

Improving the combined operation of Dynamic Positioning and motion compensation from a control engineering perspective

I.M. van der Vossen



Improving the combined operation of Dynamic Positioning and motion compensation from a control engineering perspective

MASTER OF SCIENCE THESIS

For the degree of Master of Science in Systems and Control at Delft
University of Technology

I.M. van der Vossen

February 13, 2017

Faculty of Mechanical, Maritime and Materials Engineering (3mE) · Delft University of
Technology

SIEMENS

The work in this thesis was supported by Siemens. Their cooperation is hereby gratefully acknowledged.



DCSC

Copyright © Delft Center for Systems and Control (DCSC)
All rights reserved.

DELFT UNIVERSITY OF TECHNOLOGY
DEPARTMENT OF
DELFT CENTER FOR SYSTEMS AND CONTROL (DCSC)

The undersigned hereby certify that they have read and recommend to the Faculty of
Mechanical, Maritime and Materials Engineering (3mE) for acceptance a thesis
entitled

IMPROVING THE COMBINED OPERATION OF DYNAMIC POSITIONING AND MOTION
COMPENSATION FROM A CONTROL ENGINEERING PERSPECTIVE

by

I.M. VAN DER VOSSEN

in partial fulfillment of the requirements for the degree of

MASTER OF SCIENCE SYSTEMS AND CONTROL

Dated: February 13, 2017

Supervisor(s): _____
prof.dr.ir. J. Hellendoorn

ir. R. van der Groep

Reader(s): _____
dr.ir. J. Alonso-Mora

ir. S. Boersma

Abstract

The starting point of this research is to asses possible shortcomings of the combined operation of a Dynamic Positioning (DP) vessel and a motion compensation system, with respect to the amount of energy that is used. The motion compensation system is used to allow a safe transfer from the vessel to a static offshore structure. Both systems have the objective to track a fixed reference position. In the current situation these two systems are controlled independently, raising the idea that they could counteract each other.

For a DP vessel operating on its own the ultimate goal is to track the reference position as close as possible using a reasonable amount of energy. However, for the combined operation the vessel just needs to stay close enough to the reference point so that the motion compensation system can do the rest. It is assumed that the latter needs less energy than the vessel to overpass the same distance.

The goal of this thesis is to investigate options to adjust the existing or build a new DP controller containing a certain variable that can be used to make a trade-off. The displacement of the vessel from the reference point can be weighed against the energy consumption.

Simulation models of a DP vessel and of a motion compensation system are built in Simulink. Next to this, models for the energy consumption are derived for both systems.

The proposed methods for energy consumption reduction are: the use of the integrated velocity as an estimation of the position of the vessel, the use of a reference circle instead of a reference point, the tuning of the thrust allocation optimization, and the use of Model Predictive Control (MPC).

After Simulating two different scenarios it can be concluded that all methods yield energy consumption reductions, and taking into account some more preferences, overall MPC gives the best results.

Table of Contents

1	Introduction	1
1-1	Main thesis goal	1
1-2	Assumptions and simplifications	3
1-3	Problem Statement	3
1-3-1	Sub problems	4
1-4	Outline of the Report	5
2	Preliminaries on Vessel Modelling and Dynamic Positioning	7
2-1	Generalized Vectors	7
2-2	Reference Frames	8
2-3	Kinematics	9
2-4	Wave Filtering	10
2-5	Vessel Modelling	11
2-6	Conclusion	13
3	Dynamic Positioning Vessel Simulation Model	15
3-1	Process Plant Model	16
3-2	Conventional DP Controller	17
3-3	Disturbance and Noise	17
3-4	Observer	20
3-5	Thrust Allocation	23
3-6	Energy Consumption	25
3-7	Conclusion	25
4	Motion Compensation System Simulation Model	27
4-1	Reference Signal Generator	28
4-2	Process Plant Model	30
4-3	Controller Structure	31
4-4	Energy Consumption	31
4-5	Conclusion	33

5 Energy Reduction Strategies	35
5-1 Adjustments of the standard DP controller	35
5-1-1 Dead Reckoning	35
5-1-2 Reference Circle	36
5-1-3 Thrust Allocation Tuning	37
5-2 Model Predictive Control	38
5-2-1 Matlab implementation	40
5-2-2 AMPL implementation	41
5-3 Conclusion on Energy Reduction Strategies	42
6 Case Study	45
6-1 Input Data	45
6-2 Requirements and Preferences	46
6-3 Simulation Results	48
6-3-1 Tuning	48
6-3-2 Controller Behaviour	54
6-4 Conclusions	56
7 Conclusion and Discussion	59
7-1 Conclusions of the Research	59
7-2 Discussion and Recommendations	61
A Parametrization of the Vessel Simulation Model	63
B Parametrization of the Motion Compensation System Simulation Model	67
C Matlab MPC code	69
D AMPL MPC codes	71
E Simulation results	75
Bibliography	93
Glossary	95
List of Acronyms	95

Chapter 1

Introduction

In the past decade a lot of Offshore Wind Farms have been built, and they are still proliferating in seas and oceans around the world. Needless to say, regular maintenance of these windmills is required. Oil rigs also still have a place in the foreseeable future. As a result, a lot of people will need to make transfers from floating vessels in motion to static offshore structures and vice versa. In the past, these transfers were a troublesome task if the weather conditions were rough and waves were high. Nowadays, two systems are in use to attenuate this problem.

On the one hand, the vessel can partly control its position and heading by using its own propellers, rudders and thrusters, a technique which is called Dynamic Positioning (DP), to stay at a short distance from the offshore structure. On the other hand a motion compensation system is needed to counteract the remaining motions of the vessel, mainly caused by waves. This system has a base platform mounted to the deck of the vessel, following the motion of the waves, and a top platform which can be kept motionless with respect to the offshore structure, so that a gangway from this platform to the offshore structure allows a relatively safe transfer of people. A visualization is given in Figure 1-1 [13]. Here a certain motion compensation system, called the “Ampelmann”, is used. In this system the top platform is supported by six cylinders with adjustable lengths, but this is just an example, there are other systems with different structures.

The combination of DP and motion compensation is being used in practice and achieves acceptable results but there is still room for improvement.

1-1 Main thesis goal

The starting point of this research is to asses possible shortcomings of the combined operation of a DP vessel and a motion compensation system, with respect to the amount of energy that is used. Both systems have the objective to track a fixed reference position. In the current situation these two systems are controlled independently, raising the idea that they could counteract each other.



Figure 1-1: A ship with a gangway to an offshore structure.

During the literature study it appeared that the reference tracking capability of a vessel is much more limited than that of a motion compensation system. The average DP system of a vessel only considers the Degrees of Freedom (DOF) in the horizontal plane, where a motion compensation system usually compensates for pitch, roll and heave as well. Next to this, motion compensation systems have much faster system dynamics than the vessel DP systems. Roughly speaking, the motion compensation system compensates for the fast wave induced motions, and the DP system compensates only slowly varying motions induced by wind and current. The frequency at which the motion compensation system is controlled, is compared to the vessel at least ten times higher. Due to this it is not of much use to incorporate knowledge of the vessel and its system states into the motion compensation controller.

Moreover, the vessel is a starting point in the concept of the motion compensation systems and underlies its existence to begin with. But on the contrary, a Dynamic Positioning system is not designed with the use of a motion compensation system in mind. The same DP system is used for many different purposes next to people transfer, like drilling and cable laying. This suggests that there could be room for improvement, if a DP controller mode is designed only for the purpose of people transfer with a motion compensation system. This leads to the following main question:

How can the control system of a Dynamic Positioning (DP) vessel be improved, in order to minimize the summed energy consumption of the vessel and a motion compensation system, while keeping a gangway motionless relative to an offshore structure?

1-2 Assumptions and simplifications

Even with the emphasis on the DP system and not on the motion compensation system, there are numerous ways thinkable to save energy. To narrow the search area where an answer to the main question could be found, a few assumptions and simplifications are made:

- A large vessel needs more energy than a small motion compensation system to overpass the same distance, so it will be more efficient to use the thrusters of the vessel as little as possible.
- As long as the vessel stays within a certain circle corresponding to the work space of the motion compensation system, the latter is always able to keep the gangway motionless, up to an accepted residual motion, with its existing control system in normal weather conditions.
- All forces that act on the vessel are the control forces given by the thrusters and the disturbance forces caused by wind, waves and current. The dynamic interaction between the vessel and the motion compensation system is assumed to be negligible.
- The total disturbance vector can be decoupled into two terms, the Low-Frequency (LF) and the High-Frequency (HF) disturbance. The first is an almost constant term with a slight variation with very low frequency, representing the main wind and current forces. The second term consists of a second-order wave spectrum with high frequencies, representing not only the waves but also the short-term variations in the wind and current forces like wind gusts.
- The combined system works most efficiently if the vessel reacts only to the LF disturbance term, and the motion compensation system reacts to the HF disturbance term.

1-3 Problem Statement

The standard DP controller uses Proportional Integral Derivative (PID) control to compute a generalized force vector to be applied to the vessel. The input of the controller should be the position error caused by the LF disturbance. However, the position measurement signal contains both the LF and HF motion of the vessel.

An observer is used to estimate the LF motion, but of course this can not be done perfectly. Some of the HF motions are reflected in the controller input signal and the controller responds to this. According to Liu, using a Kalman Filter the mean two dimensional LF position estimation error lies between 0.075 and 0.12 meters, depending on the number of sensors used [12]. When sailing over a distance of several meters this error is relatively small, for instance when the vessel is laying a cable. But if the reference is to stay at a fixed position this error does have an influence on the performance of the controller. The vessel manages to stay very close to the reference point, but uses high thrust forces for this. A significant inefficiency might be the reaction of the controller to a too high estimated position error, resulting in constant overcompensation.

If the estimation error of the observer is seen as given, it could be more efficient to have a

controller that accepts it if the vessel has a small displacement from the reference point. After all, the tracking of a constant reference is merely a consequence of using PID control, while for the combined operation the objective of the vessel should be to stay within a circle with a certain radius, so that the motion compensation system can compensate the remaining vessel motions.

In the light of the above made assumptions and with the estimation error as given, it could be fruitful to investigate the option to adjust the existing or build a new controller containing a certain variable that can be used to make a trade-off. The displacement of the vessel from the reference point can be weighed against the energy consumption in order to approach the scenario given in the last assumption. But first one other adjustment to the PID controller is studied, namely the use of dead reckoning.

1-3-1 Sub problems

In the first part of the research three adjustments are made to the standard DP controller to see how they affect the behaviour of the vessel.

First, as will be shown in Section 3-4, the estimation of the LF velocity of the vessel is much more accurate than the estimation of the LF position. Dead Reckoning (DR) is the consequence of using the integrated velocity as an estimation of the position, which is unwanted because of the error accumulation. Still, it would be interesting to examine the behaviour of a DP controller using this principle. Therefore the first sub question reads:

How much energy reduction could be realized by using the integrated velocity as an estimation of the position of the vessel?

Secondly, a rather rigorous approach is used to change the reference point of the PID controller into a reference circle. The LF position estimation of the observer is used to calculate the displacement of the vessel in the x-y plane. Only the part of the displacement outside of the reference circle is seen as the position error and is the input for the PID controller. The radius of the circle can be seen as a trade-off variable. The second sub question is:

How much energy reduction could be realized by changing the reference point of the PID controller into a reference circle?

Thirdly, after the DP controller has computed a generalized force vector to be applied to the vessel, a thrust allocation system determines for each individual thruster what force it should exert to match the generalized force vector. For this an optimization algorithm is used with in the objective function the thrust forces and a slack variable, representing the extent to which the actual thrust can differ from the required thrust, with different weight matrices. So in fact, the existing DP controller already has got a variable that can be used to make a trade-off. Although literature states that the weight of the slack variable should be much larger than the weight of the thrust forces, lowering the weight of the slack could result in a larger maximum displacement of the vessel but at the same time lower thrust forces, leading to the third sub question:

How much energy reduction could be realized by tuning the weight matrices in the thrust allocation objective function?

The following steps must be taken to answer these question:

- Define a model that simulates a vessel with a standard DP control system, thrust allocation and average disturbances.
- Define a model for the energy consumption of a vessel, based on the simulated DP vessel.
- Define a model of a motion compensation system and a model for the energy consumption of the system.
- Create plots of the relation between the summed energy consumption and the position of the vessel for the base case and the different adjustments to the PID controller.

In the second part of this research a more progressive approach is sought-after to trade-off displacement versus energy. A number of control methods were studied in the literature survey. Model Predictive Control (MPC) seems to be promising for this research because making a trade-off between state values and control forces is inherent in this control method. The LF position estimation is still used, so the estimation error will still have a negative influence on the controller. But the algorithm also considers predictions of the future states and disturbances of the system, here the HF disturbance does not play a role. So in total it is expected that the effect of the estimation error on the reaction of the vessel will be smaller.

Multiple publications were found on using MPC for a DP control system, but in all of them only the reference tracking capabilities were studied and the energy consumption was not elaborated upon. The new insight that is aimed for in this research is the possibility to use MPC to minimize the energy consumption of the vessel. The last sub question is:

How much energy reduction could be realized by using MPC for the vessel DP controller?

The following steps must be taken to answer this question:

- Define a prediction model for the MPC controller based on the discretized vessel simulation model.
- Define the MPC weight matrices, constraints and parameters.
- Create plots of the relation between the energy consumption and the position of the vessel for the MPC controller.

1-4 Outline of the Report

First some preliminaries on vessel modelling and DP will be given in Chapter 2.

In Chapter 3 a simulation model of a DP vessel will be defined.

Chapter 4 gives a simulation model of a motion compensation system. Though in this work the focus will be on a platform with a gangway, a similar approach could as well be used for other applications like a helicopter platform or a crane foundation system.

In Chapter 5 the proposed methods to reduce the energy consumption of the vessel will be explained more into detail.

In Chapter 6 a test case will be built to compare the different approaches of energy reduction of the vessel, including simplifications and constraints of the problem, and the simulation results will be evaluated.

Finally, in Chapter 7 the research will be summarized and discussed, and suggestions for further research will be given.

Chapter 2

Preliminaries on Vessel Modelling and Dynamic Positioning

Vessel modelling and Dynamic Positioning (DP) are very rich subjects in both scientific and non-scientific literature. This is a treat but at the same time troublesome, because not all authors use the same notation and definitions. The suggested notation in this chapter is for the largest part adopted from an author who's name occurs very frequently when reading about DP, professor Thor I. Fossen.

A DP vessel is defined by the International Maritime Organization (IMO) as *a vessel that maintains its position and heading (fixed location denoted as stationkeeping or predetermined track) exclusively by means of active thrusters*. Although 'ship modelling' is a more commonly used term, 'vessel modelling' would be more appropriate for DP, because this technique is used not only for ships, but also for other vessels like semi-submersible drilling rigs or Floating Production, Storage and Operation (FPSO) units. However, in the literature there is no clear distinction made between vessel or ship modelling, so the terms are in fact interchangeable. In this chapter first a notation and other preliminaries are determined, then a mathematical vessel model is derived [19].

2-1 Generalized Vectors

Naturally, a ship at sea has the freedom to move in all possible directions, three translations and three rotations. In 1950 a commonly used notation for forces, velocities and positions of marine vessels was defined by the Society of Naval Architects and Marine Engineers, as set out in Table 2-1 [5, 16].

Table 2-1: A widely used notation for marine vessels.

DOF	force/moment	linear/angular velocity	position/Euler angle
surge	X	u	x
sway	Y	v	y
heave	Z	w	z
roll	K	p	ϕ
pitch	M	q	θ
yaw	N	r	ψ

For convenient modelling many authors, among who Fossen, Sørensen, Perez and Blanke, use generalized position, velocity and force vectors, $\boldsymbol{\eta}$, $\boldsymbol{\nu}$ and $\boldsymbol{\tau}$, defined as:

$$\boldsymbol{\eta} = [x \ y \ z \ \phi \ \theta \ \psi]^\top \in \mathbb{R}^3 \times \mathcal{S}^3 \quad (2-1)$$

$$\boldsymbol{\nu} = [u \ v \ w \ p \ q \ r]^\top \in \mathbb{R}^6 \quad (2-2)$$

$$\boldsymbol{\tau} = [X \ Y \ Z \ K \ M \ N]^\top \in \mathbb{R}^6 \quad (2-3)$$

where \mathbb{R}^n denotes the Euclidean space of dimension n and \mathcal{S}^n denotes a torus in n dimensions. These vectors will later be used in the equations of motion for the mathematical vessel model.

However, when designing control systems for ships usually not all Degrees of Freedom (DOF) are taken into account. Which ones are used in a certain model depends on the purpose of the controller and on the available actuators of the vessel. Most DP vessels are modelled in three DOF, because control of heave, pitch and roll is unnecessary for most applications, and those directions are not actuated. In both cases the same symbols are used but with a different definition [5, 14, 17, 7]:

$$\boldsymbol{\eta} = [x \ y \ \psi]^\top \quad (2-4)$$

$$\boldsymbol{\nu} = [u \ v \ r]^\top \quad (2-5)$$

2-2 Reference Frames

To model the equations of motion of a vessel the generalized vectors are used in different reference frames, depicted in Figure 2-1 [15]. Each of these frames has a specific use:

- The **North-east-down frame (n-frame)** is fixed to the earth. The x_n -axis points north, the y_n -axis points east and the z_n -axis points towards the centre of the earth. This frame is used to define the position and orientation of the vessel, $\boldsymbol{\eta}$, as well as the directions of external forces and moments, $\boldsymbol{\tau}_{ext}$. The origin of this frame is a certain point on the still water surface.

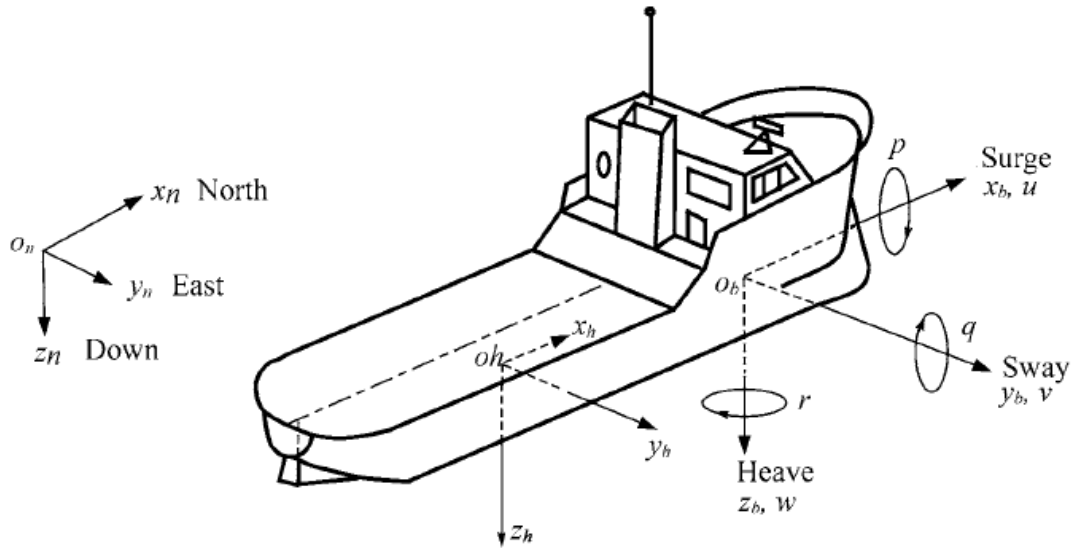


Figure 2-1: Notation and sign conventions for ship motions.

- The **Body-fixed frame (b-frame)** is fixed to the vessel. The x_b -axis points towards the bow, the y_b -axis points to starboard and the z_b -axis points downwards. The origin of this frame is usually positioned at the centre of inertia of the ship, to conveniently formulate the equations of motion. The velocity and acceleration of the ship, ν and $\dot{\nu}$, coincide with the b-frame.
- The **Hydrodynamic frame (h-frame)** is not fixed to the ship, but follows the path of the vessel at its average speed. The positive x_h -axis is aligned with the Low-Frequency (LF) heading angle of the ship, neglecting the motions of the waves, and accordingly the y_h - and z_h -axes point to the right and downwards. The origin of this frame is defined as the time-average position of the centre of gravity of the ship and lies in a plane parallel to the still water surface. The wave-induced motions of the ship make the vessel oscillate around the h-frame, so it can be used to define local wave elevation. The generalized position vector in this frame is defined as:

$$\xi = [\xi_x \quad \xi_y \quad \xi_z \quad \xi_\phi \quad \xi_\theta \quad \xi_\psi]^\top \quad (2-6)$$

where ξ_i is the position or rotation of the vessel with respect to the b-frame [5, 15].

2-3 Kinematics

A kinematic transformation matrix can be constructed to translate between $\dot{\eta}$ in the n-frame and ν in the b-frame:

$$\dot{\boldsymbol{\eta}} = \mathbf{J}(\boldsymbol{\eta})\boldsymbol{\nu} \quad (2-7)$$

$$\mathbf{J}(\boldsymbol{\eta}) := \begin{bmatrix} \mathbf{R}(\boldsymbol{\Theta}) & \mathbf{0}_{3 \times 3} \\ \mathbf{0}_{3 \times 3} & \mathbf{T}(\boldsymbol{\Theta}) \end{bmatrix} \quad (2-8)$$

where $\boldsymbol{\Theta} = [\phi \ \theta \ \psi]^\top$, and

$$\mathbf{R}(\boldsymbol{\Theta}) = \begin{bmatrix} \cos \psi \cos \theta & -\sin \psi \cos \phi + \cos \psi \sin \theta \sin \phi & \sin \psi \sin \phi + \cos \psi \cos \phi \sin \theta \\ \sin \psi \cos \theta & \cos \psi \cos \phi + \sin \phi \sin \theta \sin \psi & -\cos \psi \sin \phi + \sin \theta \sin \psi \cos \phi \\ -\sin \theta & \cos \theta \sin \phi & \cos \theta \cos \phi \end{bmatrix} \quad (2-9)$$

$$\mathbf{T}(\boldsymbol{\Theta}) = \begin{bmatrix} 1 & \sin \phi \tan \theta & \cos \phi \tan \theta \\ 0 & \cos \phi & -\sin \phi \\ 0 & \sin \phi / \cos \theta & \cos \phi / \cos \theta \end{bmatrix}, \quad \theta \neq \pm \frac{\pi}{2} \quad (2-10)$$

The matrix R is often denoted as the Euler angle rotation matrix. The matrix is orthogonal, so the inverse rotation matrix is equal to the transpose, $\mathbf{R}^{-1} = \mathbf{R}^\top$ [7].

In the three DOF case the kinematic matrix is reduced to:

$$\dot{\boldsymbol{\eta}} = \mathbf{R}(\psi)\boldsymbol{\nu} = \begin{bmatrix} \cos \psi & -\sin \psi & 0 \\ \sin \psi & \cos \psi & 0 \\ 0 & 0 & 1 \end{bmatrix} \begin{bmatrix} u \\ v \\ r \end{bmatrix} \quad (2-11)$$

The transformation matrices will later be needed because the vessel position is measured in the n-frame, but the vessel itself and the actuation of it is in the b-frame [19].

2-4 Wave Filtering

Liu and Willemse both give an overview of the reference sensors that are used for DP, including Differential Global Positioning System (DGPS), Inertial Measurement Unit (IMU), Hydro-acoustic Position Reference (HPR), laser, radar and gyroscope for position and orientation determination and an anemometer to measure the wind speed [12, 26]. Sometimes multiple sensors are used to measure the same variables, in that case sensor fusion is needed. Two options for this are using a weighting system or using the Unscented Kalman Filter (UKF), as explained in the thesis of Liu. Of course not all sensors are positioned at the Center of Gravity (CoG), so the rotations of the vessel result in errors in the position measurements of the DGPS. The kinematic transformation matrices from Subsection 2-3 and the pitch and roll measurements from the IMU are used to rectify this [12, 26].

For a DP system it is common practice to filter the measurement signals, as shown in Figure 2-2 [12], resulting in a LF and a High-Frequency (HF) motion signal:

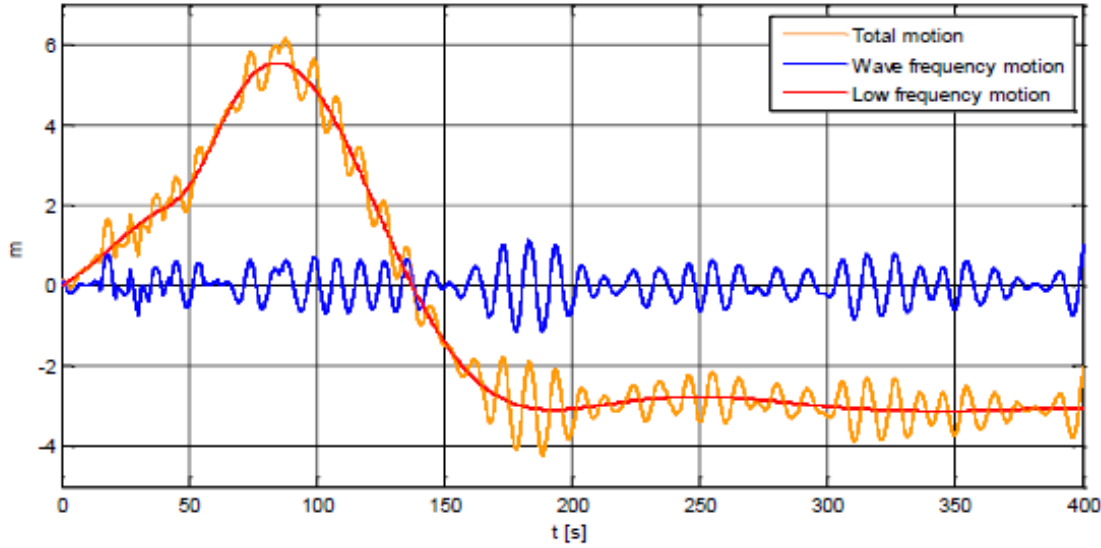


Figure 2-2: Low frequency motion and high frequency motion.

$$\mathbf{y} = \mathbf{y}_{LF} + \mathbf{y}_{HF} \quad (2-12)$$

The LF motion is mainly induced by the thruster system, the wind force and the second-order wave load. The latter can be said to be the current.

The HF motion is caused by the first-order wave load, and is usually treated as measurement noise. The DP control system should only act on the LF motions to prevent wear and tear of the propulsion system, and it is expected that in combination with a motion compensation system this will be most efficient in terms of energy. According to Liu, with a Kalman Filter the LF position can be estimated from the measurement signal with an error as low as 0.075 m if seven different sensors are used. But a DP system with only two or three different sensors available will have an error of around 0.1 m [19, 5, 12].

2-5 Vessel Modelling

Low Frequency model The nonlinear LF equation of motion of a vessel is modelled most generally as [19]:

$$\mathbf{M}\dot{\nu} + \mathbf{C}(\nu)\nu + \mathbf{D}(\nu)\nu + \mathbf{G}(\eta) = \boldsymbol{\tau}_{wave2} + \boldsymbol{\tau}_{wind} + \boldsymbol{\tau}_{thr} + \boldsymbol{\tau}_{moor} \quad (2-13)$$

On the right-hand side the force vectors are second-order wave forces (current), and wind, thruster and mooring forces. The latter is not taken into account in the rest of this thesis, as it is assumed the vessel is unmoored. The forces are directed along the b-frame. On the left-hand side, $\mathbf{M} \in \mathbb{R}^{6 \times 6}$ is the inertia matrix with rigid body and added mass included, $\mathbf{M} = \mathbf{M}_{RB} + \mathbf{M}_A$. *Added mass* is a hydrodynamic modelling term that incorporates the effect of the fluid surrounding the vessel that needs to be moved when the ship accelerates or

decelerates. The added mass coefficients depend on the shape of the hull. The $\mathbf{C}(\boldsymbol{\nu})$ matrix contains the skew-symmetric Coriolis and centripetal matrices of the rigid body and the added mass, $\mathbf{C}(\boldsymbol{\nu}) = \mathbf{C}_{RB}(\boldsymbol{\nu}) + \mathbf{C}_A(\boldsymbol{\nu})$. These terms appear due to formulating the equations of motion in the b-frame. The damping matrix $\mathbf{D}(\boldsymbol{\nu})$ can be divided into linear and nonlinear terms, modelling both potential and viscous damping effects. $\mathbf{G}(\boldsymbol{\eta})$ is a vector of generalized restoring forces, namely buoyancy and gravitation, which mainly affect the roll and pitch of the vessel [6, 7, 17, 18].

High Frequency model In the HF equations of motion small waves and amplitudes of motion are assumed. A linear model is formulated as:

$$\mathbf{M}(\omega)\ddot{\boldsymbol{\eta}}_{Rw} + \mathbf{D}_p(\omega)\dot{\boldsymbol{\eta}}_{Rw} + \mathbf{G}\boldsymbol{\eta}_{Rw} = \boldsymbol{\tau}_{wave1} \quad (2-14)$$

$$\dot{\boldsymbol{\eta}}_w = \mathbf{J}(\boldsymbol{\eta})\dot{\boldsymbol{\eta}}_{Rw} = \mathbf{J}(\boldsymbol{\eta})\boldsymbol{\nu} \quad (2-15)$$

where $\boldsymbol{\tau}_{wave1}$ contains the first-order wave forces (waves), $\boldsymbol{\eta}_{Rw}$ is the HF position vector in the h-frame and $\boldsymbol{\eta}_w$ in the n-frame, and $\mathbf{J}(\boldsymbol{\eta})$ is as defined in Equation (2-8). In the $\mathbf{M}(\omega)$ matrix the added mass is now frequency dependent, $\mathbf{D}_p(\omega)$ is the wave radiation (potential) damping and \mathbf{G} is the linearised restoring coefficient matrix, affecting only heave, roll and pitch [19].

Note that normally a time domain function cannot contain frequency coefficients because of the memory effect it incorporates, but this formulation is commonly used in vessel modelling and is denoted as a pseudo-differential equation. As shown by Fossen, memory effects can be taken into account by using a state space model [5]. In case the speed of the vessel is zero, Equation (2-14) can be assumed to be a second-order linear model driven by white noise, given in state space form as:

$$\dot{\boldsymbol{\chi}}_w = \mathbf{A}_w\boldsymbol{\chi}_w + \mathbf{E}_w\mathbf{w}_w \quad (2-16)$$

where $\boldsymbol{\chi}_w$ is the state of the HF model with $\boldsymbol{\chi}_w(0) = \mathbf{0}$, \mathbf{w}_w is a white noise signal, and \mathbf{A}_w is assumed Hurwitz [17, 18, 19].

Unified model For zero forward speed the Coriolis term disappears and the \mathbf{D} matrix can be assumed to be constant. All external forces that act on the vessel are merged in the $\boldsymbol{\tau}_{ext}$ vector. Using (2-7), (2-13) and (2-14), LF and HF can be combined in the following unified model which will be the basis for the process plant model and observer of the DP simulation model in the next chapter:

$$\dot{\boldsymbol{\eta}}_{LF} = \mathbf{J}(\boldsymbol{\eta})\boldsymbol{\nu} \quad (2-17)$$

$$\mathbf{M}\dot{\boldsymbol{\nu}} + \mathbf{D}\boldsymbol{\nu} + \mathbf{G}\boldsymbol{\eta}_{LF} = \boldsymbol{\tau}_{ext} + \boldsymbol{\tau}_{thr} \quad (2-18)$$

$$\dot{\boldsymbol{\chi}}_w = \mathbf{A}_w\boldsymbol{\chi}_w + \mathbf{E}_w\mathbf{w}_w \quad (2-19)$$

$$\boldsymbol{\eta}_{HF} = \mathbf{C}_w\boldsymbol{\chi}_w \quad (2-20)$$

$$\boldsymbol{\eta}_{tot} = \boldsymbol{\eta}_{LF} + \boldsymbol{\eta}_{HF} \quad (2-21)$$

where \mathbf{A}_w , \mathbf{E}_w and \mathbf{C}_w are constant matrices of appropriate dimensions [5, 6].

2-6 Conclusion

In this chapter an insight is given into the basics of vessel modelling. The studied theoretics will be used in the development of the Dynamic Positioning Vessel Simulation Model in Chapter 3.

Generalized vectors are used to define the equations of motion of a vessel, η , v and τ , in either three or six Degrees of Freedom. Kinematic transformation matrices were introduced to translate the vessel position which is measured in the n-frame into the position in the b-frame. The thrust forces are computed and applied to the vessel in the b-frame. Furthermore the concept of wave filtering was introduced. The measured vessel displacement and velocity are divided into a high and a low frequency part. The vessel should only react to the low frequency to prevent wear and tear of the thrusters.

Chapter 3

Dynamic Positioning Vessel Simulation Model

As a basis for the vessel simulation model the Marine Systems Simulator (MSS) developed by Fossen and Perez is used [9]. This is a Matlab/Simulink library and simulator, including vessel models and guidance, navigation and control blocks for real-time simulation. Elements of different demonstration models are used to get a basic simulation model including a vessel model, a controller, disturbance and noise generation, an observer, and a thrust allocation model. And finally, a simple model is added to estimate the energy consumption of the vessel. Figure 3-1 shows a block scheme with the most important parts of the Dynamic Positioning (DP) control system.

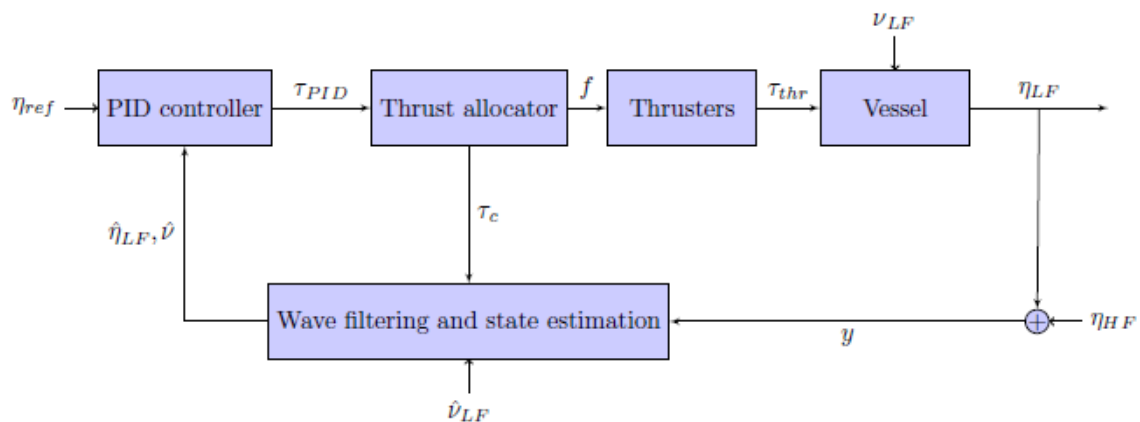


Figure 3-1: A block scheme of a DP control system.

3-1 Process Plant Model

The process plant model in this research is based on a Simulink model of a supply vessel from the MSS, depicted in Figure 3-2 [9]. It has a length of 76.2 meters and a mass of 6×10^6 kg. As the name suggests a vessel like this is used to supply goods, tools, equipment and personnel to oil platforms and other offshore structures. The vessel could benefit very well of having a motion compensation system aboard. For instance if routinely maintenance needs to be done at a wind farm. The personnel needs to transfer from and to the vessel multiple times in a day.

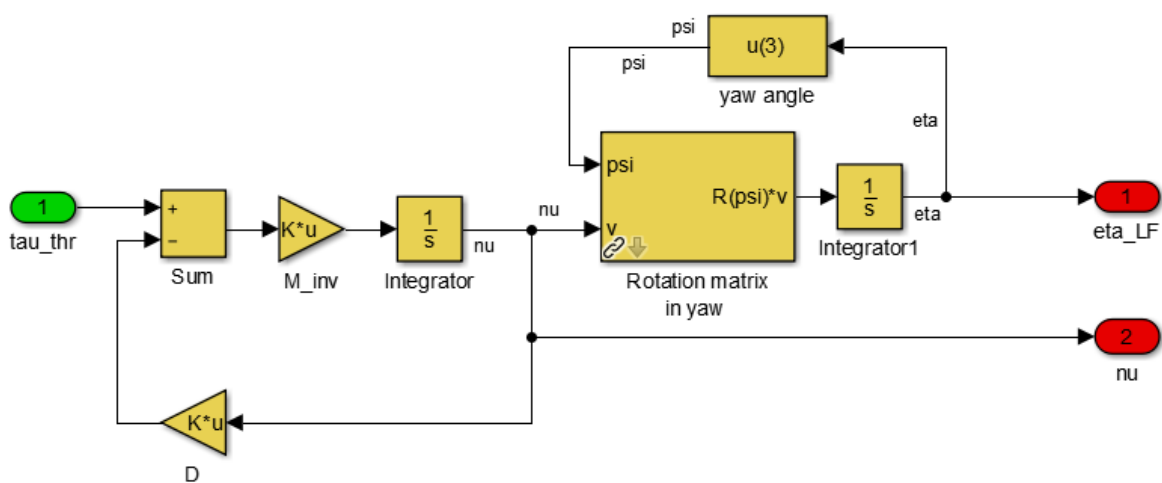


Figure 3-2: Picture and Simulink model of the supply vessel.

The vessel model is based on the first two equations of the unified model, (2-17) and (2-18). In the first $\mathbf{J}(\boldsymbol{\eta})$ is replaced by $\mathbf{R}(\psi)$, as given in (2-11), because only the three dimensions of the horizontal plane are modelled. For the same reason the buoyancy term is omitted in the second equation, and disturbance is not yet taken into account so $\boldsymbol{\tau}_{thr}$ is the only force acting on the vessel. The non-linear Low-Frequency (LF) equations of motion become:

$$\dot{\boldsymbol{\eta}}_{LF} = \mathbf{R}(\psi)\boldsymbol{\nu} \quad (3-1)$$

$$\mathbf{M}\dot{\boldsymbol{\nu}} + \mathbf{D}\boldsymbol{\nu} = \boldsymbol{\tau}_{thr} \quad (3-2)$$

3-2 Conventional DP Controller

For the base case of the simulation model a discrete time Proportional Integral Derivative (PID) controller is used to control the LF vessel position, the Simulink model is shown in Figure 3-3. It is a non-linear controller because a transposed rotation matrix $\mathbf{R}^\top(\psi)$ is needed to translate the regulation error, $\mathbf{e}_n = \boldsymbol{\eta}_{ref} - \hat{\boldsymbol{\eta}}_{LF}$, between frameworks. The system states of the vessel are measured in the North-east-down frame (n-frame) but the required control force $\boldsymbol{\tau}_{PID}$ will be calculated in the Body-fixed frame (b-frame). Furthermore, the LF position error is integrated with the forward Euler method:

$$\boldsymbol{\tau}_{PID}(k) = \mathbf{K}_p \mathbf{e}_b(k) + \mathbf{K}_i \mathbf{z}(k) - \mathbf{K}_d \hat{\boldsymbol{\nu}}(k) \quad (3-3)$$

$$\mathbf{e}_b(k) = \mathbf{R}^\top(\psi)(\boldsymbol{\eta}_{ref}(k) - \hat{\boldsymbol{\eta}}_{LF}(k)) = \mathbf{R}^\top(\psi)\mathbf{e}_n(k) \quad (3-4)$$

$$\mathbf{z}(k) = \mathbf{z}(k-1) + \mathbf{K}[t(k) - t(k-1)]\mathbf{e}_b(k-1) \quad (3-5)$$

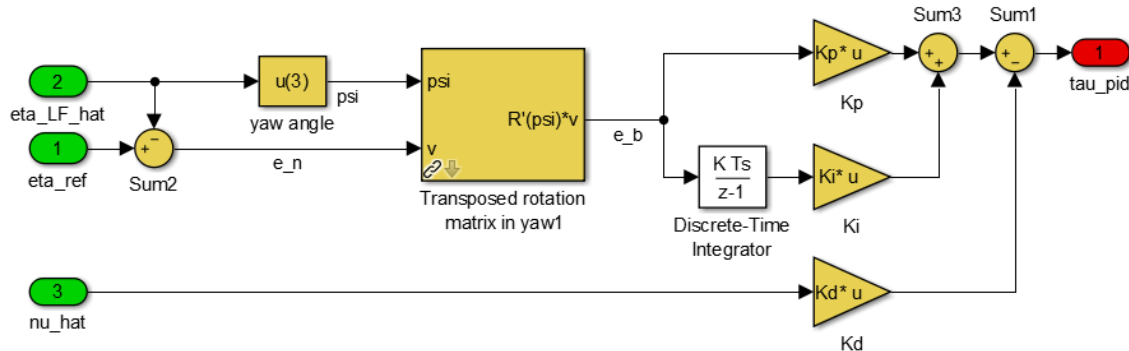


Figure 3-3: Simulink model of the PID controller.

3-3 Disturbance and Noise

As discussed before the intended vessel motion gets disturbed by wind, waves and current. For simplicity it is chosen not to model each of these separately, but to describe the total

disturbance by one LF and one High-Frequency (HF) term.

The disturbances are not modelled as forces but as a velocity and a displacement for the LF and HF term respectively. This might be counter intuitive but is in line with the demonstration models of the MSS, and this method will give valuable information for evaluating the controller performance as will be explained in this subsection.

LF Disturbance The LF disturbance is incorporated in the model by slightly adjusting the process plant model. In the damping term of the equation of motion the relative velocity of the vessel is used, $\nu_r = \nu - \nu_{LF}$, this is the vessel velocity minus the LF disturbance velocity caused by current and wind. The process plant model including LF disturbance becomes:

$$\dot{\eta}_{LF} = \mathbf{R}(\psi)\nu \quad (3-6)$$

$$\mathbf{M}\dot{\nu} + \mathbf{D}(\nu - \nu_{LF}) = \tau_{thr} \quad (3-7)$$

with the LF disturbance velocity ν_{LF} , depicted in Figure 3-4, modelled as two constant values, $c_{1,i}$, for the main current velocities in x and y -direction, and both have a small sinusoidal fluctuation with amplitude $c_{2,i}$ and frequency ω_{cur} :

$$\nu_{LF}(t) = \begin{bmatrix} c_{1,x} + c_{2,x} \sin(\omega_{cur}t) \\ c_{1,y} + c_{2,y} \sin(\omega_{cur}t) \\ 0 \end{bmatrix} \quad (3-8)$$

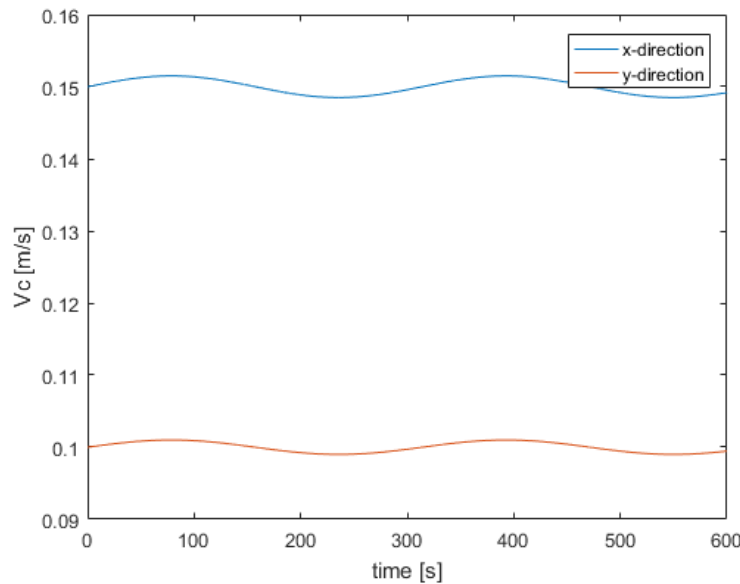


Figure 3-4: An example of the LF disturbance ν_{LF} .

HF Disturbance The HF disturbance is modelled by a linear second order wave spectrum, induced by white noise. It is evident that if a ship is excited by one single wave or wind gust,

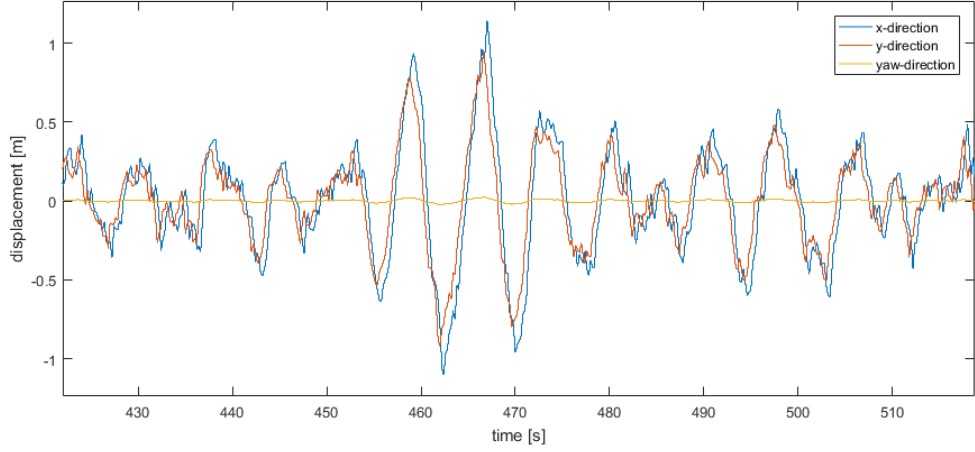


Figure 3-5: An example of $\boldsymbol{\eta}_{HF}$.

it will oscillate for some time and then come to rest, so the HF disturbance can be modelled by harmonic oscillators with damping and white-noise, which are uncoupled in the three Degrees of Freedom (DOF). The oscillators correspond to the following transfer function:

$$\frac{\eta_{wi}}{w_{wi}}(s) = \frac{K_{wi}s}{s^2 + 2\zeta_i\omega_is + \omega_i^2} \quad (3-9)$$

An example of the resulting vessel position due to the HF disturbance is shown in Figure 3-5. For the observer a state space form of the HF disturbance model will be needed, based on the third and fourth equations of the unified model, (2-19) and (2-20):

$$\dot{\boldsymbol{\chi}}_w = \mathbf{A}_w \boldsymbol{\chi}_w + \mathbf{E}_w \mathbf{w}_w \quad (3-10)$$

$$\boldsymbol{\eta}_{HF} = \mathbf{C}_w \boldsymbol{\chi}_w \quad (3-11)$$

where $\boldsymbol{\eta}_{HF} \in \mathbb{R}^3$ is the position and orientation vector, $\mathbf{w}_w \in \mathbb{R}^3$ is zero-mean Gaussian white noise, and $\boldsymbol{\chi}_w = [\boldsymbol{\eta}_w^\top / s \quad \boldsymbol{\eta}_w^\top]^\top \in \mathbb{R}^6$.

$$\mathbf{A}_w = \begin{bmatrix} \mathbf{0}_{3 \times 3} & \mathbf{I}_{3 \times 3} \\ -\boldsymbol{\Omega}^2 & -2\boldsymbol{\Lambda}\boldsymbol{\Omega} \end{bmatrix} \quad (3-12)$$

$$\mathbf{C}_w = \begin{bmatrix} \mathbf{0}_{3 \times 3} & \mathbf{I}_{3 \times 3} \end{bmatrix} \quad (3-13)$$

$$\mathbf{E}_w = \begin{bmatrix} \mathbf{0}_{3 \times 3} \\ \mathbf{K}_w \end{bmatrix} \quad (3-14)$$

with $\boldsymbol{\Omega} = \text{diag}\{\omega_1, \omega_2, \omega_3\}$, $\boldsymbol{\Lambda} = \text{diag}\{\zeta_1, \zeta_2, \zeta_3\}$ and $\mathbf{K}_w = \text{diag}\{K_{w1}, K_{w2}, K_{w3}\}$ [17, 18].

As shown in Figure 3-1, the resulting wave pattern is added to the displacement of the

process plant model and the total vessel displacement η_{tot} will be the input signal of the observer:

$$\eta_{tot} = \eta_{LF} + \eta_{HF} \quad (3-15)$$

Modelling the HF disturbance as a displacement and not as a force that acts on the vessel might be less realistic, and good wave force models do exist. However, with the chosen method more information on the controller performance is available.

If the disturbance would be modelled as a force acting on the process plant, then in the simulation this force would be added up to the thruster forces and only η_{tot} would be known. The distinction between η_{LF} and η_{HF} would be lost.

As will be shown in the next section, the estimated displacement $\hat{\eta}_{LF}$ is not very accurate, it would not suffice to only study this variable. So though it is a less realistic model, for the simulation model this method will give valuable information for evaluating the controller performance as also η_{LF} can be taken into account.

Noise In the observer and in the MPC controller the constant parts of the velocities are taken as an estimation of the LF disturbance, $\hat{\nu}_{LF}$. The sinusoidal fluctuations of ν_{LF} can be seen as process noise.

In the MSS demonstration models, measurement noise is not taken into account as the assumption is made that sensor noise is negligible compared to the wave-induced motion. The HF disturbance is already treated as noise on the measurement signal η_{tot} and filtered out by the observer.

3-4 Observer

In the MSS a continuous time non-linear passive observer is used. The simulated measurement signal $\mathbf{y} = \eta_{tot} = \eta_{LF} + \eta_{HF}$, the desired control force τ_c as computed by the thrust allocation algorithm explained in the next subsection, and the known part of the LF disturbance $\hat{\nu}_{LF}$ are the input signals of the observer.

A bias vector, \mathbf{b} , is added to account for process noise. A frequently used bias model is the first order Markov model:

$$\dot{\mathbf{b}} = -\mathbf{T}_b^{-1}\mathbf{b} + \mathbf{E}_b\mathbf{w}_b \quad (3-16)$$

where $\mathbf{w}_b \in \mathbb{R}^3$ is zero-mean Gaussian white noise, $\mathbf{T}_b \in \mathbb{R}^{3 \times 3}$ is a diagonal matrix of bias time constants and \mathbf{E}_b is a diagonal scaling matrix [18].

The process plant including LF disturbance, and the HF disturbance model are copied from (3-6), (3-7), (3-10) and (3-11), resulting in the following observer:

$$\dot{\hat{\chi}}_w = \mathbf{A}_w \hat{\chi}_w + \mathbf{K}_1 \tilde{\mathbf{y}} \quad (3-17)$$

$$\hat{\boldsymbol{\eta}}_{HF} = \mathbf{C}_w \hat{\chi} \quad (3-18)$$

$$\dot{\hat{\boldsymbol{\eta}}}_{LF} = \mathbf{R}(\psi_y) \hat{\boldsymbol{\nu}} + \mathbf{K}_2 \tilde{\mathbf{y}} \quad (3-19)$$

$$\dot{\hat{\mathbf{b}}} = -\mathbf{T}_b^{-1} \hat{\mathbf{b}} + \mathbf{K}_3 \tilde{\mathbf{y}} \quad (3-20)$$

$$\mathbf{M} \dot{\hat{\boldsymbol{\nu}}} + \mathbf{D}(\hat{\boldsymbol{\nu}} - \hat{\boldsymbol{\nu}}_{LF}) = \boldsymbol{\tau}_c + \mathbf{R}^\top(\psi_y) \hat{\mathbf{b}} + \mathbf{K}_4 \mathbf{R}^\top(\psi_y) \tilde{\mathbf{y}} \quad (3-21)$$

$$\hat{\mathbf{y}} = \hat{\boldsymbol{\eta}}_{LF} + \hat{\boldsymbol{\eta}}_{HF} \quad (3-22)$$

with the estimation error $\tilde{\mathbf{y}} = \mathbf{y} - \hat{\mathbf{y}}$ and observer gain matrices \mathbf{K}_1 , \mathbf{K}_2 , \mathbf{K}_3 and \mathbf{K}_4 [17].

Because small angles of ψ are assumed the system can be linearised around $\psi_y = 0$. The equations are combined in a unified state space model. This state space model is discretised in Matlab to get a discrete time observer. The continuous input signals are sampled with a Zero-Order Hold function. The Zero-Order Hold block holds its input value at the beginning of each sample period, for a specified sample time, to get discrete signals.

To evaluate the performance of the observer two indicators are looked at, the x - and y -position mean errors and the Variance Accounted For (VAF) values. A VAF value indicates to what extend the output of a certain model equals the real data it is based on. The higher the VAF, the lower the prediction error and the better the model. It is a value between 0 and 100%, calculated with the following formula [25]:

$$VAF(y(k), \hat{y}(k)) = \max \left(0, \left(1 - \frac{\frac{1}{N} \sum_{k=1}^N \|y(k) - \hat{y}(k)\|_2^2}{\frac{1}{N} \sum_{k=1}^N \|y(k)\|_2^2} \right) \cdot 100\% \right) \quad (3-23)$$

Figure 3-6 shows plots of $\boldsymbol{\eta}_{LF}$, $\hat{\boldsymbol{\eta}}_{LF}$, $\boldsymbol{\nu}$ and $\hat{\boldsymbol{\nu}}$ for different reference points. The mean estimation errors for the x - and y -positions are the same for each reference point, namely $\bar{e}_x = 0.0513$ and $\bar{e}_y = 0.0426$.

In Figure 3-7 the VAF values for the LF position and velocity are plotted for multiple different reference points. It can be seen that while the mean estimation errors stay the same, the VAF values rapidly decrease when the reference position comes close to zero. So the estimated $\hat{\boldsymbol{\eta}}_{LF}$, which is the input signal for the PID controller, loses its relevance. The PID controller still manages to keep $\boldsymbol{\eta}_{LF}$ really small, which seems like a good thing, but there is a good chance that the controller is constantly overcompensating and thereby wasting energy. On the other hand, the VAF values of the velocity stay more or less the same, indicating that estimating the displacement by integrating the velocity over time might be an improvement for the DP control system.

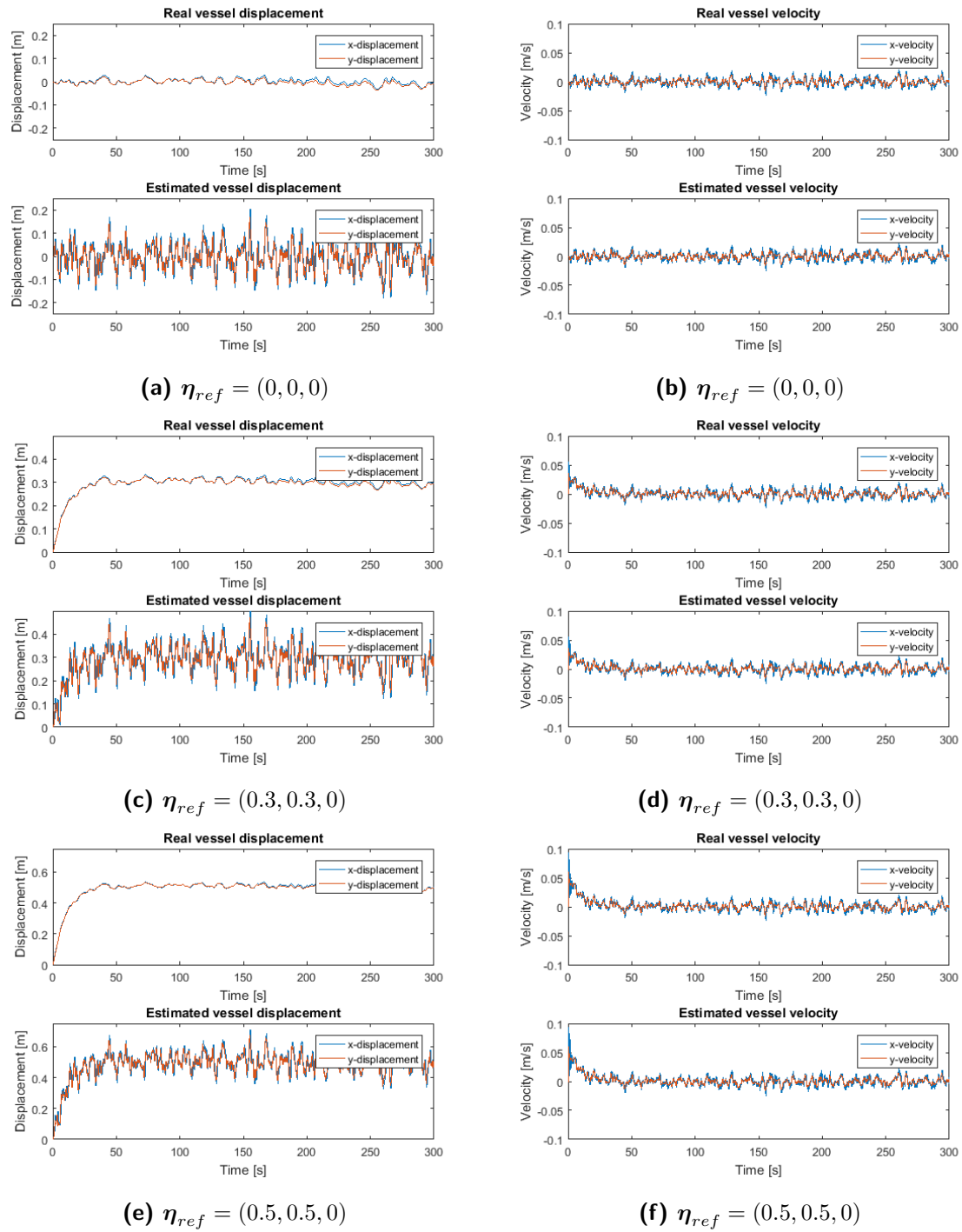


Figure 3-6: η_{LF} , $\hat{\eta}_{LF}$, ν and $\hat{\nu}$ for different reference points.

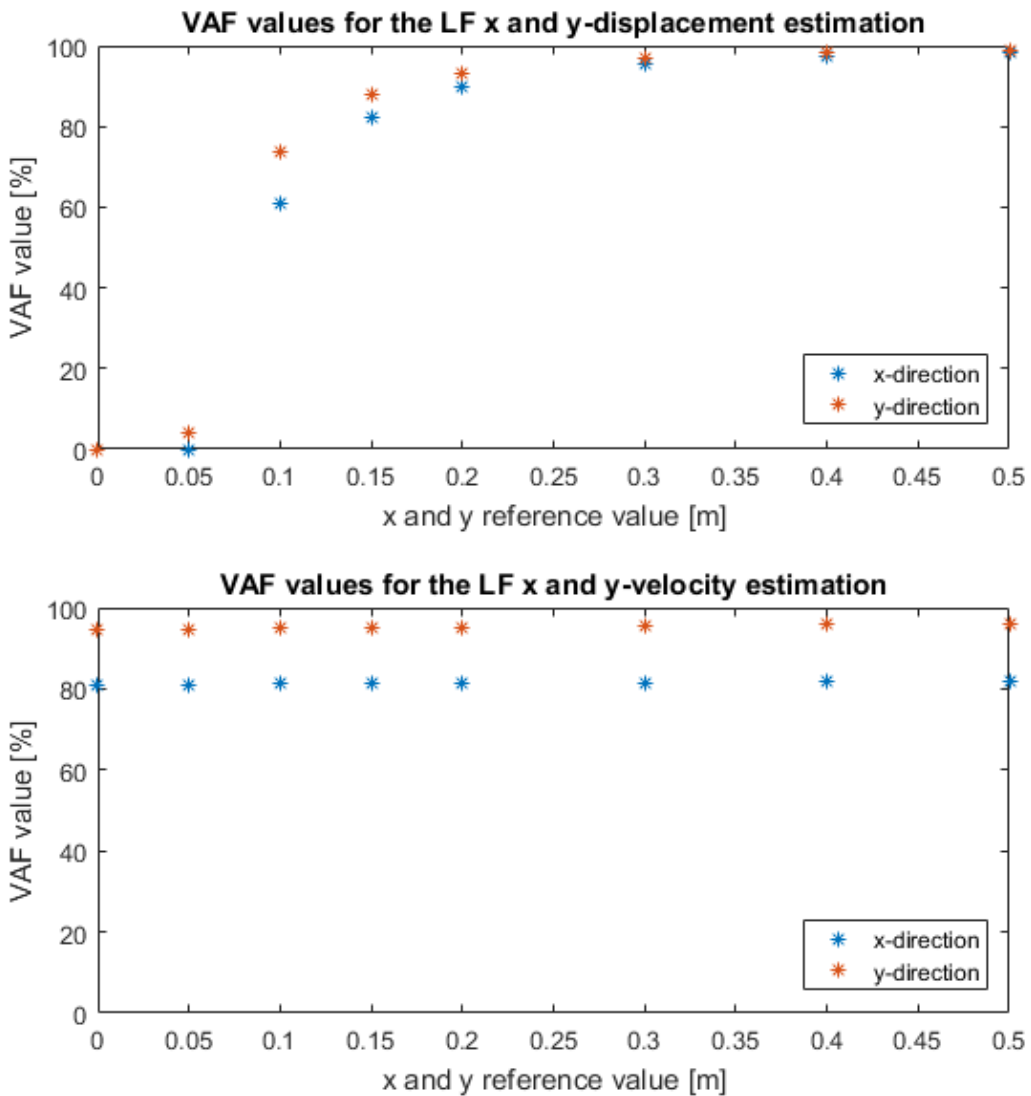


Figure 3-7: VAF values of $\hat{\eta}_{LF}$ and $\hat{\nu}$ for different reference points.

3-5 Thrust Allocation

The motion control algorithm has calculated the forces and moments that are required to keep the vessel at the reference point, contained by the thrust vector τ_{PID} . However, it is not directly evident how to control each individual thruster or propeller to let the actual produced thrust τ_{thr} coincide with this. And this problem can be further complicated by taking into account the physical limitations of the thrusters.

The variable τ_c is introduced to represent the desired generalized thrust force to be acted out on the vessel. The desired τ_c is allowed to differ from the required τ_{PID} to take into account the thruster limitations and to minimize the individual thruster forces as will be explained

later in this section. The relation between τ_c and the produced thrust could be modelled as:

$$\tau_c = \mathbf{T}(\alpha)\mathbf{f} \approx \tau_{PID} \quad (3-24)$$

where $\alpha \in \mathbb{R}^r$ is the vector containing the orientations of all thrusters (fixed or variable), r is the number of thrusters, and $\mathbf{f} \in \mathbb{R}^r$ encompasses the control forces for each thruster.

The variable τ_{thr} was already introduced as the actual produced thrust. The distinction between the desired τ_c and the actual τ_{thr} lies in the dynamical interaction between the thruster blades and the water. The same control signal will not always result in exactly the same thrust force. In the simulation model this is not taken into account, so in this case $\tau_{thr} = \mathbf{T}(\alpha)\mathbf{f} = \tau_c$.

For n DOF, the actuator configuration matrix $\mathbf{T}(\alpha) \in \mathbb{R}^{n \times r}$ holds one column vector $\mathbf{t}_i \in \mathbb{R}^n$ for each actuator. For the three dimensions of the horizontal plane holds:

$$\mathbf{t}_i = \begin{bmatrix} \cos \alpha_i \\ \sin \alpha_i \\ l_{x_i} \sin \alpha_i - l_{y_i} \cos \alpha_i \end{bmatrix} \quad (3-25)$$

where the moment arms are defined as $l_{x_i} = x_i - x_{iCoG}$ and $l_{y_i} = y_i - y_{iCoG}$ for each thruster.

The thrust allocation is modelled as a linear quadratic constrained control problem:

$$\begin{aligned} \min_{\mathbf{f}, \mathbf{s}} \quad & J = \mathbf{f}^\top \mathbf{W} \mathbf{f} + \mathbf{s}^\top \mathbf{Q} \mathbf{s} \\ \text{s.t.} \quad & \mathbf{T}(\alpha)\mathbf{f} = \tau_{PID} + \mathbf{s} \\ & \mathbf{f}_{\min} \leq \mathbf{f} \leq \mathbf{f}_{\max} \end{aligned} \quad (3-26)$$

where $\mathbf{s} \in \mathbb{R}^r$ is a vector of slack variables, introduced to let the problem remain solvable in case the control force \mathbf{f} needed to equal τ_{PID} exceeds \mathbf{f}_{\max} . Using the slack variables will result in the ships position deviating from the reference position. To keep this departure within a small limit, the weighting matrices should be chosen as $\mathbf{Q} \gg \mathbf{W} > \mathbf{0}$. Though later on in this thesis the ratio of these weights will be studied in order to lower the energy consumption of the vessel [8].

The thrust allocation is implemented in the simulation model as a separate Matlab function. The linear quadratic optimization problem is solved with the Matlab function `quadprog`.

For the supply vessel in the MSS a thruster lay-out is not specified. To define a lay-out and find appropriate thruster dimensions the Wind Farm Service Vessel, designed by Royal IHC, was used as a basis. This vessel is comparable with the vessel of the simulation model in size and purpose. The vessel of IHC has two azimuth thrusters (variable α) at the stern, one retractable azimuth thruster at the bow, and two tunnel thrusters (fixed α) at the bow. However, the thrust allocation optimization does not handle a matrix \mathbf{T} with a varying α . So

the vessel in the simulation model is equipped with two thrusters at the stern that are fixed at $\alpha = 0^\circ$, at 5 m port side and starboard of the Center of Gravity (CoG) of the vessel. At the bow three thrusters fixed at $\alpha = 90^\circ$ are used, at 24, 27 and 30 m from the CoG [11].

3-6 Energy Consumption

A simple model for the power consumption of a thrusters is given by de Wit [4]:

$$P(f) = (P_{max} - P_{min}) \left(\frac{|f|}{f_{max}} \right)^\eta + P_{min} \quad (3-27)$$

where P is the power in kW, f is the thrust force in kN and η usually lies between 1.3 and 1.7.

To be able to include the power consumption into the thrust allocation model an approximation can be made with a quadratic function using the least squares method:

$$P_i(f) \approx w_i f_i^2 + c_i \quad (3-28)$$

Where w_i and c_i are constant values modelling the behaviour of the i -th thruster.

As the constant term c_i will not have any influence on an optimization procedure, the power consumption can be included in the thrust allocation by scaling the weights of the matrix \mathbf{W} relative to each other to reflect the thruster specifications contained in the parameter w_i for the different thrusters.

Note that (3-28) is only needed to find \mathbf{W} for the thrust allocation algorithm. After the different thrust forces are calculated for the current time step, the (3-27) can be used to calculate the power consumption for the simulated vessel operation.

3-7 Conclusion

In this chapter the development of the Dynamic Positioning Vessel Simulation Model was discussed. The Simulink model includes the simulation of a supply vessel with a conventional DP system as found in the literature. The DP system consists of a PID controller, an observer that performs wave filtering, and a thrust allocation algorithm. The vessel is subjected to LF and HF disturbance. The HF disturbance is modelled as a displacement instead of a force, which is less realistic, but this method provides a better insight into the controller performance.

Furthermore a model for the energy consumption of the thrusters is added. Later on a number of adjustments will be suggested to reduce the energy consumption of the vessel. The adjustments will be included in the Simulink model and simulations will be run, where the models as has been described in this chapter will serve as the base case.

Chapter 4

Motion Compensation System Simulation Model

In 1965 a paper was published by D. Stewart, titled “A Platform with Six Degrees of Freedom”. This platform described in the paper was meant to be used as an aircraft cockpit simulator and is still called the Stewart Platform. The structure consists of a base and a platform, connected by six arms with adjustable length, shown in Figure 4-1 [2]. Traditionally these are hydraulic cylinders because of the high force they can exert. Recently the use of linear electromechanical actuators, making the system faster and cheaper and requiring less space, has been studied by Thöndel [21]. In 2007 a patent was filed for using a Stewart Platform to compensate for motions of a vessel with a gangway to transfer personnel and/or load, later brought to the market as the Ampelmann system [23].

The Ampelmann is certainly not the only motion compensation system used in the offshore industry, but unique about it is the ability to compensate all six Degrees of Freedom (DOF), and its objective to keep the gangway completely motionless. Crane foundation systems exist compensating mainly heave, pitch and roll, because the ship already has a Dynamic Positioning (DP) system for surge, sway and yaw. For transfer of personnel the positioning of the ship would not be accurate enough but for most crane operations it suffices. Other gangway systems use hinging elements. Part of the motions of the waves are compensated by movement of the gangway.

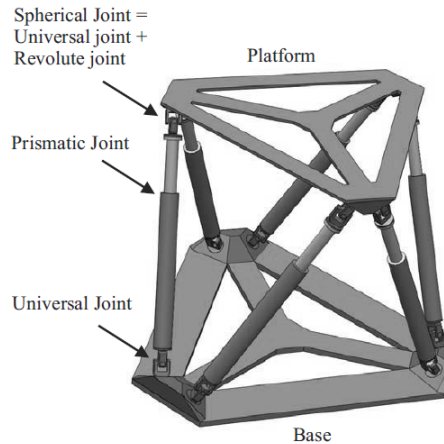


Figure 4-1: The Stewart Platform.

A good model of a Stewart Platform is provided at the Mathworks file exchange by Jeff Wendlandt [20]. The model is built in the Simscape Multibody environment. This Matlab module provides a simulation environment for 3D mechanical systems. It allows to create complicated models with building blocks of different types of actuators, sensors, joints and more. The Stewart Platform model consists of a reference signal generator, a process plant model and a Proportional Integral Derivative (PID) controller.

4-1 Reference Signal Generator

In reality the motion compensation system would use its own motion sensor, sensing the accelerations of the base platform, to define a reference path for the position of the top platform in six DOF. However in the simulation, this is modelled differently to allow a simple connection between the two models.

The DP Vessel Simulation Model is connected to the Motion Compensation System Simulation Model via the reference signal generator. For simplicity it is assumed the motion compensation system is placed at the Center of Gravity (CoG) of the vessel. The real displacements in the vessel simulation, $\eta_{tot} = \eta_{LF} + \eta_{HF}$, multiplied by -1 are used as the surge, sway and yaw reference position of the platform. For the other three DOF (pitch, roll and heave) the same wave spectrum model is used as for the High-Frequency (HF) disturbance of the vessel, though the roll and the pitch have a phase lag of 0.5π rad on the other signals. It is expected that the heave will be in phase with the surge and sway, but the roll and pitch will be zero at the top and bottom dead centres of the heave motion and will be maximal in between. The amplitudes are scaled for the different DOF, but the fluctuation is relatively the same with respect to time. A large wave will lead to large translations and rotations and a small wave will induce small translations and rotations.

In the reference signal generator the desired platform position and orientation is translated into desired leg lengths with the use of some kinematics. As well as the vessel models, the Stewart Platform model is also expressed in Cartesian coordinates using the Newton-Euler

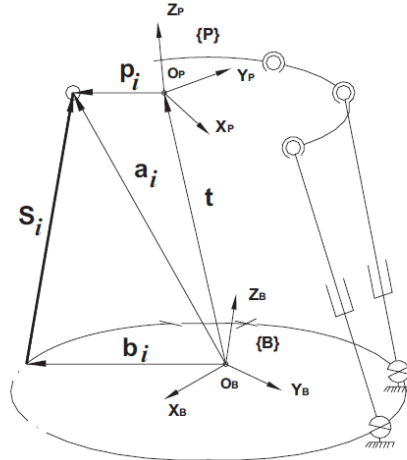


Figure 4-2: A schematic view of the Stewart Platform.

approach. The position and orientation of the center of the moving platform are represented by q , defined as:

$$\mathbf{q} = \begin{bmatrix} \mathbf{t}^\top & \boldsymbol{\Theta}^\top \end{bmatrix}^\top \quad (4-1)$$

with

$$\mathbf{t} = [x \ y \ z]^\top \quad (4-2)$$

$$\boldsymbol{\Theta} = [\phi \ \theta \ \psi]^\top \quad (4-3)$$

The *inverse kinematics* equation is used to compute the leg lengths for a desired position and orientation of the platform. The leg lengths are the norms of the leg vectors:

$$\mathbf{S}_i = \mathbf{R}(\boldsymbol{\Theta})\mathbf{p}_i + \mathbf{t} - \mathbf{b}_i \quad (4-4)$$

A schematic view of this is given in Figure 4-2 [2]. \mathbf{S}_i is the leg vector of the i -th leg ($i = 1, 2, \dots, 6$), \mathbf{p}_i is the position vector of the i -th platform joint seen from the center of the platform O_P , \mathbf{b}_i is the position vector of the i -th base point seen from the center of the base O_B , and $\mathbf{R}(\boldsymbol{\Theta})$ is the rotation matrix of the platform frame $\{\mathbf{P}\}$ relative to the base frame $\{\mathbf{B}\}$ defined the same as the rotation matrix for vessel modelling given in (2-9):

$$\mathbf{R}(\boldsymbol{\Theta}) = \begin{bmatrix} \cos \psi \cos \theta & -\sin \psi \cos \phi + \cos \psi \sin \theta \sin \phi & \sin \psi \sin \phi + \cos \psi \cos \phi \sin \theta \\ \sin \psi \cos \theta & \cos \psi \cos \phi + \sin \phi \sin \theta \sin \psi & -\cos \psi \sin \phi + \sin \theta \sin \psi \cos \phi \\ -\sin \theta & \cos \theta \sin \phi & \cos \theta \cos \phi \end{bmatrix} \quad (4-5)$$

4-2 Process Plant Model

The dynamics of the Stewart Platform could be described as:

$$\mathbf{M}(\mathbf{q})\ddot{\mathbf{q}} + \mathbf{C}(\mathbf{q}, \dot{\mathbf{q}})\dot{\mathbf{q}} + \mathbf{G}(\mathbf{q}) = \boldsymbol{\tau} = \mathbf{J}^T(\mathbf{q})\mathbf{u} \quad (4-6)$$

where $\mathbf{M}(\mathbf{q})$ is the inertia matrix, $\mathbf{C}(\mathbf{q}, \dot{\mathbf{q}})$ contains the coriolis and centripetal forces, $\mathbf{G}(\mathbf{q})$ is the gravitational force, $\mathbf{J}(\mathbf{q})$ is the Jacobian matrix, and $\boldsymbol{\tau}$ and \mathbf{u} are the generalized and actuation forces respectively [10]. However, in Simscape Multibody the platform model is built with several system components, all with their own underlying (differential) equations.

Rigid bodies are used for the top plate, base plate, and upper and lower legs. The upper and lower leg are connected to each other via a cylindrical joint block, which allows the entire leg to adjust its length by moving in one translational and one rotational degree of freedom. The top en lower leg are connected to the top and base plate with universal joint blocks, allowing rotations but no translational motion.

The cylindrical joint in between the upper and lower leg is connected to actuator and sensor blocks. The actuator block receives the control signal from the PID controller and translates this to the force applied between the legs. The sensor block extracts the position and velocity, and these signals will be led back to the controller.

An m-file is used for the initialisation of the model, in which the geometry of the connection points of the legs and the plates is defined. The dimensions of the simulated motion compensation system are based on the parameters that were found in the Ampelmann Demonstrator model documentation. This demonstrator model is designed to be able to compensate up to $H_s = 2 \text{ m}$ on a 50 m vessel. Important design parameters are the radius's of the two platforms R_t and R_b , the spacing between a pair of gimbals, defined by s_b and s_t and shown in Figure 4-3, and the cylinders stroke and dead lengths. The dead length of a cylinder is defined as the minimum cylinder length (gimbal to gimbal) minus the stroke length, depicted in Figure 4-4. An overview of these parameters is given in Table 4-1 and a full parametrization of the Motion Compensation System Simulation model can be found in Appendix B [24, 20].

Table 4-1: Motion compensation system design parameters.

Parameter	Value
Radius top platform	$R_t = 2.75 \text{ m}$
Radius base platform	$R_b = 3.00 \text{ m}$
Half separation top gimbal pairs	$s_t = 0.25 \text{ m}$
Half separation base gimbal pairs	$s_b = 0.25 \text{ m}$
Cylinder minimum length	$l_{min} = 3.25 \text{ m}$
Cylinder stroke length	$l_{stroke} = 2.00 \text{ m}$
Cylinder dead length	$l_{dead} = 1.25 \text{ m}$

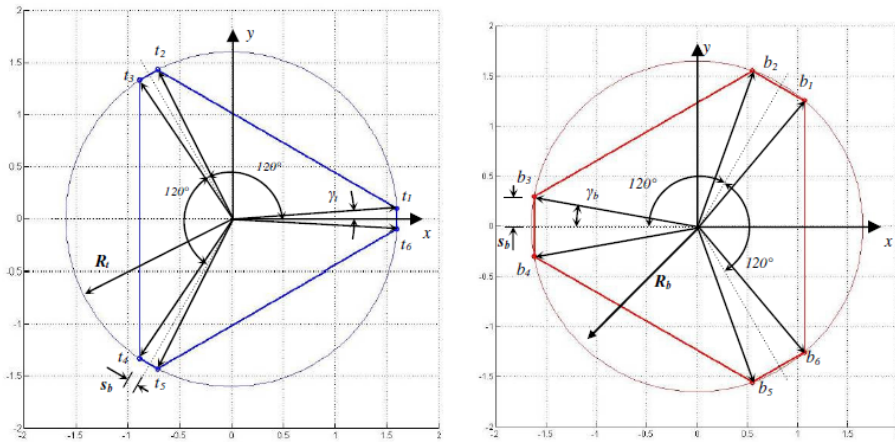


Figure 4-3: Top and base platform lay-out.



Figure 4-4: Cylinder minimum length and stroke length.

4-3 Controller Structure

In the Stewart Platform model from Mathworks it is possible to use a PID controller or an H_∞ controller. For this research the continuous time PID controller is chosen:

$$F_{PID,i} = K_p E_i + K_i \int_0^t E_i dt - K_d (dE_i/dt) \quad (4-7)$$

where $F_{PID,i}$ is the computed control force, and E_i is the desired leg length \mathbf{S}_i , given by the reference signal generator, minus the actual leg length that is measured by the sensor block, both for the i -th leg. So if E_i is positive the leg is too short and the positive control force $F_{PID,i}$ makes the leg expand [20].

4-4 Energy Consumption

A model for the average energy consumption of a Stewart Platform with hydraulic cylinders, Ψ_v , is given by Cleasby[3]:

$$\Psi_v = \frac{1}{\eta_v} (Q_{av} P_s + \Psi_r) + \Psi_l \quad (4-8)$$

where η_v is the electric motor/pump efficiency, Q_{av} is the average absolute volumetric flow for all six cylinders, P_s is the supply pressure of the Hydraulic Power Unit (HPU), Ψ_r is power loss through the relief valve, and Ψ_l is water pump and leakage related power loss.

From this average power consumption the time dependent power consumption, $\Psi(t)$, can be deducted. The efficiency and the loss factors are given by Cleasby as constant values, and for steady operation the HPU pressure needs to be kept constant. So the required power fluctuates parallel to the absolute volumetric flow, in order to keep P_s constant. This results in:

$$\Psi(t) = \frac{1}{\eta_v} (Q_{av}(t)P_s + \Psi_r) + \Psi_l \quad (4-9)$$

The volumetric flow rate fully depends on the cylinder stroke velocities and the cylinder surfaces, depicted in Figure 4-5:

$$q(t) = A_1 v_j(t) \quad \text{for } v_j(t) \geq 0 \quad (4-10)$$

$$q(t) = A_2 v_j(t) \quad \text{for } v_j(t) < 0 \quad (4-11)$$

where q is the flow rate of one cylinder and v_j is the cylinder velocity.

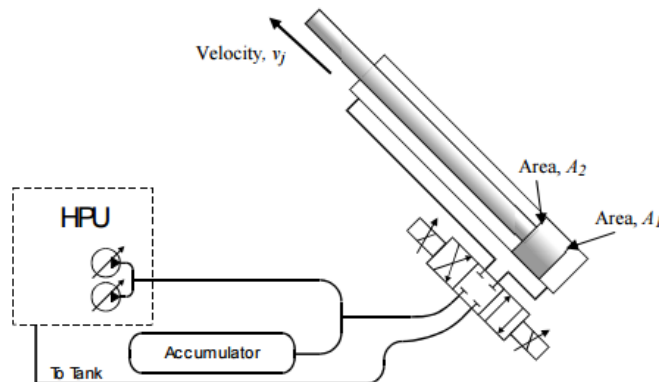


Figure 4-5: Cylinder velocity and surfaces.

The power consumption depends on the absolute volumetric flow, because power is needed for expansion as well as retraction of the cylinders. It can be assumed that the wave pattern of the cylinder velocities is symmetrical in the up and down strokes, so the average of the areas A_1 and A_2 can be used, and as all six cylinders have the same dimensions the average of the different absolute velocities can be used:

$$\Psi(t) = \frac{1}{\eta_v} \left(\frac{A_1 + A_2}{2} \cdot 6 \cdot |v_j(t)|_{avg} \cdot P_s + \Psi_r \right) + \Psi_l \quad (4-12)$$

4-5 Conclusion

In addition to the Dynamic Positioning Vessel Simulation Model, also a simulator of a motion compensation system was built. The two simulators are connected via the reference signal generator of the latter. The real vessel displacement multiplied by minus one is the input for the motion compensation system.

As a basis for the Motion Compensation System Simulation Model, a Simulink model of the Stewart Platform is used. The model parameters are adjusted to match the Ampelmann Demonstrator model, which is designed to compensate for wave motions on a 50 m vessel up to a significant wave height of $H_s = 2.0 \text{ m}$.

Also for the motion compensation platform the energy consumption is modelled. The methods that will be used to reduce the energy consumption of the vessel should not result in an increase in the energy consumption of the platform that is larger. So after performing a case study, as will be discussed in Chapter 6, the summed energy consumption will be assessed.

Chapter 5

Energy Reduction Strategies

As was seen in Section 3-4 the observer of the Dynamic Positioning (DP) Vessel Simulation Model can estimate the position of the vessel with an estimation error of approximately 0.05 m . A significant inefficiency might be the reaction of the controller to a too high estimated position error, resulting in constant overcompensation. If the estimation error of the observer is seen as a given, it could be more efficient to have a controller that accepts it if the vessel has a small displacement from the reference point. After all, the tracking of a constant reference is merely a consequence of using Proportional Integral Derivative (PID) control, while the objective of the vessel control should be to stay within a circle with a certain radius. Multiple different methods that could possibly reduce the influence of the estimation error on the control signal of the DP system are introduced in this chapter. The main focus lies on making a trade-off between vessel displacement and thrust forces. But first another possibility is looked into, namely the use of Dead Reckoning (DR), the vessel position is estimated to be the integrated vessel velocity.

5-1 Adjustments of the standard DP controller

5-1-1 Dead Reckoning

In Section 3-4 it was shown that the estimation of the Low-Frequency (LF) vessel position, $\hat{\eta}_{LF}$, loses its relevance if the vessel displacements are smaller than 0.1 m . However, the estimation of the velocity, $\hat{\nu}$, is much more accurate. The position of the vessel can of course also be calculated by integrating the velocity over time. This is a form of DR; the position of the vessel is based on the position in the former time step. A downside of this method is the error accumulation. But if the mean error stays smaller than the original position estimation error, an improvement could be made with this method.

For the integration the Forward Euler method is used:

$$\hat{\eta}_{LF}(k) = \hat{\eta}_{LF}(k-1) + K[t(k) - t(k-1)]\hat{\nu} \quad (5-1)$$

5-1-2 Reference Circle

In Section 3-2 a conventional DP controller was given, which is a standard PID controller. The tracking of a constant reference point is merely a consequence of using PID control, while the objective should be to stay within a circle with a certain radius, so that the motion compensation system can cover the remaining vessel motions. So a second approach to improve the DP system is to change the reference point of the PID controller into a reference circle. The LF position estimation of the observer is used to calculate the displacement of the vessel in the xy-plane. Only the part of the displacement outside of the reference circle is seen as the position error, which is used as the input for the PID controller. This is shown graphically in Figure 5-1.

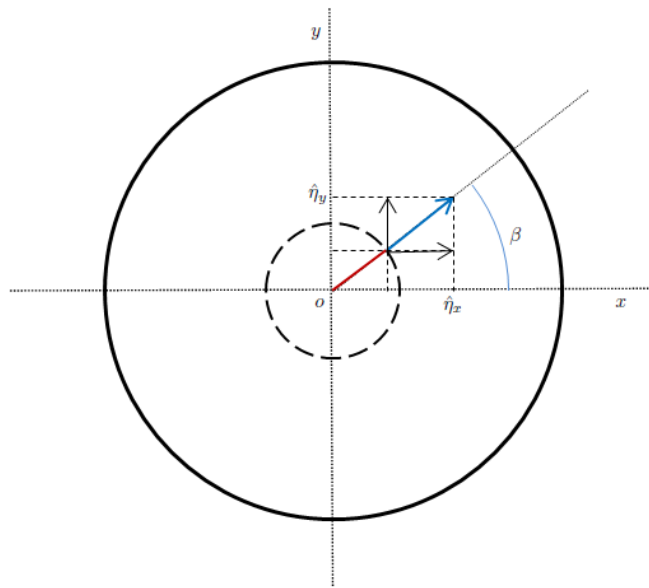


Figure 5-1: PID reference circle

The radius of the outer circle is the maximum allowed LF two dimensional vessel displacement d_{max} . The inner circle is the reference circle with radius r_{ref} , the red part of the arrow. The red and blue part of the arrow together equal the total LF vessel displacement, $d_{tot} = \sqrt{\hat{\eta}_x^2 + \hat{\eta}_y^2}$. Only the distance between the vessel and the reference circle, the blue part of the arrow, is the displacement that needs to be compensated for, it is denoted by d_{error} , with $d_{error} = d_{tot} - r_{ref}$. The angle between the displacement direction and the x -axis can easily be found; $\beta = \arctan(|\hat{\eta}_y|/|\hat{\eta}_x|)$.

The black arrows are the new PID controller inputs for the x and y -direction, d_x and d_y . They are derived from d_{error} and β . The values are always calculated in the first quadrant, and then given the right signs, corresponding to the signs of $\hat{\eta}_x$ and $\hat{\eta}_y$. A decision variable j is used to make the PID input signal zero if the vessel is inside of the reference circle.

The control input for the yaw direction will not be changed.

Summarizing, the new controller inputs are calculated with the following formulas:

$$d_{tot} = \sqrt{\hat{\eta}_x^2 + \hat{\eta}_y^2} \quad (5-2)$$

$$d_{error} = d_{tot} - r_{ref} \quad (5-3)$$

$$\beta = \arctan(|\hat{\eta}_y|/|\hat{\eta}_x|) \quad (5-4)$$

$$j = \begin{cases} 1 & \text{for } d_{tot} \geq r_{ref} \\ 0 & \text{for } d_{tot} < r_{ref} \end{cases} \quad (5-5)$$

$$d_x = \text{sign}(\hat{\eta}_x) \cdot d_{error} \cdot \cos(\beta) \cdot j \quad (5-6)$$

$$d_y = \text{sign}(\hat{\eta}_y) \cdot d_{error} \cdot \sin(\beta) \cdot j \quad (5-7)$$

The value for the radius of the reference circle, r_{ref} , will be varied to find how much energy reduction could be realised with this method.

5-1-3 Thrust Allocation Tuning

In Section 3-5 the standard thrust allocation system was explained. Recall, the DP controller computes a generalized force vector τ_{PID} to be applied to the vessel, containing forces in x and y -direction and a yaw-moment. The thrust allocation system determines for each individual thruster what force it should exert to approximately match the generalized force vector. An optimization algorithm is used to solve the linear quadratic objective function, defined as:

$$\begin{aligned} \min_{\mathbf{f}, \mathbf{s}} \quad & J = \mathbf{f}^\top \mathbf{W} \mathbf{f} + \mathbf{s}^\top \mathbf{Q} \mathbf{s} \\ \text{s.t.} \quad & \mathbf{T}(\boldsymbol{\alpha}) \mathbf{f} = \tau_{PID} + \mathbf{s} \\ & \mathbf{f}_{\min} \leq \mathbf{f} \leq \mathbf{f}_{\max} \end{aligned} \quad (5-8)$$

The objective contains the thrust forces \mathbf{f} and a slack vector \mathbf{s} , representing the extent to which the desired thrust τ_c can differ from the required thrust τ_{PID} . The weighting matrices should be chosen as $\mathbf{Q} \gg \mathbf{W} > \mathbf{0}$ to have optimal reference tracking [8].

Although literature states that the weight of the slack variable should be much larger than the weight of the thrust forces, lowering the weight of the slack will probably result in a larger maximum displacement of the vessel but at the same time lower thrust forces. So the proportional relationship between \mathbf{Q} and \mathbf{W} can be used to tune the possible energy reduction. For tuning the parameter c_{alloc} is introduced, which scales the order of magnitude of \mathbf{Q} with respect to \mathbf{W} :

$$\mathbf{Q} = c_{alloc} \cdot \begin{bmatrix} Q_1 & 0 & 0 \\ 0 & Q_2 & 0 \\ 0 & 0 & Q_3 \end{bmatrix} \quad (5-9)$$

Note that defining $c_{alloc} = \mathbf{W}/\mathbf{Q}$ would be incorrect as the matrices have different dimensions.

c_{alloc} will be varied between 1 and 10,000. The latter seems like an extremely high value, but this comes forth from the forces having a maximum value up to 180,000 Newton. The high c_{alloc} is used to represent the conventional DP controller where the slack is only used if the needed forces exceed the thruster limitations. In the case study in the next chapter this will be referred to as the base case.

For lower values of c_{alloc} the difference between τ_c and τ_{PID} will become larger, but \mathbf{f} can be lower. For $c_{alloc} = 1$ \mathbf{Q} and \mathbf{W} will have the same order of magnitude, so $\mathbf{Q} \gg \mathbf{W}$ no longer holds, but as will be seen in the case study acceptable vessel behaviour will still be achieved.

5-2 Model Predictive Control

A number of less conventional control methods were evaluated in the literature survey, like Integrator Backstepping, Sliding-Mode Control, Passivity-Based Control and Model Predictive Control (MPC). The latter seems to be promising for this research because making a trade-off between state values and control forces is inherent in this control method. Multiple publications were found on using MPC for a DP control system, but in all of them only the reference tracking capabilities were studied and the energy consumption was not elaborated upon. The new insight that is aimed for in this research is the possibility to use MPC to minimize the energy consumption of the vessel.

The LF position estimation is still used as an input signal for the MPC controller, so the estimation error will still have a negative influence. But the algorithm also considers predictions of the future states and disturbances of the system and here the High-Frequency (HF) disturbance does not play a role. So in total it is expected that the effect of the estimation error on the reaction of the vessel will be smaller.

In this section it is shown how the the DP control problem is implemented as an MPC problem. Two different optimization programs are used.

An MPC controller was built in Matlab because the simulation models of the vessel and the motion compensation system are modelled in Simulink. The Standard Predictive Control Toolbox of Van den Boom is used for this.

Next to this, also AMPL was used to develop a controller. This program offers a language especially to describe optimization problems. With the AMPL syntax the user can define the model in the same way that people think about them, allowing fast and reliable modelling. The model is then translated into a code that can be read by a solver. Many different solvers can be chosen to solve the problem, for instance MINOS, CPLEX and Gurobi. Furthermore it is expected that AMPL needs a shorter computation time to solve the same optimization problem [1].

The MPC problem definition MPC does not come down to a single technique, but could be seen as a methodology. The control problem can be translated into a mathematical formulation in different ways, but the base of the design procedure always consists of the following

five items:

- Process model and disturbance model
- Performance index
- Optimization
- Constraints
- Receding horizon principle

An MPC controller uses the process and disturbance models to predict the behaviour of the system for certain control inputs, extrapolated from the known former and current system states. The number of time steps that the controller looks into the future is predefined. A performance index is formulated consisting of two or more terms, of which the first contains the reference tracking error and the second contains the control inputs. To compare these terms they are translated into operation costs, by taking the norms of the signals and multiplying them with weight factors to make them dimensionless. Then an optimization procedure is used to find the control inputs that minimize the performance index, and thus the operation costs, while satisfying all constraints. The controller calculates control inputs for the defined number of time steps ahead, but only the value for one time step ahead is used. As the process and disturbance models are not a perfect representation of the system the new states will be different from the predicted ones. So the optimization is done again for every time step, which is known as the receding horizon principle [22].

As will be seen later in this subsection the MPC controller not only replaces the PID controller, but also includes the thrust allocation. The block scheme of the DP control system that was given in the introduction of Chapter 3 changes into the scheme shown in figure 5-2.

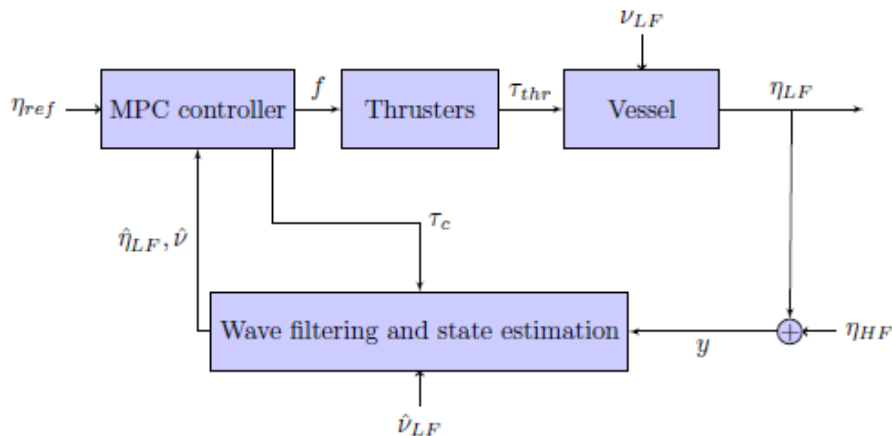


Figure 5-2: A block scheme of an MPC DP control system.

5-2-1 Matlab implementation

The Standard Predictive Control Toolbox of Van den Boom is used to construct an MPC controller in Matlab [22]. From the toolbox the function `1qpc` can be used to solve the Linear Quadratic Predictive Control problem for a state space system. An overview of the Matlab codes is given in Appendix C.

Process and disturbance model To predict the future system states the `1qpc` function requires the process and disturbance model of the vessel to be formulated in the following state space form:

$$x(k+1) = A_0x(k) + K_0e_0(k) + L_0d_0(k) + B_0u(k) \quad (5-10)$$

$$y(k) = C_0x(k) + D_He_0(k) + D_Fd_0(k) \quad (5-11)$$

A_0 and L_0 model the influence of the current state $x(k)$ and the known disturbance $d_0(k)$ on the new state $x(k+1)$. To find the matrices the LF process plant model, given in Section 3-3, needs to be translated into state space form, linearised around $\psi = 0$, and then discretised. The matrices K_0 and D_H model the influence of measurement noise. They do not need to be defined because a noiseless case is considered, so $e_0(k) = 0$ and K_0 and D_H can be anything. It is chosen to define C_0 to be an Identity matrix to leave open the possibility to study all the predicted states, which are the LF vessel displacements and velocities, but actually $y(k)$ will not be used. Only the control signal $u(k)$ will be of interest.

D_F is zero as the LF disturbance has no influence on the measurement equation.

B_0 models the influence of the control signal $u(k)$ on the system states (the LF vessel displacements and velocities). Because $u(k)$ will be optimized with respect to the system states in the performance index, (5-16), it is desired that $u(k)$ is a vector representing the thrust forces \mathbf{f} . So the thrust allocation needs to be incorporated into the matrix B_0 .

Let B_{disc} be the matrix modelling the influence of the generalized force vector $\boldsymbol{\tau}_c$ on the vessel, found from the discretised process plant:

$$x(k+1) = A_0x(k) + \dots + B_{disc}\boldsymbol{\tau}_c \quad (5-12)$$

Recall from the thrust allocation algorithm given in section 3-5:

$$\boldsymbol{\tau}_c = \mathbf{T}(\boldsymbol{\alpha})\mathbf{f} \quad (5-13)$$

As $\mathbf{T}(\boldsymbol{\alpha})$ is a constant matrix it can be included into B_0 :

$$u(k) = \mathbf{f} \quad (5-14)$$

$$B_0 = B_{disc}\mathbf{T}(\boldsymbol{\alpha}) \quad (5-15)$$

Note that the slack variable is not needed any more because where $\boldsymbol{\tau}_{PID}$ was a given value that needed to be equalled by $\mathbf{T}(\boldsymbol{\alpha})\mathbf{f} - \mathbf{s}$, see (5-8), here there is no such restriction. The vector \mathbf{f} will be optimized with respect to vessel position directly, without $\boldsymbol{\tau}_{PID}$ in between.

Performance Index The performance index that will be optimized is given by:

$$\min_{\mathbf{u}(k)} J(\mathbf{u}, k) = \sum_{j=N_m}^N \hat{\mathbf{x}}(k+j)^\top \mathbf{Q} \hat{\mathbf{x}}(k+j) + \sum_{j=1}^N \mathbf{u}(k+j-1)^\top \mathbf{W} \mathbf{u}(k+j-1) \quad (5-16)$$

The minimum cost horizon and the prediction horizon, N_m and N , can be tuned to improve the performance of the controller. But especially the weight matrices \mathbf{Q} and \mathbf{W} can be used to make a trade off between the displacement of the vessel and the thrust power needed for this.

Again \mathbf{Q} and \mathbf{W} can be used to tune the possible energy reduction. And \mathbf{Q} is defined in the same way as for the thrust allocation, given in (5-9). However, in the case of the thrust allocation \mathbf{Q} weighs the slack, and in the MPC controller the actual displacements are considered, so the values of c_{alloc} are different. For the MPC controller c_{alloc} will be varied between 50 and 5,000,000. The high value of c_{alloc} can be explained by the big difference in order of magnitude between the allowed thrust forces (up to 180,000 N) and the desired LF vessel displacement ($\ll 1 \text{ m}$).

Constraints As in the thrust allocation algorithm, also here the maximum thrust power can be constrained to incorporate the limitations of the thrusters in the model. The `1qpc` function does not allow different lower and upper limits, $u_{min} = -u_{max}$, but a vector can be used to give every thruster a different limit:

$$|\mathbf{u}(k+j)| \leq \mathbf{u}_{max} \quad (5-17)$$

Receding horizon principle To include the MPC controller into the Vessel Simulation Model the `1qpc` function is invoked from Simulink. The function has a built-in receding horizon principle, but this is not used. The prediction horizon is the same as the total length of the simulation interval of the function. In Simulink only the controller values for the first time step are used and then the `1qpc` function is invoked again. A prediction horizon of $N = 15$ will be used. By trial and error it was found that this value gives good results without a very long computation time [22].

5-2-2 AMPL implementation

Next to Matlab, also AMPL was used to develop an MPC controller. In this program it is aimed to let the syntax coincide as much as possible with the way people think about optimization problems [1]. The MPC controller codes are written in Notepad and are given in Appendix D.

Sets and indexes Unlike Matlab, AMPL does not work with matrices and vectors, but with sets and indexes. First sets must be defined, which can consist of numbers but also of non numericals. Next, variables can be declared that are indexed over one or multiple sets. An

advantage of this method is that values can be assigned to a certain variable in an infinite number of dimensions.

For the DP control problem two sets are used, both representing a time vector. One set goes from 1 to N and is used to index the control forces. The other goes from 0 to N , indexing the system states $\hat{\eta}_{LF}$ and \hat{v} that will be predicted. The states $s_i[0]$ are the current estimated system states from the observer of the Vessel Simulation Model. They are the initial values for the prediction of the future states. N is the prediction horizon.

Performance Index To get comparable results the performance index is defined to get mathematically seen the same optimization problem as in the Matlab MPC controller, given in (5-16). However, it will be formulated and solved in different ways.

In the AMPL code, see Listing D.2, the term objective function is used instead of performance index, and the weights are named $W1$ and $W2$, but they are equal to \mathbf{W} and \mathbf{Q} respectively, exactly as in the Matlab MPC controller.

Constraints In AMPL constraints can be defined as recursive equations. For the MPC controller the process and disturbance model, used to predict the future system states, are implemented as a number of constraints that the states and control forces need to satisfy.

Furthermore, variables can be constrained right away at their declaration, so the thruster limitations can be included in the optimization very easily.

Optimization To solve the optimization problem the user can choose many different solvers. For the DP MPC controller MINOS is selected, because this solver can handle non-linear constraints. AMPL translates the code given in Listing D.2 into a structure that can be read by the solver, and the output of the solver is again translated by AMPL in a way that is easy interpretable also for the less experienced user [1].

To implement the controller into the Vessel Simulation Model an Application Programming Interface (API) is used. This enables to invoke AMPL within Matlab, so the MPC model can be used in the same way as the `lqpc` function.

5-3 Conclusion on Energy Reduction Strategies

In this chapter a number of control methods were proposed, all aiming to minimize the reaction of the controller to a too high estimated position error. For all methods except the Dead Reckoning this aim coheres with making a trade-off between vessel displacement and energy consumption.

The proposed strategies are:

- using the integrated velocity as an estimation of the position of the vessel;

- the use of a reference circle instead of a reference point, where the radius of this circle, r_{ref} , is used to execute the trade-off;
- the tuning of the thrust allocation optimization, where the objective function parameter, c_{alloc} , is used to execute the trade-off;
- the use of MPC, also with the objective function parameter c_{alloc} to execute the trade-off.

For the MPC method two different software programs will be used to build the controller. Mathematically the same optimization problem will be implemented, but it will be formulated and solved in different ways.

Chapter 6

Case Study

In the previous chapter four strategies were proposed to reduce the amount of energy used by a vessel for Dynamic Positioning (DP), of which three are based on making a trade-off between displacement and thrust forces. To evaluate the proposed strategies a case study is performed, which will be discussed in this chapter.

First a simulation scenario must be defined. For this, all parameters and other input data for the simulation models and controllers must be determined. Then some hard requirements are formulated, which all solutions must meet. And lastly all feasible solutions will be compared to find the most promising energy reduction strategy.

6-1 Input Data

To define a simulation scenario all parameters of the models need to be determined.

Motion Compensation System Simulation Model The most important dimensions of the simulated motion compensation platform were already given in Chapter 4, and the full parametrization is given in Appendix B. As a basis the Ampelmann Demonstrator was used. This system must minimally be able to operate on a 50 m vessel with a significant wave height of $H_s \leq 2.0$ m. This corresponds to the wave conditions occurring 85% of the time off the Dutch coast [24]. The Proportional Integral Derivative (PID) controller is tuned by trial and error, and the model runs with a fixed step size of $h = 0.01$ s.

Vessel Simulation Model The full parametrization of the DP Vessel Simulation Model can be found in Appendix A. The Process Plant matrices are given in the Marine Systems Simulator (MSS), and the PID controller is tuned by trial and error for the case where no thrust allocation is used (the control force applied to the vessel is exactly the needed force calculated by the PID controller). The observer and controllers are discrete with a step size

of $h = 0.2 \text{ s}$. The vessel control plant model is continuous with a fixed step size fundamental sample time of $h = 0.01 \text{ s}$.

The environmental conditions of the DP vessel are captured in the disturbance terms. In the simulation model the wave peak frequency is left as it is in the MSS, $\omega_0 = 0.8$, but the wave height is scaled to have $H_s = 2.0 \text{ m}$. A mean wave direction of 40° was chosen arbitrarily.

A mean Low-Frequency (LF) disturbance velocity of 0.18 m/s was chosen, comparable to the value found in the research of Liu [12]. Liu also defines an angle for the mean disturbance direction. For DP vessels in transit mode it occurs that the direction in which the ship sails is not the same as the disturbance direction. For vessels in station-keeping mode it is usual to turn the bow towards the mean current and wind direction. To be thorough both situations are taken into account, resulting in two simulation scenarios. The first with an LF disturbance direction of 0° and the second with 35° .

The thruster specifications are based on the Wind Farm Service Vessel of IHC [11].

6-2 Requirements and Preferences

Except for the Dead Reckoning strategy, all other proposed controllers have a variable that needs to be tuned to find the maximum possible energy reduction. To select which solutions are feasible and which are not, some hard requirements are defined.

Maximum vessel displacement Filtering the measurements to make a distinction between the current LF and High-Frequency (HF) motion is one thing, but predicting what the future holds will be even more difficult. Research has been done on this subject, but in this thesis this will not be included.

In this thesis it is assumed that, based on existing sea state models, a reliable value can be determined of the maximum HF disturbance that is expected, $d_{HF,max}$. However, when the maximum HF disturbance will occur is unknown. So the first requirement for the controllers is that, irrespectively of the position or velocity of the vessel, the absolute LF displacement, d_{tot} , must always be smaller than a certain value $d_{LF,max}$, so that even with the largest expected HF displacement the vessel still stays within the workspace of the motion compensation system. This workspace is defined as a circle with radius $d_{MCS,max}$:

$$d_{LF,max} + d_{HF,max} \leq d_{MCS,max} \quad (6-1)$$

$$d_{tot} \leq d_{LF,max} \quad (6-2)$$

$$d_{tot} = \sqrt{\eta_{LF,x}^2 + \eta_{LF,y}^2} \quad (6-3)$$

$d_{MCS,max}$ is based on the values of the Ampelmann Demonstrator given in Appendix B. The motion compensation platform is able to compensate for 3.63 m in the x-direction and for 3.31 m in the y-direction. To be conservative it is assumed that if the x and y direction need to be compensated at the same time, in both directions only 1.5 m can be reached, which gives an absolute distance of $d_{MCS,max} = 2.12 \text{ m}$.

From the simulation scenario it is known that the maximum HF displacement is $d_{HF,max} = 1.43 \text{ m}$. So strictly speaking for the LF displacement holds $d_{LF,max} = d_{MCS,max} - d_{HF,max} = 0.69 \text{ m}$. To incorporate another safety margin a value of $d_{LF,max} = 0.50 \text{ m}$ will be used.

Maximum residual platform motion In Chapter 1 the assumption was made that, as long as the vessel stays within the workspace of the motion compensation system, the latter is always able to keep the gangway motionless up to an accepted residual motion.

In the simulation model the input of the motion compensation system is the real total vessel displacement in the horizontal plane, and matching references for the other three Degrees of Freedom (DOF) are generated. An output of the Motion Compensation System Simulation Model that can be used is the position of the top platform in surge sway and heave. As the input of the reference signal generator (described in Section 4-1) is supposedly the real vessel position, and the output is the real platform position, the residual of the one minus the other can be seen as the motion of the platform as experienced by a person standing on the platform. For x_{res} , y_{res} and z_{res} a maximum value of 0.05 m is yielded.

Preferences Next to the hard constraints, the controller performance can be evaluated on some other aspects that are not directly quantifiable.

First of all, the motion of the vessel and the motion compensation platform should be smooth for the comfort of the personnel using it.

Also the thrust forces should not be varying too rapidly, because this would cause wear and tear of the equipment of the vessel.

Furthermore, the computation time could be taken into account when evaluating the controllers. Especially for Model Predictive Control (MPC) this is often an issue. The controllers do not necessarily need to be able to solve the problem in real time, but the computation time should be somewhere in the same order of magnitude.

And lastly, the robustness of the controllers was not a focus point in the previous part, but it could still be taken into consideration in evaluating them by looking at how the process noise is reflected in the simulation results.

Summary Summarizing the content of this section, the hard requirements that every controller should meet are:

$$d_{tot} \leq 0.5 \quad (6-4)$$

$$x_{res} \leq 0.05 \quad (6-5)$$

$$y_{res} \leq 0.05 \quad (6-6)$$

$$z_{res} \leq 0.05 \quad (6-7)$$

Furthermore, it is preferred that:

- the vessel and the platform have smooth motions;
- the thrust forces do not vary rapidly;
- the computation time is in the same order of magnitude as the real time or shorter;
- the controller is robust with respect to process noise.

6-3 Simulation Results

The simulation results that will be studied are the LF and total displacement of the vessel, the displacement and rotation of the motion compensation platform, the thrust forces of the vessel, and the effect of varying the tuning parameters on the energy consumption and the maximum LF vessel displacement. Two scenarios will be used:

- Scenario 1: mean LF disturbance angle: 0° (bow turned towards the disturbance)
- Scenario 2: mean LF disturbance angle: 35°

As mentioned in Subsection 5-1-3, the base case represents the basic conventional DP controller as described in the literature. Thrust allocation is used, but with the conservative ratio $\mathbf{Q} \gg \mathbf{W}$; $c_{alloc} = 10,000$.

The result of using a reference circle instead of a reference point is looked into. For indication also the values for $r_{ref} = 0$ are included, which are equal to the base case simulation.

In the Thrust Allocation Tuning method c_{alloc} is tuned to find the lowest value that still gives a feasible solution. Here the last simulation, with $c_{alloc} = 10,000$, is equal to the base case. Then the PID controller is replaced by MPC control, and the ratio between displacement and thrust forces is tuned by varying c_{alloc} for the two controllers, one built in Matlab and the other in AMPL.

The Simulations are run for 600 seconds.

6-3-1 Tuning

Energy consumption When looking at Figures 6-1 and 6-2, the trends in the energy consumption for the varying tuning parameters are very clear, and all but one behave as expected. The behaviour of the AMPL MPC controller in the second scenario, Figure 6-2d, is unexpected. As later will be discussed this controller does not give stable results and will be rejected, so it can be ignored.

Both the Reference Circle and the Thrust Allocation Tuning methods have the base case simulation results included, the left-most and right-most values respectively. For the Reference Circle and the Thrust Allocation Tuning the energy consumption values are all lower than in the base case.

In the first scenario the two MPC controllers give exactly the same behaviour. For the high values of c_{alloc} the energy consumption is higher than in the base case. The controllers react very strongly to the position error because high costs are connected to it. This induces the same effect as with the base case PID controller; the vessel reacts too much because of the position estimation error resulting in constant overcompensation. For the lower values of c_{alloc} this effect diminishes and the total energy consumption is below the value of the base case for $c_{alloc} = 50,000$ or lower in both scenarios.

LF vessel displacement Along with the decreasing energy consumption, increasing LF vessel displacements were expected, resulting in higher maximum values for d_{tot} . With some imagination this can be seen in Figures 6-3 and 6-4, but the trends are not as clear as for the

Table 6-1: Comparison for mean LF disturbance angle: 0° . The base case is explained in Chapter 3, the Dead Reckoning method in Subsection 5-1-1, the Reference Circle method in Subsection 5-1-2, the Thrust Allocation Tuning method in Subsection 5-1-3, the MPC Matlab method in Subsection 5-2-1, and the MPC AMPL method in Subsection 5-2-2.

Method	Tuning	Maximum d_{tot} [m]	E_{tot} [kJ]	E_{DP} [kJ]	E_{MC} [kJ]
Base case	-	0.042	$16.2e5$	$15.9e5$	$0.33e5$
Dead Reckoning	-	0.14	$0.37e5$	$0.04e5$	$0.33e5$
Reference Circle	$r_{ref} = 0.20$	0.12	$0.59e5$	$0.26e5$	$0.33e5$
Thrust Allocation Tuning	$c_{alloc} = 1e0$	0.045	$2.52e5$	$2.19e5$	$0.33e5$
MPC Matlab	$c_{alloc} = 5e2$	0.18	$0.39e5$	$0.06e5$	$0.33e5$
MPC AMPL	$c_{alloc} = 5e2$	0.18	$0.39e5$	$0.06e5$	$0.33e5$

Table 6-2: Comparison for mean LF disturbance angle: 35° .

Method	Tuning	Maximum d_{tot} [m]	E_{tot} [kJ]	E_{DP} [kJ]	E_{MC} [kJ]
Base case	-	0.066	$17.8e5$	$17.5e5$	$0.33e5$
Dead Reckoning	-	0.14	$7.14e5$	$6.81e5$	$0.33e5$
Reference Circle	$r_{ref} = 0.20$	0.16	$7.83e5$	$7.50e5$	$0.33e5$
Thrust Allocation Tuning	$c_{alloc} = 1e0$	0.11	$8.03e5$	$7.70e5$	$0.33e5$
MPC Matlab	$c_{alloc} = 5e4$	0.35	$11.7e5$	$11.4e5$	$0.33e5$
MPC AMPL	-	-	-	-	-

energy consumption. For the first scenario the maximum displacements first decrease before they increase. Only for the Thrust Allocation tuning a minimal but steady trend can be found. For the second scenario the trends are more or less as expected, except for the AMPL controller which is rejected.

In Figure 6-4c it can be seen that the hard requirements are not met for low values of c_{alloc} , because $d_{tot} > 0.5 \text{ m}$. The best tuning for this controller is $c_{alloc} = 50,000$.

By the absence of clear trends in the maximum LF vessel displacement, the concept of making a trade-off between energy consumption and displacement is a bit misplaced. Nevertheless, it was decided to include all solutions that meet the hard requirements and take a closer look at the simulations of the controllers tuned for the lowest total energy consumption values. An overview of these for the two scenarios can be found in Tables 6-1 and 6-2.

Looking at these tables, it seems as though the energy consumption of the motion compensation system stays constant for all proposed methods, but this is not the case. In the first place, the motion compensation system has to compensate the same heave, roll and pitch displacements in both scenarios and for all methods regardless of the vessel position. This already accounts for a large part of the energy consumed by the system. Next to this, recall $d_{LF,max} = 0.5 \text{ m}$ and $d_{HF,max} = 1.43 \text{ m}$. In the horizontal plane, only the LF vessel displacements will be varying, but the HF vessel displacements, which are generally larger, are the same in each simulation. So the differences in energy consumption of the motion compensation platform are there, but they are very small.

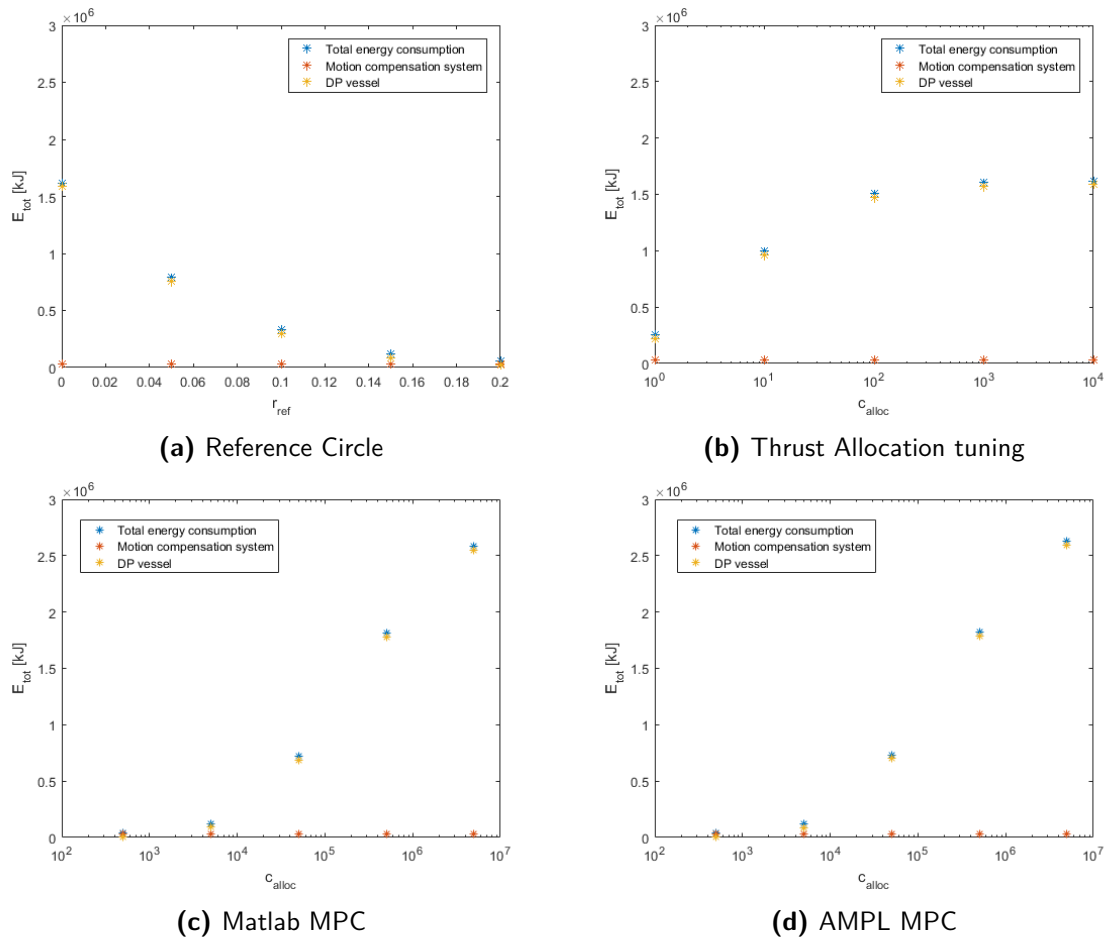


Figure 6-1: Energy consumption for varying tuning parameters, mean LF disturbance angle: 0°

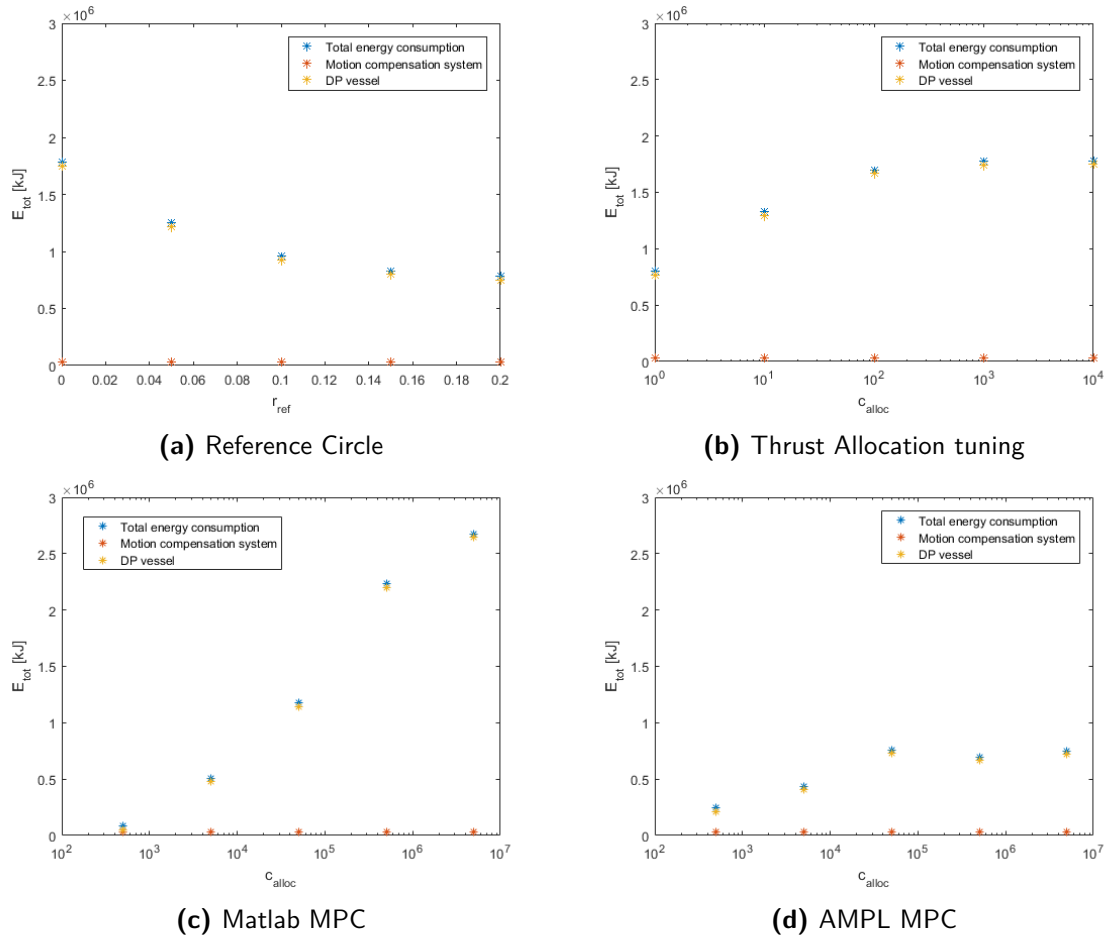


Figure 6-2: Energy consumption for varying tuning parameters, mean LF disturbance angle: 35°

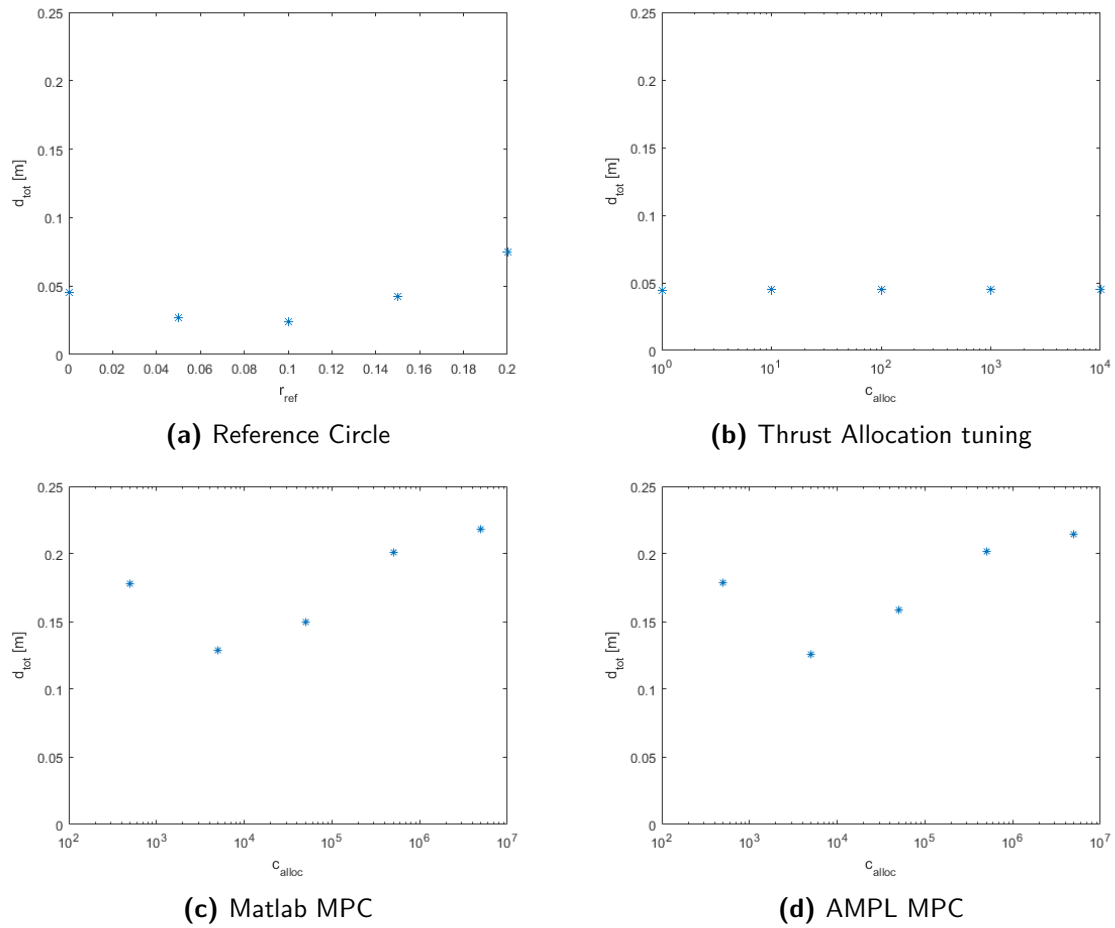


Figure 6-3: Maximum d_{tot} for varying tuning parameters, mean LF disturbance angle: 0°

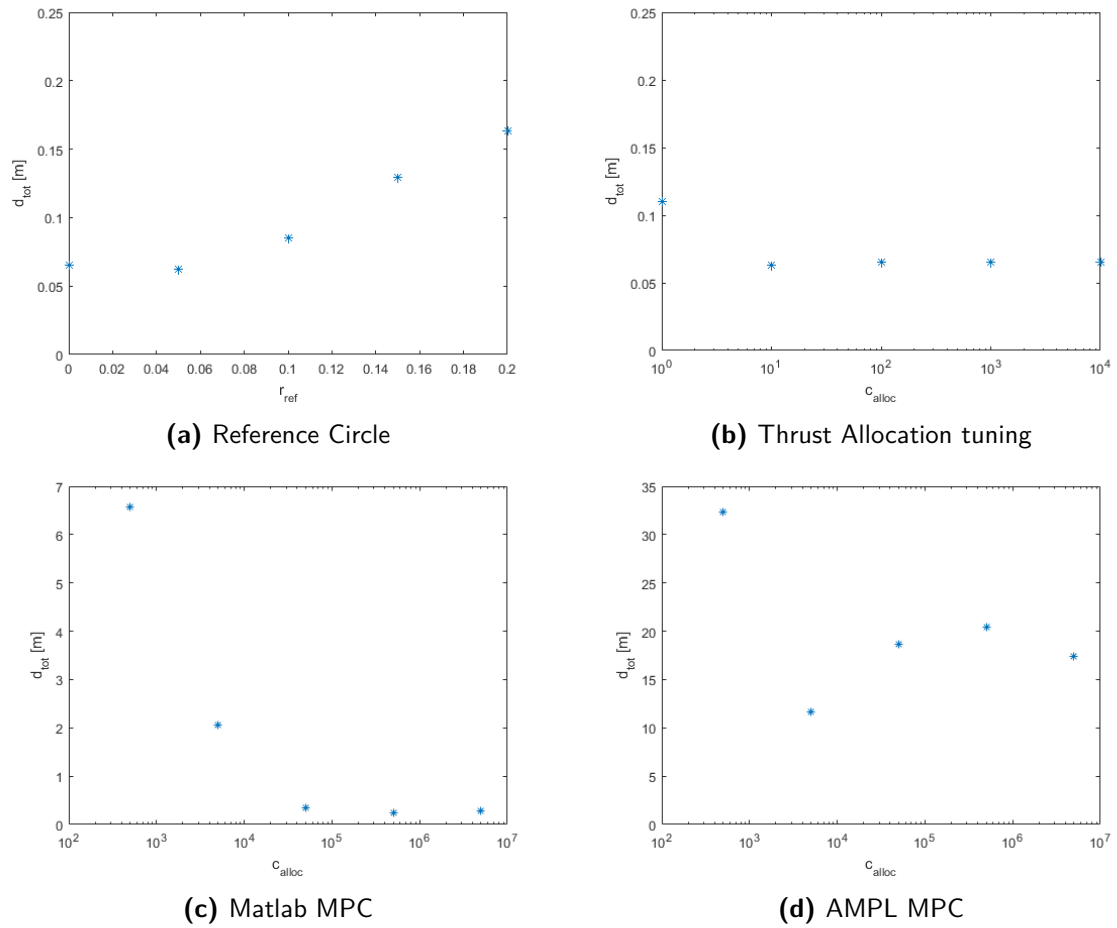


Figure 6-4: Maximum d_{tot} for varying tuning parameters, mean LF disturbance angle: 35°

6-3-2 Controller Behaviour

Recall the two scenarios:

- Scenario 1: mean LF disturbance angle: 0° (bow turned towards the disturbance)
- Scenario 2: mean LF disturbance angle: 35°

Plots of the simulations for both scenarios can be found in Appendix E. The LF and total vessel displacements and the thrust forces are plotted for all controllers.

Base Case In the base case plots, Figures E-1, E-2, E-5 and E-7, it can be seen that the controller tries to keep η_{LF} as small as possible and high forces are needed for this, hence a high energy consumption. The thrusters often use the maximum allowed thrust force. The process noise (the sinusoidal fluctuation of the LF disturbance) is visible, especially in the second scenario, but has only the slightest influence on the vessel position. In the second scenario the yaw angle of the vessel gets perturbed, but is stable and in Figure E-8 it can be seen that the motion compensation system compensates for this.

The motion compensation system plots show smooth behaviour, Figures E-3, E-4, E-8 and E-9, and the reference tracking errors are lower than the defined limits.

Only for the base case of both scenarios the plots of the motion compensation platform are shown. For the other controllers this is omitted because barely any difference can be noticed if the data is plotted in a reasonable scale. This already indicates the small influence that the LF vessel displacement has on the total vessel displacement, which can also be seen when comparing the plots of the total vessel displacement for all methods. Moreover, it underscores the small differences in the energy consumption of the motion compensation system for all simulations.

Dead Reckoning For the Dead Reckoning method a longer simulation is made to study the effect of the error accumulation. In Figure E-13, it can be seen that this effect is small. The maximum d_{tot} after 1800 seconds is only slightly larger than after 300 seconds. However, by using dead reckoning the vessel becomes very susceptible of the process noise, which degrades the robustness of the controller.

Recall it was assumed that the combined system works most efficiently if the vessel reacts only to the LF disturbance term, and the motion compensation system reacts to the HF disturbance term. As shown in Figures E-11 and E-14, after oscillating for a few second in both scenario's the controllers find the thrust forces that almost perfectly counteract the LF disturbance, resulting in a very low total energy consumption (given in Tables 6-1 and 6-2) which could almost be called ideal.

Reference Circle Especially in the results of the 1800 s simulations, Figures E-16 and E-19, it can be seen that the behaviour of the Reference Circle method resembles the behaviour of the Dead Reckoning method to some extend. In both cases the input of the PID controller is near zero most of the time and due to the integral action the computed thrust forces approach

the needed values to counteract the LF disturbance.

The robustness is higher for the Reference Circle method because when the vessel is outside of the reference circle the controller roughly behaves as the base case PID controller, and generally the robustness of PID controllers is good. A downside of the method is the aggressive controller reaction when the vessel displacement approaches the reference circle radius, as can be seen in Figures E-17 and E-20.

Thrust Allocation Tuning As for the base case, in the Thrust Allocation Method again the process noise is reflected in the LF vessel displacement, but has no major influence, shown in Figures E-21 and E-23. In the first scenario the energy reduction is substantially less than with the other methods, but in the second scenario an average value for this is reached. The thrust forces, Figures E-22 and E-24, behave good and are more smooth than in the base case.

The thrust allocation algorithm with a low c_{alloc} can allow high slack values regardless of the position of the vessel. This makes the controller less robust. Still, with the PID controller as a basis adequate robustness properties are expected.

Model Predictive Control In the first scenario the two MPC controllers give exactly the same behaviour, as can be seen in Figures E-25 and E-29. However for the second scenario, while the Matlab controller shows quite promising results, Figure E-27, the AMPL controller gives unstable behaviour, Figure E-31. For an unknown reason the controller is unable to keep the vessel from rotating in the yaw direction. As the rotation becomes larger the linearisation of the vessel model becomes inaccurate and thereby also the position of the vessel becomes unstable. So as indicated earlier, the AMPL MPC controller is rejected for the second scenario. For the first scenario it is still taken into account, because although the behaviour is the same, for the AMPL controller the computation time is a bit lower than for the Matlab controller. Recall Tables 6-1 and 6-2. For the first scenario the MPC controller gives the highest d_{tot} , but it is still far below the allowed value of 0.5 m, and the behaviour is really smooth for both LF vessel displacement and thrust forces, Figures E-26 and E-30. Moreover, the thrust forces are very low and the total energy consumption comes close to the almost ideal value of the Dead Reckoning method.

For the second scenario only the Matlab MPC controller is evaluated. Here the MPC controller has again the highest d_{tot} and also the highest energy consumption (apart from the base case), making it the least favourable energy reduction method. On the other hand, the controller shows so to say ‘smart behaviour’ in the vessel displacement plots, Figure E-27. The vessel is rotated a few degrees towards the mean LF disturbance direction. Hereby the vessel needs less energy to maintain its position. Furthermore, a shift has occurred in the y-position of the vessel. The controller reacts adequately to prevent the vessel from drifting off further, but sees no need to make the vessel sail back to the reference position. And there is no need, because the motion compensation system can compensate for it.

The robustness of MPC controllers in general is a difficult subject, because of the great variety in models, constraints and solvers that can be used. For the simulated scenarios the controller seems to have adequate robustness as the process noise is not reflected in the behaviour of the vessel. Next to this, the prediction model and constraints are kept simple, so this will not be a problem. And because the thrust forces and the vessel displacement are linked in the

objective function, the robustness should be better than with the Thrust Allocation Tuning method.

6-4 Conclusions

In this chapter the case study was discussed that was performed to evaluate the different methods that were proposed to reduce the energy consumption of a DP vessel equipped with a motion compensation system.

A supply vessel, based on the IHC Wind Farm Service Vessel, was simulated, with environmental conditions based on different sources, namely the MSS, the research of Liu, and the Ampelmann Demonstrator documentation. The latter was also the for the Motion Compensation System Simulator model parameters.

The combined system of the simulated vessel and motion compensation system should be able to operate in a sea state with $H_s \leq 2.0 \text{ m}$.

The hard requirements that every controller should meet are:

$$d_{tot} \leq 0.5 \quad (6-8)$$

$$x_{res} \leq 0.05 \quad (6-9)$$

$$y_{res} \leq 0.05 \quad (6-10)$$

$$z_{res} \leq 0.05 \quad (6-11)$$

Furthermore, it is preferred that:

- the vessel and the platform have smooth motions;
- the thrust forces do not vary rapidly;
- the computation time is in the same order of magnitude as the real time or shorter;
- the controller is robust with respect to process noise.

The simulation results were studied for two different scenarios, a mean LF disturbance angle of 0° and of 35° . For the Reference Circle method r_{ref} was varied, and the Thrust Allocation and the Matlab and AMPL MPC methods were tuned with c_{alloc} .

Trends were found clearly in the values of the energy consumption for the different methods. All behaved as expected, except for the AMPL controller in the second scenario, which did not give stable results and was rejected.

For the maximum vessel displacement d_{tot} no trends were found, but for all simulations d_{tot} stayed far lower than the maximum allowed value of 0.5 m .

The behaviour of all control methods was studied for the controllers tuned to have the lowest

possible energy consumption.

The Dead Reckoning method resulted in the lowest energy consumption, but the robustness of this controller could be a problem.

The Reference Circle method achieved good energy reduction values and is more robust than the Dead Reckoning method, but the high amplitude oscillations in the thrust forces could cause wear and tear of the vessel.

The Thrust Allocation Tuning method has the least energy reduction in the first scenario, and an average value in the second. The robustness of the controller is questionable, as the given slack to reduce the thrust forces is not related to the position of the vessel.

With the MPC controllers, the robustness is better because the thrust forces and vessel position are related in the objective function. In the first scenario the energy reduction approached the lowest value, found with Dead Reckoning. In the second scenario the controller has the least energy reduction, but the controller shows so to say 'smart behaviour' by turning the bow towards the LF disturbance direction and accepting a small shift in the vessel position.

Chapter 7

Conclusion and Discussion

The last chapter will be used to present the conclusions that can be drawn from the previous chapters. Then this thesis will be concluded by giving recommendations for further research on the subject of energy reduction for Dynamic Positioning (DP) vessels equipped with a motion compensation system.

7-1 Conclusions of the Research

In Chapter 1 the following main question for this research was formulated:

How can the control system of a Dynamic Positioning (DP) vessel be improved, in order to minimize the summed energy consumption of the vessel and a motion compensation system, while keeping a gangway motionless relative to an offshore structure?

It was chosen to approach this question with a very general perspective, because the control problem resulting from the combination of DP and motion compensation is not the most ordinary one. Reference tracking would be preferred if the Low-Frequency (LF) displacements were exactly known, but a significant estimation error impedes this. Instead of tracking the reference as close as possible, in this case the vessel can just stay in the vicinity of the reference point and the motion compensation system will compensate for the remaining vessel motions.

While much research has been done on various control techniques for both subjects, control of the specific combination of the two was not found in literature. Therefore in this research multiple methods were proposed that could yield a reduction of the energy consumption, without going far into detail, but merely to give an indication where the highest gains could be obtained.

All methods that were proposed, except for the Dead Reckoning method, were based on making a trade-off between the displacement of the vessel and the thrust forces. In the model that was used the energy consumption of the vessel solely depends on the thrust forces.

As a starting point a simulation model was made of the standard DP controller as described in the literature, including a vessel control plant model, an observer, a Proportional Integral Derivative (PID) controller and a thrust allocation algorithm. A simulation model of a motion compensation platform was connected to the vessel simulation by using the position and yaw rotation of the vessel as input for the compensation system. The proposed adjustments were implemented, two Model Predictive Control (MPC) controllers were built, and simulations were run to answer the following sub questions:

- How much energy reduction could be realized by using the integrated velocity as an estimation of the position of the vessel?
- How much energy reduction could be realized by changing the reference point of the PID controller into a reference circle?
- How much energy reduction could be realized by tuning the weight matrices in the thrust allocation objective function?
- How much energy reduction could be realized by using MPC for the vessel DP controller?

The short answers to these questions can be found in Table 7-1, but next to the energy consumption also some other properties were studied, which are the smoothness of all motions and the thrust forces, and the computation time and the robustness of the controllers.

All methods have their own downsides. With Dead Reckoning and Thrust Allocation Tuning the robustness could be an issue, but this depends on the accuracy with which the LF disturbance can be measured or predicted. Current and wind measurement systems should be studied more into depth to draw conclusion on this.

The Reference Circle method causes strong thrust force oscillations, which could cause wear and tear of the thrusters. Also the effect of this on the power supply system of the vessel could be a problem.

For the MPC controllers the computation time is the most important hold-back. Although the prediction model and constraints are kept to a minimum the run time of the simulations was approximately equal to the real time. With AMPL the computation time is a bit lower than with Matlab. However, the main advantage of using AMPL was the natural way of formulating the model and constraints. This allows easy implementation of additional constraints, but thereby the computation time increases rapidly.

Table 7-1: Energy reduction for the different methods

Method	Energy reduction in kJ	
	Scenario 1	Scenario 2
Dead Reckoning	15.83e5	10.66e5
Reference Circle	15.61e5	9.97e5
Thrust Allocation Tuning	13.68e5	9.77e5
MPC Matlab	15.80e5	6.8e5
MPC AMPL	15.80e5	-

All together, to answer the main question, all proposed methods yield energy consumption reductions. Despite the lower value for energy reduction in the second scenario MPC seems

to be the most promising method for energy consumption reduction. With a faster computer the computation time will no longer be a problem. A very simple controller formulation already achieves good results, especially if the vessel has the bow turned towards the mean LF disturbance, which is usually the case for wind farm service vessels. If the disturbance has an angle of attack the controller shows ‘smart behaviour’ by rotating the bow a few degrees towards it. And, at least in this case study, this method shows good robustness with respect to the process noise.

7-2 Discussion and Recommendations

This thesis was focussed on researching the feasibility of a number of different methods to reduce the energy consumption of the combined operation of a DP vessel and a motion compensation system. The results that were found look promising, but many assumptions and simplifications were made, leaving many opportunities for further research, of which a few are highlighted here.

Robustness In the previous section already some condoned matters came to light. In the case study the robustness was the main drawback for the Dead Reckoning and the Thrust Allocation Tuning methods. However, the LF disturbance was modelled very simplistically by a constant term that was assumed to be known and a light sinusoidal fluctuation as the unknown process noise. A good improvement would be to get a clearer picture of the actual robustness of all different methods. A good start for this would be to look into modelling and measuring current and wind.

Force oscillations The Reference Circle method was written off because of the strong oscillations of the thruster forces. It was assumed that this will harm the thruster and the power supply system of the vessel. Probably with better signal processing the oscillations could be averted. Also using a more gradual approach with different stages of abating the reference signal could be a solution.

Energy reduction versus fuel reduction Ultimately, the energy reduction is pursued in order to save costs for fuel and to lower polluting emissions. So actually the fuel consumption should be minimized and this does not completely go one on one with minimizing the energy consumption of the thrusters. Much research has been done on power management systems and fuel consumption of ships. It would be a great gain to extend the vessel simulation model in order to minimize the fuel consumption.

Appendix A

Parametrization of the Vessel Simulation Model

Process Plant

$$\dot{\eta}_{LF} = \mathbf{R}(\psi)\boldsymbol{\nu} \quad (\text{A-1})$$

$$\mathbf{M}\dot{\boldsymbol{\nu}} + \mathbf{D}\boldsymbol{\nu} = \boldsymbol{\tau}_{thr} \quad (\text{A-2})$$

with

$$\mathbf{M} = \begin{bmatrix} 5.3122e6 & 0 & 0 \\ 0 & 8.2831e6 & 0 \\ 0 & 0 & 3.7454e9 \end{bmatrix} \quad (\text{A-3})$$

$$\mathbf{D} = \begin{bmatrix} 5.0242e4 & 0 & 0 \\ 0 & 2.7229e5 & -4.3933e6 \\ 0 & -4.3933e6 & 4.1894e8 \end{bmatrix} \quad (\text{A-4})$$

Proportional Integral Derivative (PID) controller

$$\boldsymbol{\tau}_{PID}(k) = \mathbf{K}_p \mathbf{e}_b(k) + \mathbf{K}_i \mathbf{z}(k) - \mathbf{K}_d \hat{\boldsymbol{\nu}}(k) \quad (\text{A-5})$$

$$\mathbf{e}_b(k) = \mathbf{R}^\top(\psi)(\boldsymbol{\eta}_{ref}(k) - \hat{\boldsymbol{\eta}}_{LF}(k)) = \mathbf{R}^\top(\psi)\mathbf{e}_n(k) \quad (\text{A-6})$$

$$\mathbf{z}(k) = \mathbf{z}(k-1) + \mathbf{K}[t(k) - t(k-1)]\mathbf{e}_b(k-1) \quad (\text{A-7})$$

with $\mathbf{K}_p = 5e6 \cdot \mathbf{I}_3$, $\mathbf{K}_i = 1e4 \cdot \mathbf{I}_3$, $\mathbf{K}_d = 5e7 \cdot \mathbf{I}_3$ and $\mathbf{K} = 1$.

Low-Frequency (LF) disturbance

$$\boldsymbol{\nu}_{LF}(t) = \begin{bmatrix} c_{1,x} + c_{2,x} \sin(\omega_{cur} t) \\ c_{1,y} + c_{2,y} \sin(\omega_{cur} t) \\ 0 \end{bmatrix} \quad (\text{A-8})$$

For a mean LF disturbance angle of 0° ;

$c_{1,x} = -0.18 \text{ m/s}$, $c_{2,x} = 0.0015 \text{ m/s}$, $c_{1,y} = 0 \text{ m/s}$, $c_{2,y} = 0.001 \text{ m/s}$ and $\omega_{cur} = 0.02 \text{ rad/s}$.

For a mean LF disturbance angle of 35° ;

$c_{1,x} = -0.15 \text{ m/s}$, $c_{2,x} = 0.0015 \text{ m/s}$, $c_{1,y} = 0.10 \text{ m/s}$, $c_{2,y} = 0.001 \text{ m/s}$ and $\omega_{cur} = 0.02 \text{ rad/s}$.

High-Frequency (HF) disturbance

$$\frac{\eta_{w_i}}{w_{w_i}}(s) = \frac{K_{w_i}s}{s^2 + 2\zeta_i\omega_i s + \omega_i^2} \quad (\text{A-9})$$

with $K_{w_i} = 0.08$, $\zeta_i = 0.1$ and $\omega_i = 0.8 \text{ rad/s}$.

Observer

$$\dot{\boldsymbol{\chi}}_w = \mathbf{A}_w \boldsymbol{\chi}_w + \mathbf{E}_w \mathbf{w}_w \quad (\text{A-10})$$

$$\hat{\boldsymbol{\eta}}_{HF} = \mathbf{C}_w \boldsymbol{\chi}_w \quad (\text{A-11})$$

with $\boldsymbol{\chi}_w = [\boldsymbol{\eta}_w^\top / s \quad \boldsymbol{\eta}_w^\top]^\top \in \mathbb{R}^6$ and

$$\mathbf{A}_w = \begin{bmatrix} \mathbf{0}_{3 \times 3} & \mathbf{I}_{3 \times 3} \\ -\boldsymbol{\Omega}^2 & -2\boldsymbol{\Lambda}\boldsymbol{\Omega} \end{bmatrix} \quad (\text{A-12})$$

$$\mathbf{C}_w = \begin{bmatrix} \mathbf{0}_{3 \times 3} & \mathbf{I}_{3 \times 3} \end{bmatrix} \quad (\text{A-13})$$

$$\mathbf{E}_w = \begin{bmatrix} \mathbf{0}_{3 \times 3} \\ \mathbf{K}_w \end{bmatrix} \quad (\text{A-14})$$

with $\boldsymbol{\Omega} = \text{diag}\{0.8, 0.8, 0.8\}$, $\boldsymbol{\Lambda} = \text{diag}\{0.1, 0.1, 0.1\}$ and $\mathbf{K}_w = \text{diag}\{1.44, 1.44, 1.44\}$.

$$\dot{\hat{\boldsymbol{\chi}}}_w = \mathbf{A}_w \hat{\boldsymbol{\chi}}_w + \mathbf{K}_1 \tilde{\mathbf{y}} \quad (\text{A-15})$$

$$\hat{\boldsymbol{\eta}}_{HF} = \mathbf{C}_w \hat{\boldsymbol{\chi}} \quad (\text{A-16})$$

$$\dot{\hat{\boldsymbol{\eta}}}_{LF} = \mathbf{R}(\psi_y) \hat{\boldsymbol{\nu}} + \mathbf{K}_2 \tilde{\mathbf{y}} \quad (\text{A-17})$$

$$\dot{\hat{\mathbf{b}}} = -\mathbf{T}_b^{-1} \hat{\mathbf{b}} + \mathbf{K}_3 \tilde{\mathbf{y}} \quad (\text{A-18})$$

$$\mathbf{M} \dot{\hat{\boldsymbol{\nu}}} + \mathbf{D}(\hat{\boldsymbol{\nu}} - \hat{\boldsymbol{\nu}}_{LF}) = \boldsymbol{\tau}_c + \mathbf{R}^\top(\psi_y) \hat{\mathbf{b}} + \mathbf{K}_4 \mathbf{R}^\top(\psi_y) \tilde{\mathbf{y}} \quad (\text{A-19})$$

$$\hat{\mathbf{y}} = \hat{\boldsymbol{\eta}}_{LF} + \hat{\boldsymbol{\eta}}_{HF} \quad (\text{A-20})$$

with $\mathbf{K}_1 = \mathbf{E}_w$, $\mathbf{K}_2 = \text{diag}\{1.04, 1.04, 1.04\}$, $\mathbf{K}_3 = \text{diag}\{0.1, 0.1, 0.01\}$, $\mathbf{K}_4 = \text{diag}\{0.1, 0.1, 0.01\}$, and $\mathbf{T}_b = \text{diag}\{100, 100, 100\}$.

Thrust Allocation

$$\boldsymbol{\tau}_c = \mathbf{T}(\boldsymbol{\alpha})\mathbf{f} \quad (\text{A-21})$$

with

$$\mathbf{T}(\boldsymbol{\alpha}) = \begin{bmatrix} 1 & 1 & 0 & 0 & 0 \\ 0 & 0 & 1 & 1 & 1 \\ -5 & 5 & 24 & 27 & 30 \end{bmatrix} \quad (\text{A-22})$$

Furthermore

$$\begin{aligned} \min_{\mathbf{f}, \mathbf{s}} \quad & J = \mathbf{f}^\top \mathbf{W} \mathbf{f} + \mathbf{s}^\top \mathbf{Q} \mathbf{s} \\ \text{s.t.} \quad & \mathbf{T}\mathbf{f} = \boldsymbol{\tau}_{PID} + \mathbf{s} \\ & \mathbf{f}_{\min} \leq \mathbf{f} \leq \mathbf{f}_{\max} \end{aligned} \quad (\text{A-23})$$

with \mathbf{f} in Newton, and

$$\mathbf{f}_{\max} = [180e3 \quad 180e3 \quad 95e3 \quad 125e3 \quad 125e3]^\top \quad (\text{A-24})$$

$$\mathbf{f}_{\min} = -\mathbf{f}_{\max} = [-180e3 \quad -180e3 \quad -95e3 \quad -125e3 \quad -125e3]^\top \quad (\text{A-25})$$

$$\mathbf{W} = \begin{bmatrix} 1 & 0 & 0 & 0 & 0 \\ 0 & 1 & 0 & 0 & 0 \\ 0 & 0 & 1.5 & 0 & 0 \\ 0 & 0 & 0 & 1.3 & 0 \\ 0 & 0 & 0 & 0 & 1.3 \end{bmatrix} \quad (\text{A-26})$$

$$\mathbf{Q} = c_{alloc} \cdot \begin{bmatrix} 1 & 0 & 0 \\ 0 & 1 & 0 \\ 0 & 0 & 100 \end{bmatrix} \quad (\text{A-27})$$

Power Consumption

$$P_i(f) = (P_{i,max} - P_{i,min}) \left(\frac{|f_i|}{f_{i,max}} \right)^\eta + P_{i,min} \quad (\text{A-28})$$

with $\eta = 1.6$, $P_{1,max} = P_{2,max} = 1200$ kW, $P_{3,max} = 650$ kW, $P_{4,max} = P_{5,max} = 850$ kW, $P_{i,min} = 0$ kW for $i = 1,..,5$, and $f_{1,max} = f_{2,max} = 180$ kN, $f_{3,max} = 95$ kN, $f_{4,max} = f_{5,max} = 125$ kN.

$$P_i(f) \approx w_i f_i^2 + c_i \quad \text{for } i = 1,..,5 \quad (\text{A-29})$$

with $w_1 = w_2 = 0.30$, $w_3 = 0.45$, $w_4 = w_5 = 0.38$, and $c_1 = c_2 = c_3 = c_4 = c_5 = 0$.

Appendix B

Parametrization of the Motion Compensation System Simulation Model

Motion compensation system parameters The settled platform height is measured with the cylinders at minimum length and the neutral platform height with half cylinder strokes.

Table B-1: Motion compensation system design parameters.

Parameter	Value
Radius top platform	$R_t = 2.75 \text{ m}$
Radius base platform	$R_b = 3.00 \text{ m}$
Half separation top gimbal pairs	$s_t = 0.25 \text{ m}$
Half separation base gimbal pairs	$s_b = 0.25 \text{ m}$
Cylinder minimum length	$l_{min} = 3.25 \text{ m}$
Cylinder stroke length	$l_{stroke} = 2.00 \text{ m}$
Cylinder dead length	$l_{dead} = 1.25 \text{ m}$
Settled platform height	$h_s = 2.15 \text{ m}$
Neutral platform height	$h_n = 3.40 \text{ m}$
Maximum excursions	$x_{max} = 3.63 \text{ m}$ $y_{max} = 3.31 \text{ m}$ $z_{max} = 2.50 \text{ m}$ $\phi_{max} = 55^\circ$ $\theta_{max} = 53^\circ$ $\psi_{max} = 76^\circ$

Proportional Integral Derivative (PID) controller

$$F_{PID,i} = K_p E_i + K_i \int_0^t E_i dt - K_d (dE_i/dt) \quad (\text{B-1})$$

with $K_p = 2e7$, $K_i = 1e6$ and $K_d = 4.5e5$.

Energy consumption

$$\Psi(t) = \frac{1}{\eta_v} \left(\frac{A_1 + A_2}{2} \cdot 6 \cdot |v_j(t)|_{avg} \cdot P_s + \Psi_r \right) + \Psi_l \quad (\text{B-2})$$

with $\eta_v = 0.85$, $A_1 = 0.015 \text{ m}^2$, $A_2 = 0.009 \text{ m}^2$, $P_s = 2.5e5 \text{ Pa}$, $\Psi_r = 20e3 \text{ W}$, and $\Psi_l = 25e3 \text{ W}$.

Appendix C

Matlab MPC code

Listing C.1: Matlab MPC controller set-up

```
1 clc
2
3 %% Vessel Parameters
4 Bu = eye(3);
5 Dsv = [5.0242e4 0 0; 0 2.7229e5 -4.3933e6; 0 -4.3933e6 4.1894e8];
6 Msv = [5.3122e6 0 0; 0 8.2831e6 0; 0 0 3.7454e9];
7
8 Talpha = [1 1 0 0 0; 0 0 1 1 1; -5 5 24 27 30];
9
10 %% Prediction Model
11 Ampc = [zeros(3,3) eye(3);
12          zeros(3,3) -inv(Msv)*Dsv];
13 Bmpc = [zeros(3,3); inv(Msv)*Bu];
14 Empc = [zeros(3,3); inv(Msv)*Dsv];
15 Hmpc = [eye(3) zeros(3,3); zeros(3,3) eye(3)];
16 Dmpc = zeros(6,6);
17
18 h = 0.2;
19 sys_mpc = ss(Ampc, [Bmpc Empc], Hmpc, Dmpc);
20 sysd_mpc = c2d(sys_mpc, h);
21
22 %% Controller
23 W1 = [1 0 0 0 0; 0 1 0 0 0; 0 0 1.5 0 0; 0 0 0 1.3 0; 0 0 0 0 1.3];
24 W2 = 5e2;
25
26 Ao = sysd_mpc.A;
27 Ko = eye(6);
28 Lo = sysd_mpc.B(:, 4:6);
29 Bo = 1e4.*sysd_mpc.B(:, 1:3)*[1 1 0 0 0; 0 0 1 1 1; -5 5 24 27 30];
30 Co = sysd_mpc.C;
31 DH = eye(6);
32 DF = zeros(6, 3);
```

```
33 Q = [W2*[1 0 0;0 1 0;0 0 100] zeros(3,3);zeros(3,3) zeros(3,3)];  
34 R = [W1];  
35 Nm = 1;  
36 N = 15;  
37 Nc = 15;  
38 lensim = 15;  
39 umax = [18 18 9.5 12.5 12.5]';  
40 apr = 1;  
41 rhc = 0;  
42  
43 %% Disturbance (scenario 1)  
44 do = [-0.18*ones(1,lensim);zeros(1,lensim);zeros(1,lensim)];  
45 eo = zeros(6,lensim);
```

Appendix D

AMPL MPC codes

Listing D.1: AMPL MPC preprocessing

```
1 ## pre_mpc.run
2
3 param s_init1;
4 param s_init2;
5 param s_init3;
6 param s_init4;
7 param s_init5;
8 param s_init6;
```

Listing D.2: AMPL MPC model

```
1 ## mpc_ampl.run
2
3 param fin := 15;                      # Number of steps in prediction horizon
4
5 set Step := 1..fin;                     # Set from 1 to N
6 set Inits := 0..fin;                    # Set from 0 to N
7
8                         # Disturbance scenario 2
9 param Vc1 := -0.15;                   # Current velocity in x-direction
10 param Vc2 := -0.1;                    # Current velocity in y-direction
11 param Vc3 := 0;                      # Rotational current
12
13 param W1 := 1;                       # Weight on forces
14 param W2 := 5e5;                     # Weight on displacement
15
16 var s1 {i in Inits};                 # Position in x-direction
17 var s2 {i in Inits};                 # Position in y-direction
18 var s3 {i in Inits};                 # Position in yaw-direction
19 var s4 {i in Inits};                 # Velocity in x-direction
20 var s5 {i in Inits};                 # Velocity in y-direction
21 var s6 {i in Inits};                 # Velocity in yaw-direction
```

```

22
23 var tau1 {h in Step};          # Generalized force in x-direction
24 var tau2 {h in Step};          # Generalized force in y-direction
25 var tau3 {h in Step};          # Generalized moment in yaw-direction
26
27 var f1 {h in Step} >=-18 <=18;      # Force of thruster 1
28 var f2 {h in Step} >=-18 <=18;      # Force of thruster 2
29 var f3 {h in Step} >=-9.5 <=9.5;    # Force of thruster 3
30 var f4 {h in Step} >=-12.5 <=12.5;   # Force of thruster 4
31 var f5 {h in Step} >=-12.5 <=12.5;   # Force of thruster 5
32
33 data;
34
35 # Objective function
36 minimize cost: sum {h in Step} (W1*(f1[h]^2+f2[h]^2+1.5*f3[h]^2+1.3*f4
37 [h]^2+1.3*f5[h]^2) + W2*(s1[h]^2+s2[h]^2+100*s3[h]^2));
38
39 # Constraints
40 subject to con_s1 {i in Inits}: s1[i] = if i=0 then s_init1 else s1[i
41 -1]+0.1998*s4[i-1]+3.763e-9*tau1[i]+0.000189*Vc1;
42 subject to con_s2 {i in Inits}: s2[i] = if i=0 then s_init2 else s2[i
43 -1]+0.1993*s5[i-1]+0.01051*s6[i-1]+2.409e-9*tau2[i]+1.875e-13*tau3[i
44 ]+0.0006552*Vc2-0.01051*Vc3;
45 subject to con_s3 {i in Inits}: s3[i] = if i=0 then s_init3 else s3[i
46 -1]+2.3235e-05*s5[i-1]+0.1978*s6[i-1]+1.875e-13*tau2[i]+5.3e-12*tau3[i
47 ]-2.3235e-05*Vc2+0.00222*Vc3;
48 subject to con_s4 {i in Inits}: s4[i] = if i=0 then s_init4 else
49 0.9981*s4[i-1]+3.761e-8*tau1[i]+0.00189*Vc1;
50 subject to con_s5 {i in Inits}: s5[i] = if i=0 then s_init5 else
51 0.9935*s5[i-1]+0.1046*s6[i-1]+2.407e-8*tau2[i]+2.805e-12*tau3[i
52 ]+0.006541*Vc2-0.1046*Vc3;
53 subject to con_s6 {i in Inits}: s6[i] = if i=0 then s_init6 else 2.3123
54 e-04*s5[i-1]+0.9779*s6[i-1]+2.805e-12*tau2[i]+5.281e-11*tau3[i
55 ]-0.0002312*Vc2+0.02211*Vc3;
56
57 subject to con_tau1 {h in Step}: tau1[h] = (f1[h]+f2[h])*1e4;
58 subject to con_tau2 {h in Step}: tau2[h] = (f3[h]+f4[h]+f5[h])*1e4;
59 subject to con_tau3 {h in Step}: tau3[h] = (-5*f1[h]+5*f2[h]+24*f3[h
60 ]+27*f4[h]+30*f5[h])*1e4;
61
62 option minos_options 'Hessian_dimension=80';
63 option solver minos;

```

Listing D.3: Matlab function calling AMPL MPC preprocessing and model

```

1 function [output] = AMPL_mpc(in1,in2,in3,in4,in5,in6,in7,in8,in9)
2     %% Create an AMPL instance
3     ampl = AMPL;
4
5     % Initialisation
6     basef = fileparts(which('dietModel'));
7     addpath(fullfile(basef, '../..//matlab'));
8     modeldirectory = fullfile(basef, 'models', 'diet');

```

```

9
10 %% 
11 % Input values for requested load
12 ampl.read([modeldirectory '/pre_mpc.run']);
13
14 ampl.getParameter('s_init1').setValues(in4);
15 ampl.getParameter('s_init2').setValues(in5);
16 ampl.getParameter('s_init3').setValues(in6);
17 ampl.getParameter('s_init4').setValues(in7);
18 ampl.getParameter('s_init5').setValues(in8);
19 ampl.getParameter('s_init6').setValues(in9);
20
21 % Load from file the ampl model
22 ampl.read([modeldirectory '/mpc_ampl.run']);
23
24 %% Solve
25 ampl.solve
26
27 %% Output
28 matrix = ones(15,5);
29
30 % Print objective
31 fprintf('Objective is: %f\n' ,ampl.getObjective('cost').value());
32
33 % Print Variables
34 f1 = ampl.getVariable('f1').getValues('val','dual');
35 f2 = ampl.getVariable('f2').getValues('val','dual');
36 f3 = ampl.getVariable('f3').getValues('val','dual');
37 f4 = ampl.getVariable('f4').getValues('val','dual');
38 f5 = ampl.getVariable('f5').getValues('val','dual');
39
40 % Get values to MATLAB vector
41 matrix(:,1) = f1.getColumnAsDoubles('val');
42 matrix(:,2) = f2.getColumnAsDoubles('val');
43 matrix(:,3) = f3.getColumnAsDoubles('val');
44 matrix(:,4) = f4.getColumnAsDoubles('val');
45 matrix(:,5) = f5.getColumnAsDoubles('val');
46
47 output = 1e4.*matrix(1,:)';
48
49 % Close the AMPL object
50 ampl.close();
51 end

```

Appendix E

Simulation results

Base case Proportional Integral Derivative (PID) controller

Scenario 1: mean Low-Frequency (LF) disturbance angle is 0°

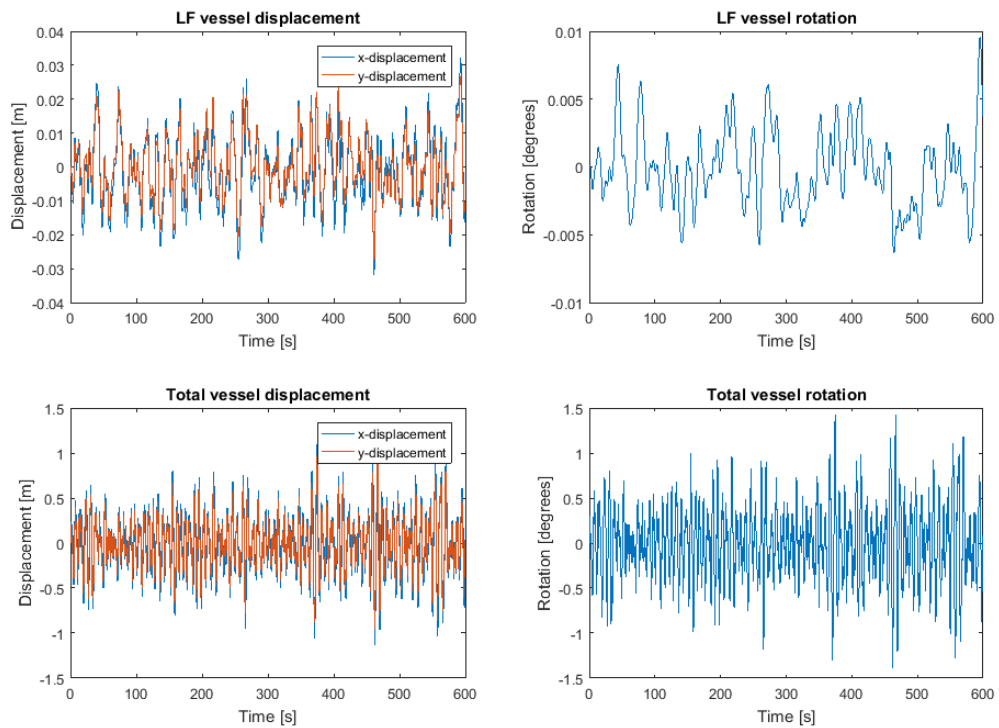


Figure E-1: η_{LF} and η_{tot} for the base case simulation.

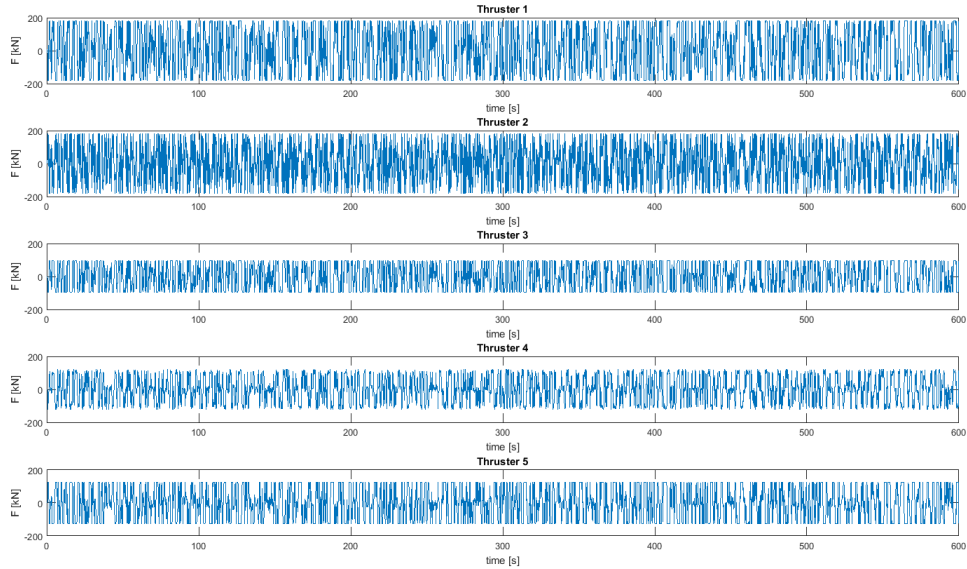


Figure E-2: Thrust forces used in the base case simulation.

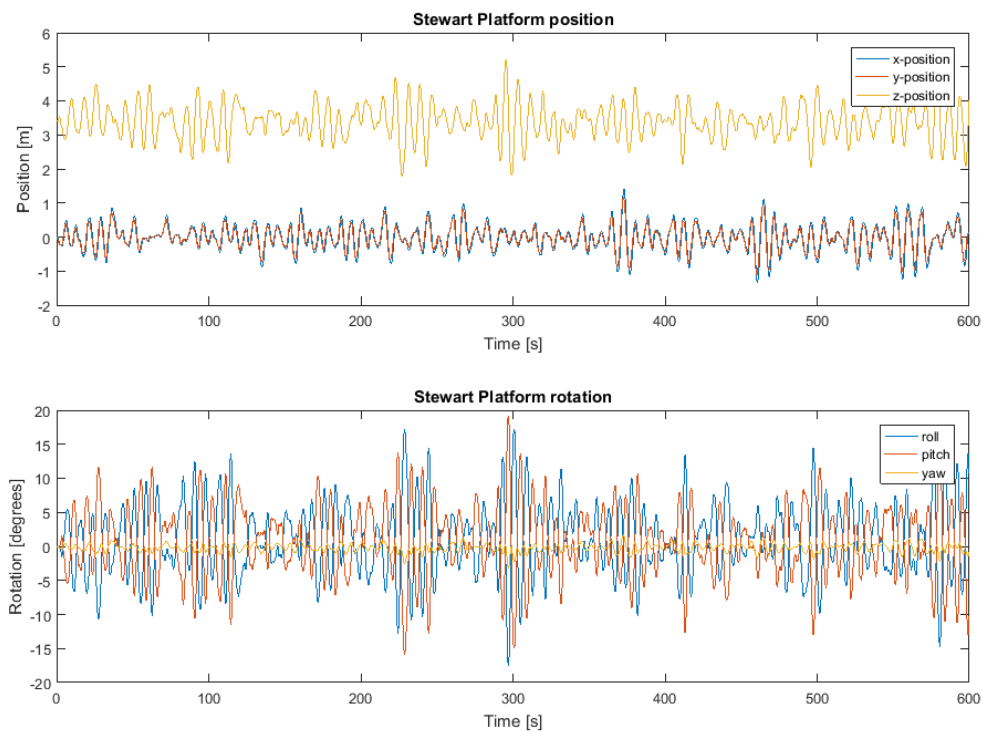


Figure E-3: Displacements and rotations of the top platform relative to the base platform.

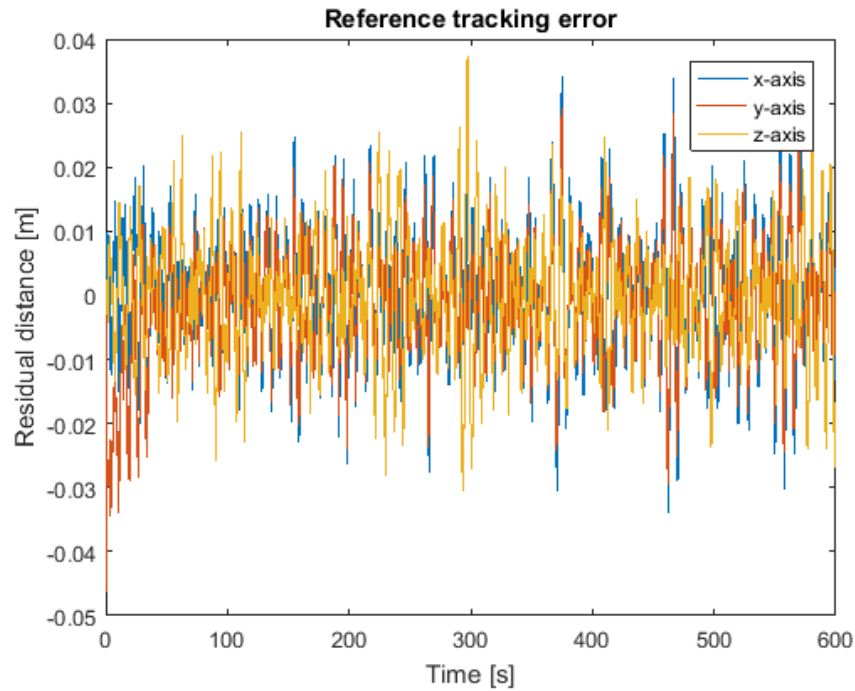


Figure E-4: Reference tracking errors of the motion compensation platform.

Scenario 2: mean LF disturbance angle is 35°

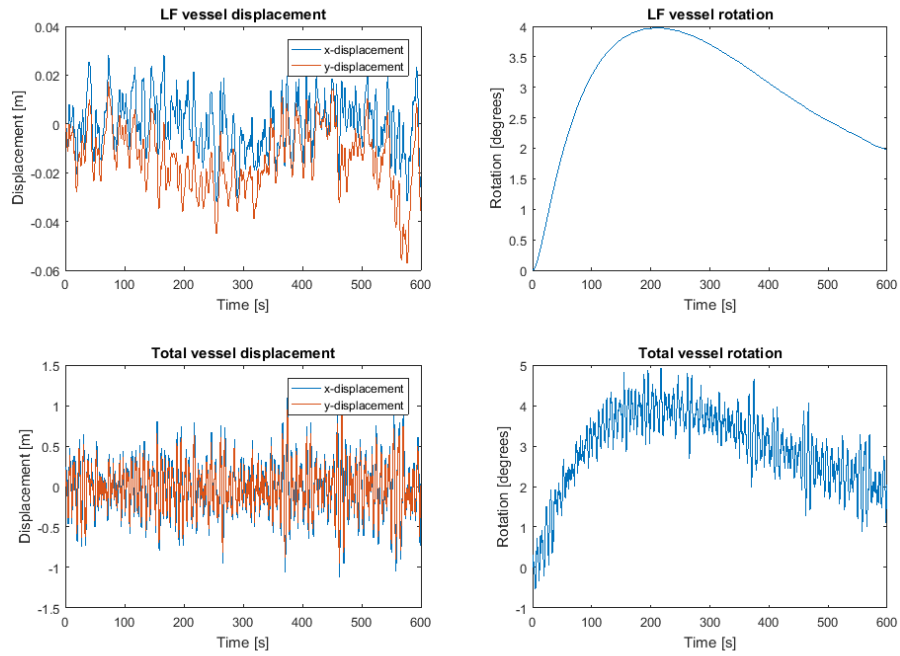


Figure E-5: η_{LF} and η_{tot} for the base case simulation.

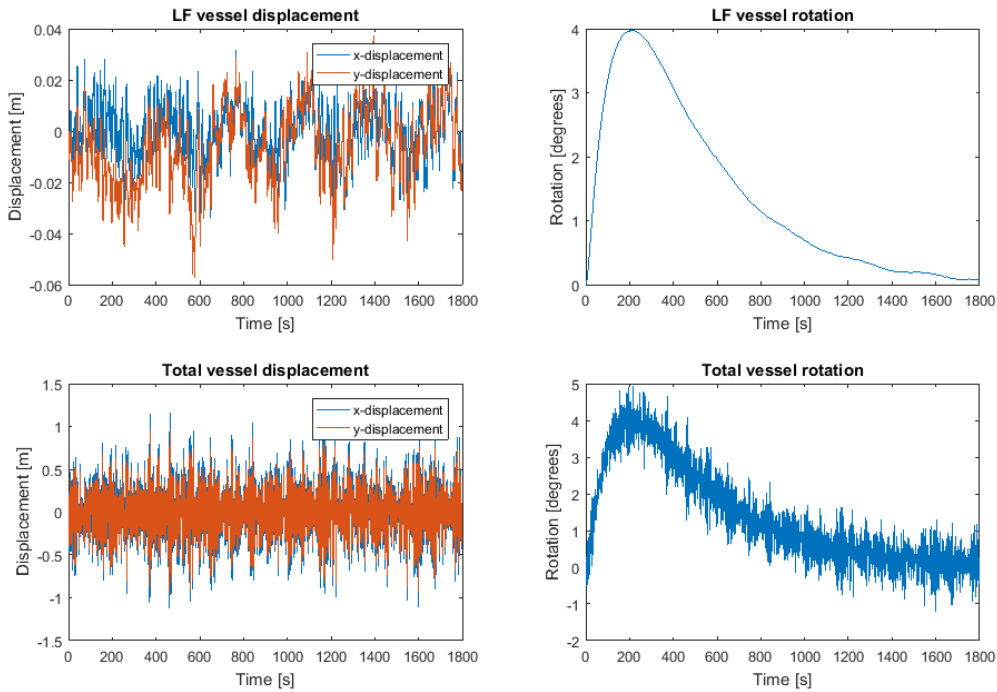


Figure E-6: η_{LF} and η_{tot} for 1800 s.

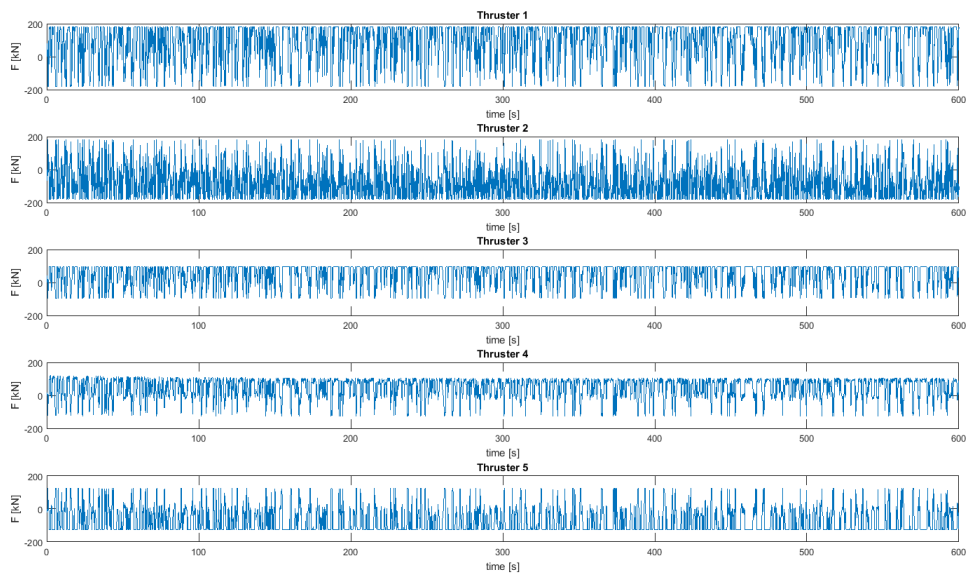


Figure E-7: Thrust forces used in the base case simulation.

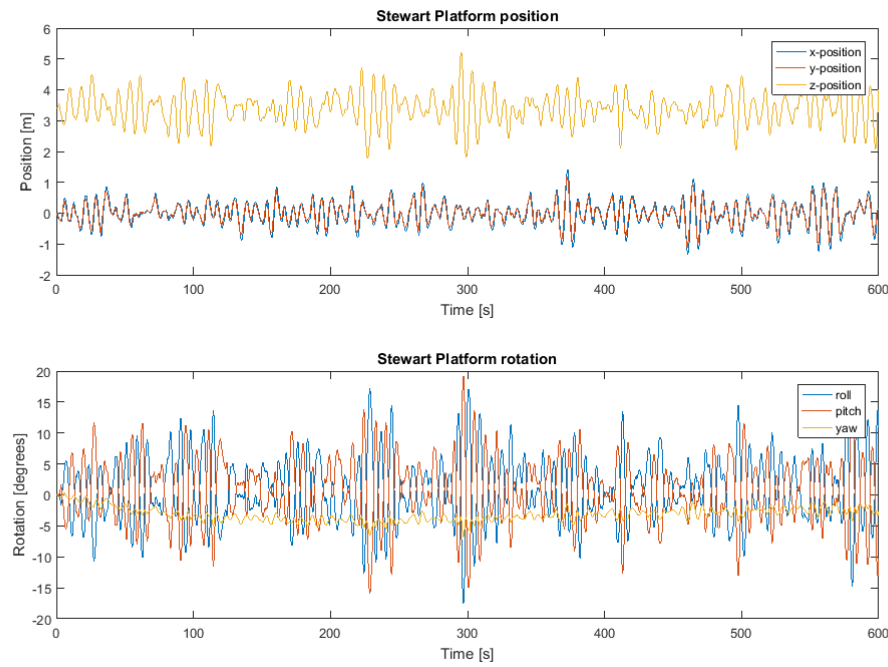


Figure E-8: Displacements and rotations of the top platform relative to the base platform.

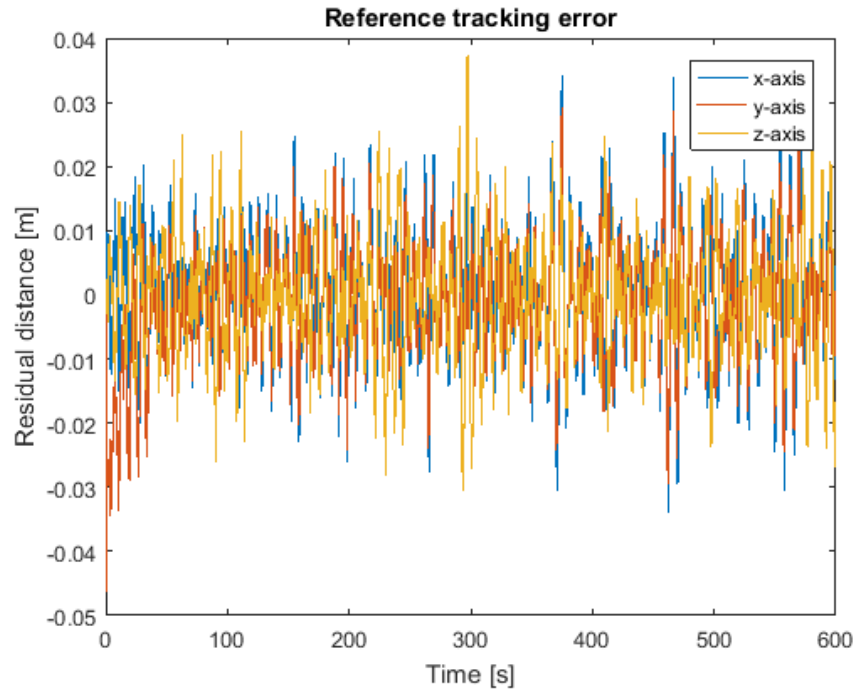


Figure E-9: Reference tracking errors of the motion compensation platform.

Dead Reckoning

Scenario 1: mean LF disturbance angle is 0°

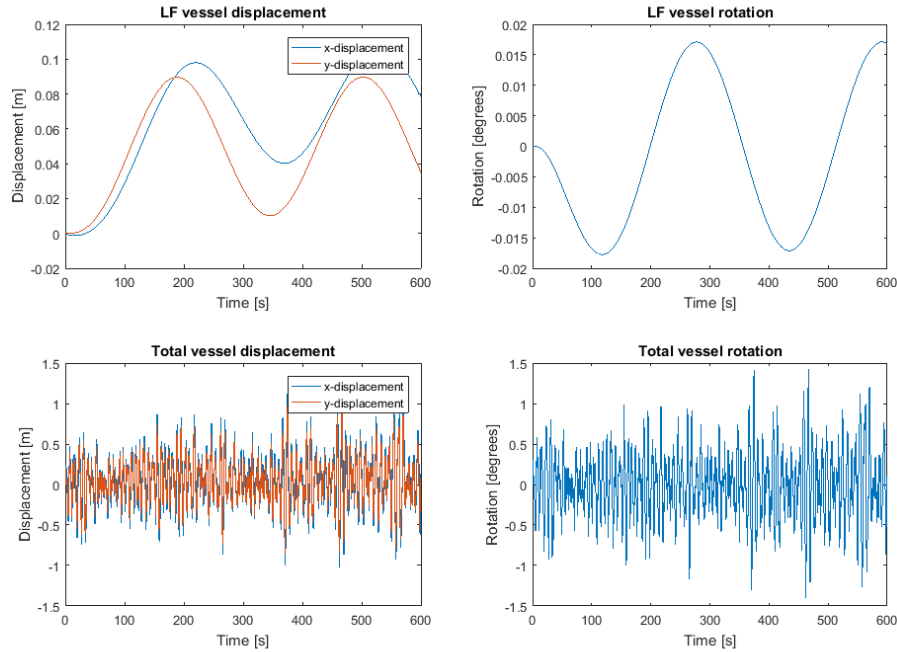


Figure E-10: η_{LF} and η_{tot} for the dead reckoning simulation.

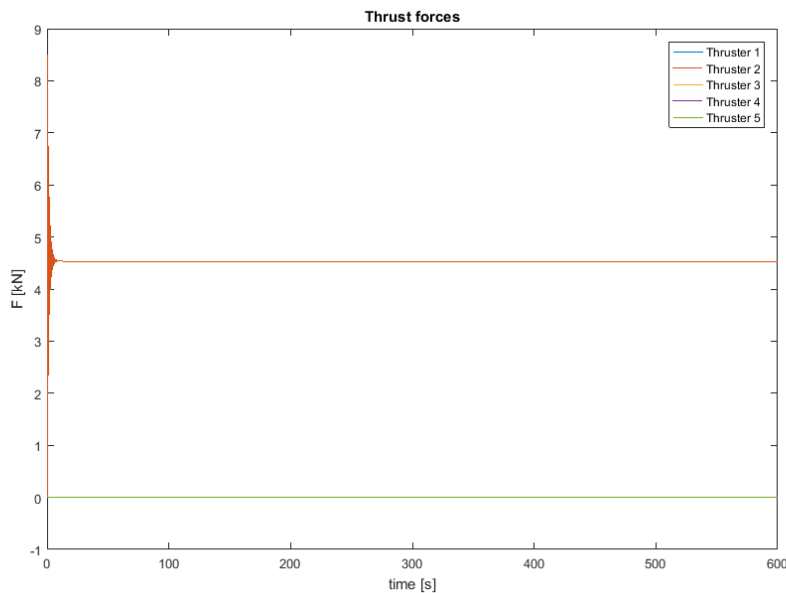


Figure E-11: Thrust forces used in the dead reckoning simulation.

Scenario 2: mean LF disturbance angle is 35°

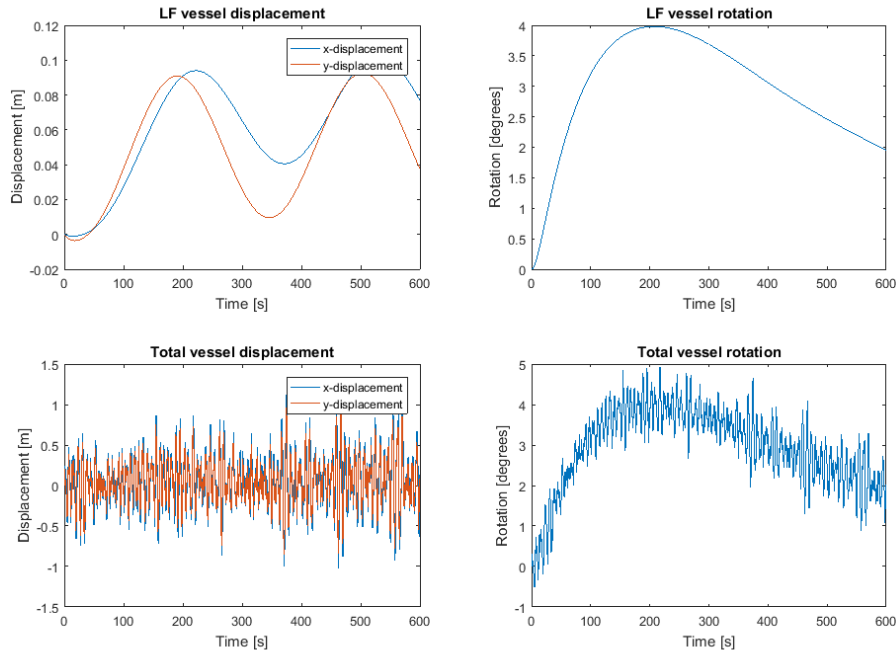


Figure E-12: η_{LF} and η_{tot} for the dead reckoning simulation.

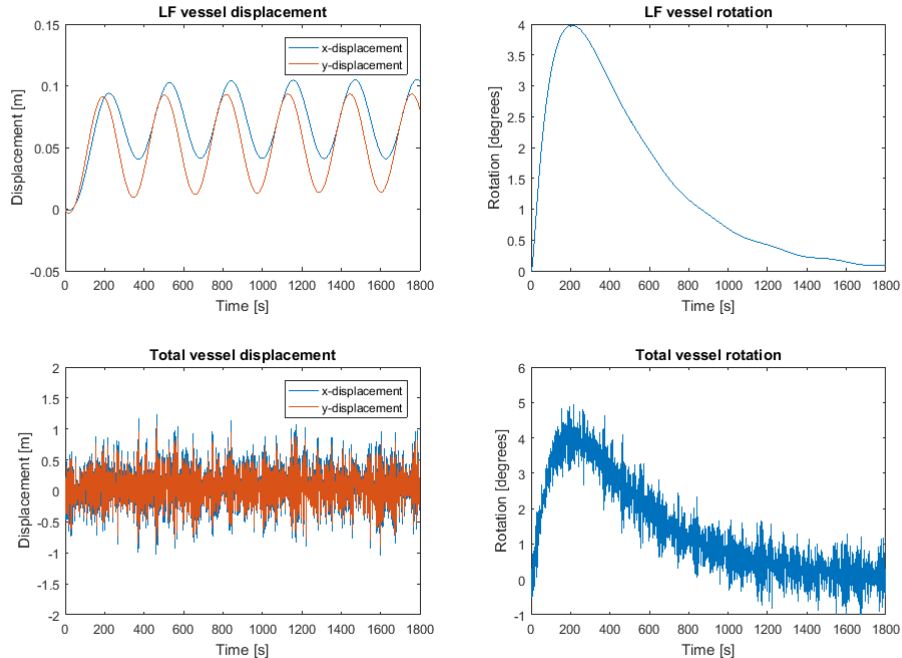


Figure E-13: η_{LF} and η_{tot} for 1800 s.

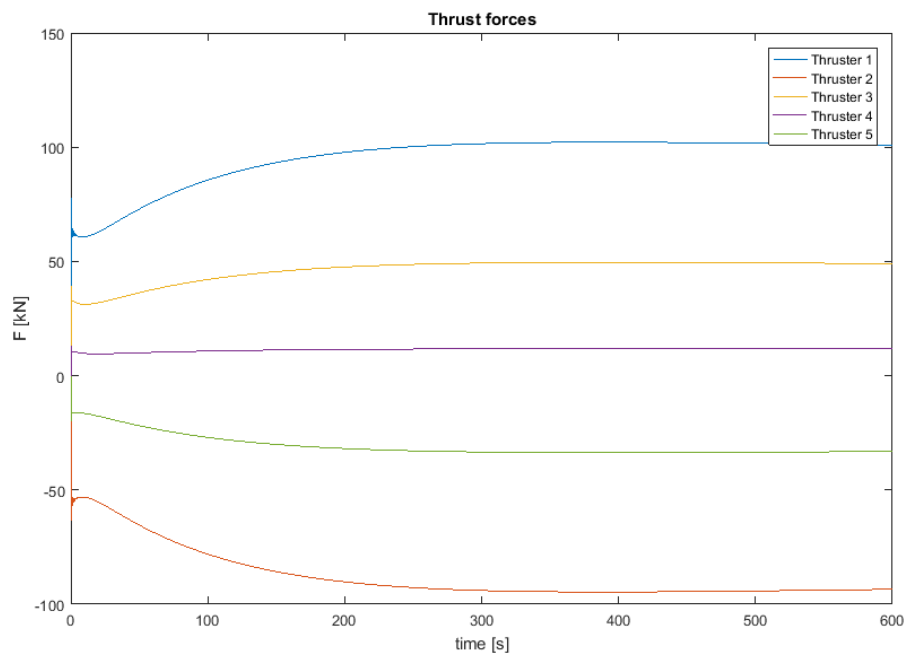


Figure E-14: Thrust forces used in the dead reckoning simulation.

PID Reference Circle

Scenario 1: mean LF disturbance angle is 0°

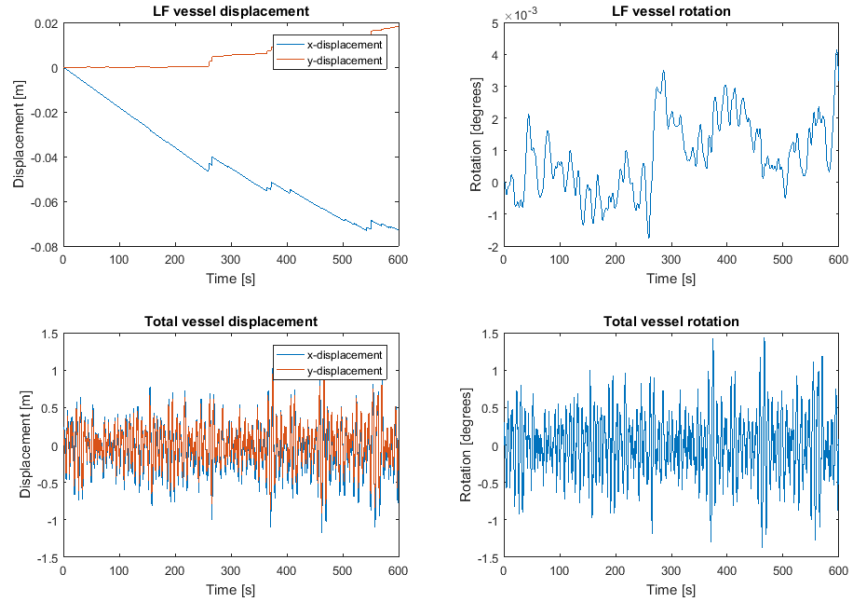


Figure E-15: η_{LF} and η_{tot} for $r_{ref} = 0.20$

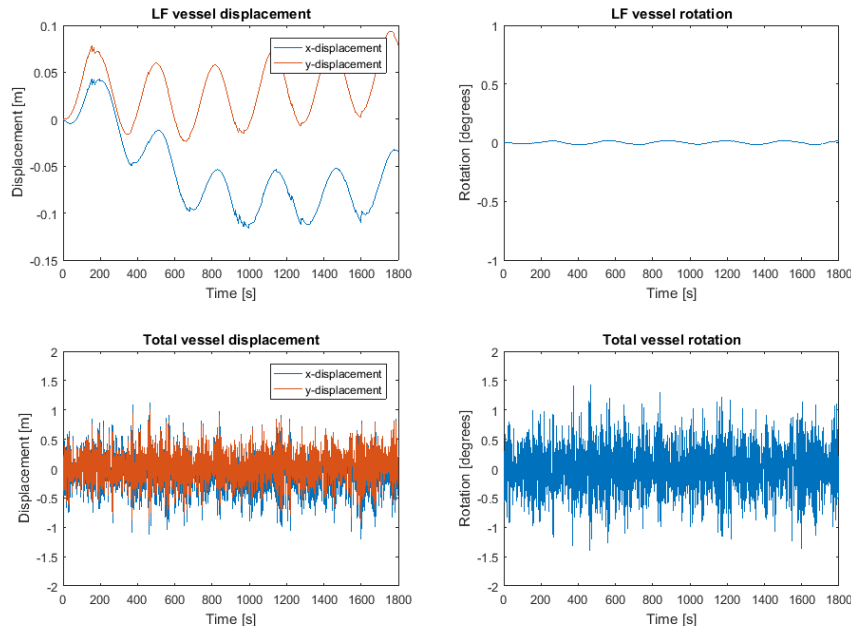


Figure E-16: η_{LF} and η_{tot} with $r_{ref} = 0.20$ for 1800 s.

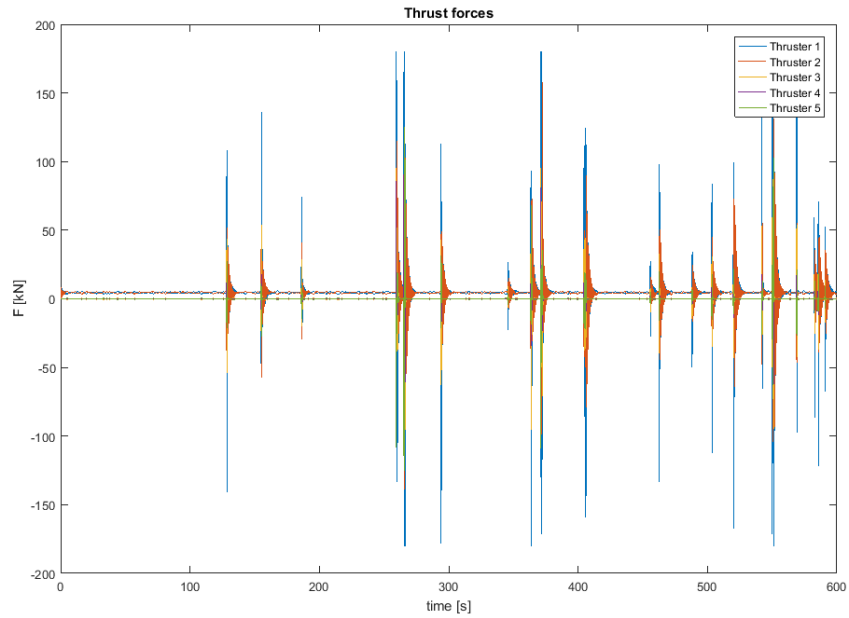


Figure E-17: Thrust forces for $r_{ref} = 0.20$

Scenario 2: mean LF disturbance angle is 35°

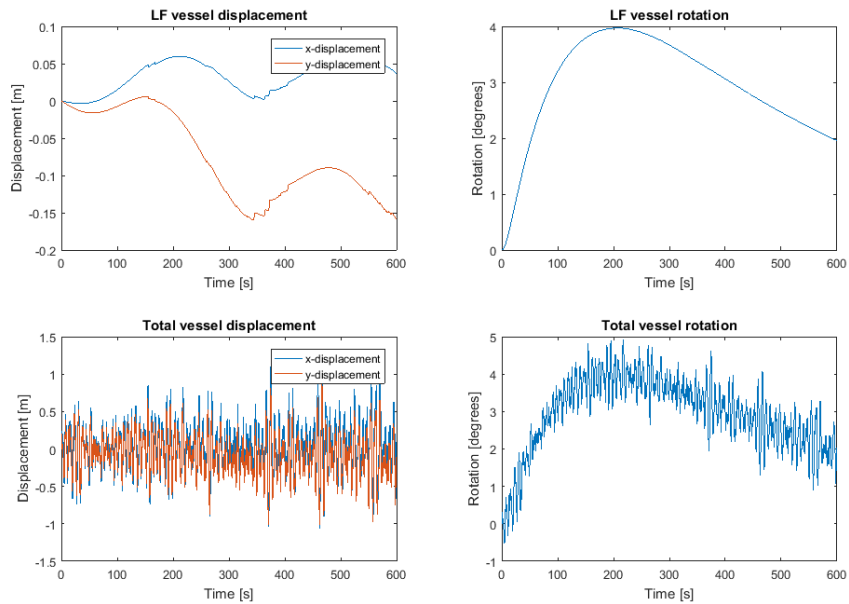


Figure E-18: η_{LF} and η_{tot} for $r_{ref} = 0.20$

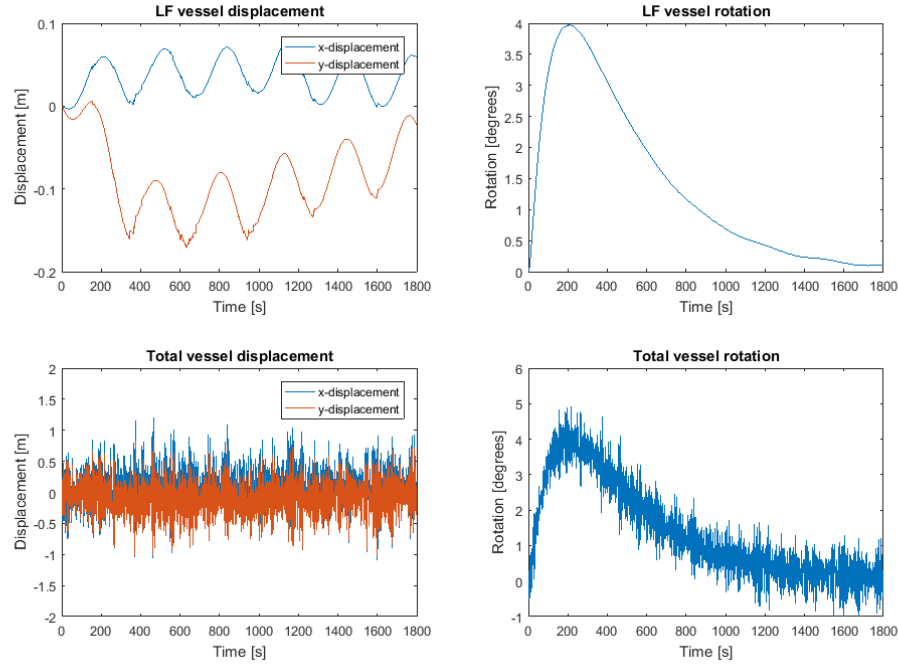


Figure E-19: η_{LF} and η_{tot} for 1800 s.

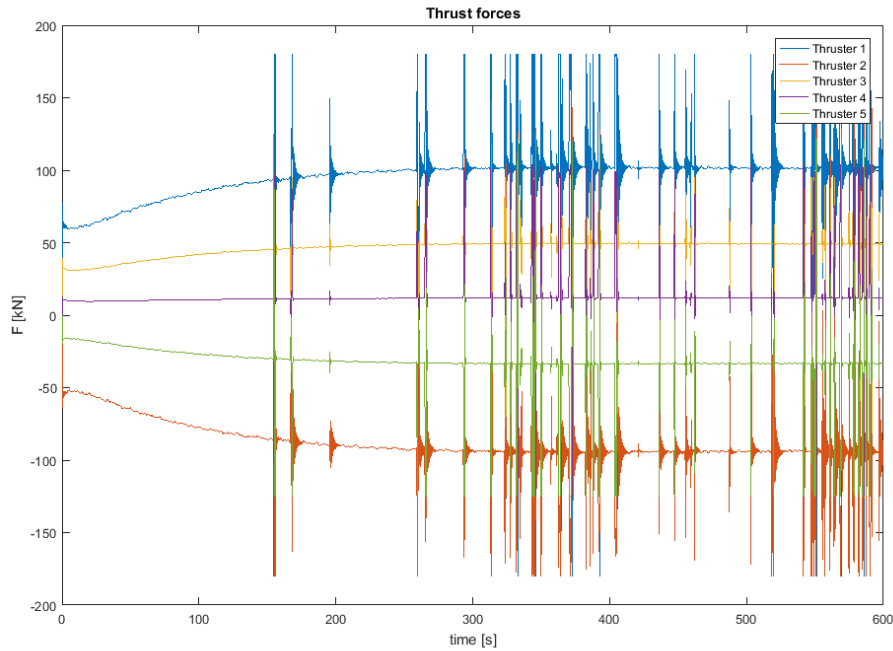


Figure E-20: Thrust forces for $r_{ref} = 0.20$

Thrust Allocation Tuning

Scenario 1: mean LF disturbance angle is 0°

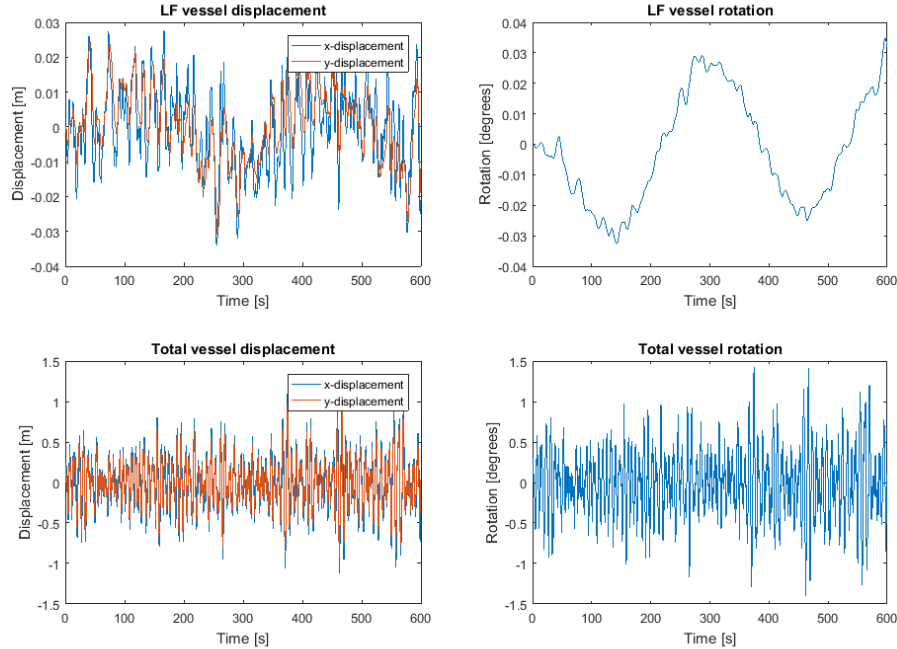


Figure E-21: η_{LF} and η_{tot} for $c_{alloc} = 10^0$

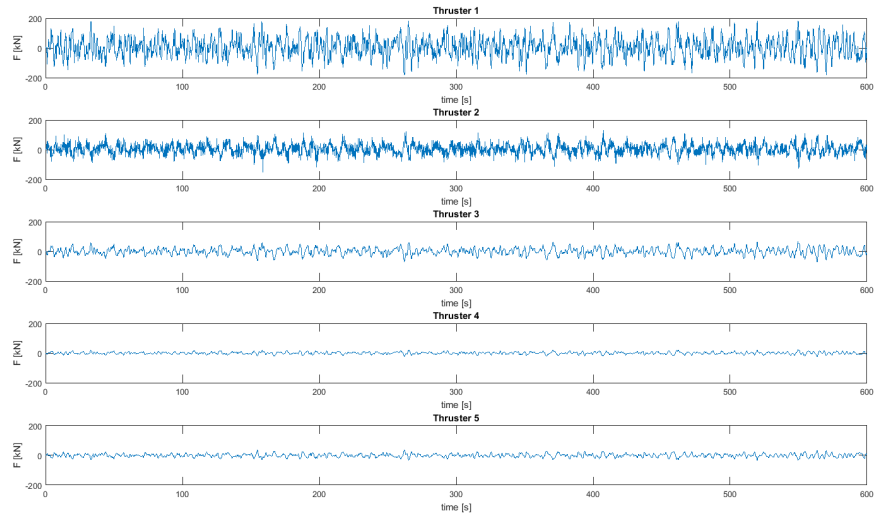


Figure E-22: Thrust forces for $c_{alloc} = 10^0$

Scenario 2: mean LF disturbance angle is 35°

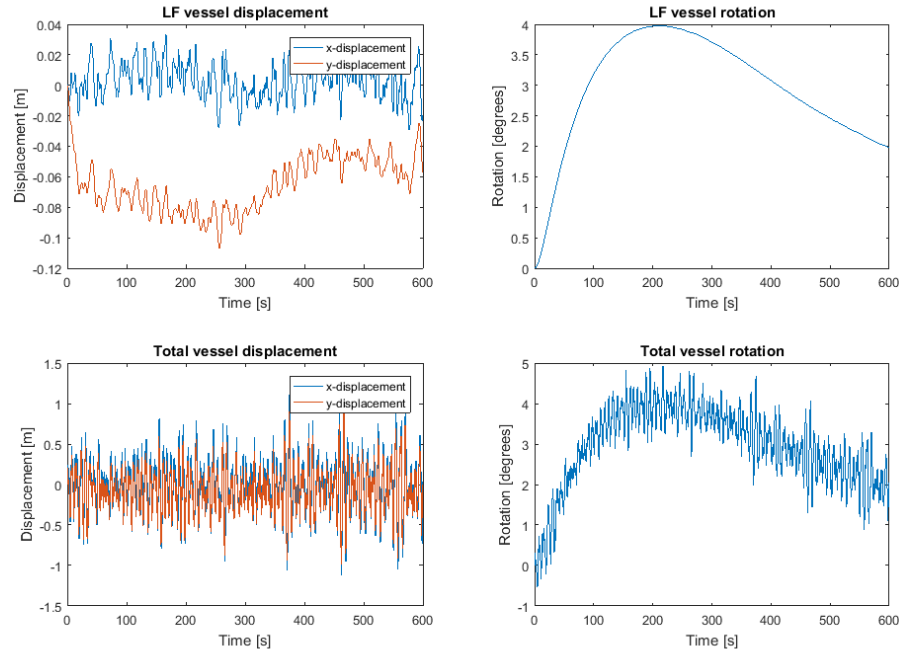


Figure E-23: η_{LF} and η_{tot} for $c_{alloc} = 10^0$

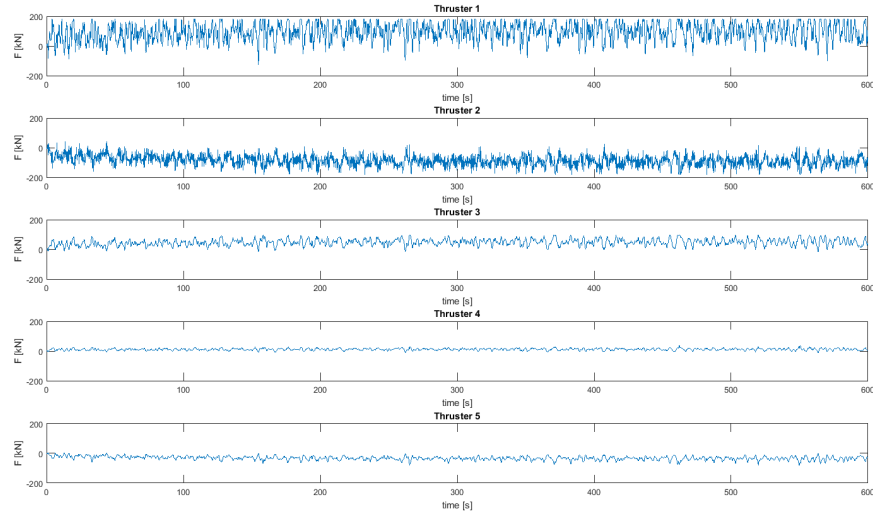


Figure E-24: Thrust forces for $c_{alloc} = 10^0$

Model Predictive Control (MPC) Matlab

Scenario 1: mean LF disturbance angle is 0°

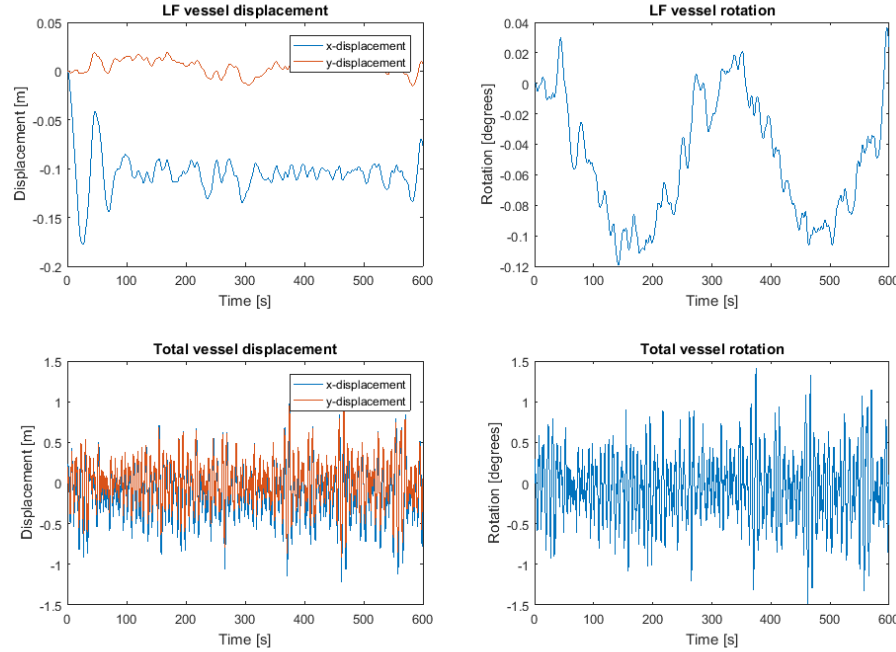


Figure E-25: η_{LF} and η_{tot} for $c_{alloc} = 5e2$

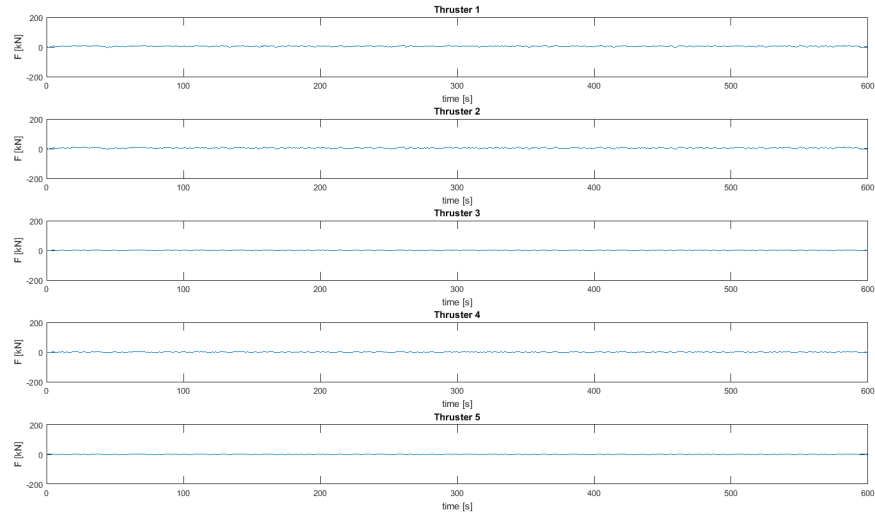


Figure E-26: Thrust forces for $c_{alloc} = 5e2$

Scenario 2: mean LF disturbance angle is 35°

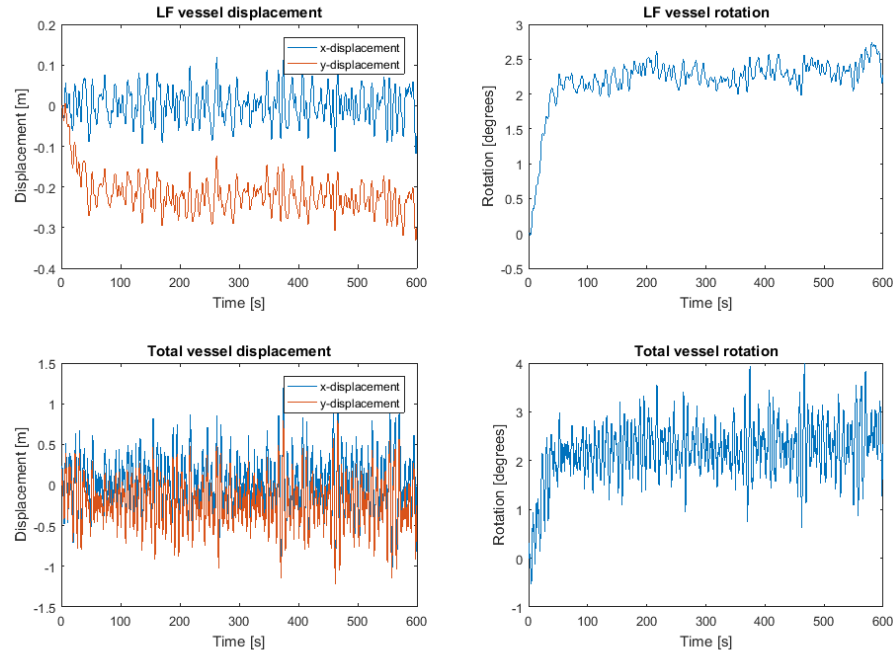


Figure E-27: η_{LF} and η_{tot} for $c_{alloc} = 5e4$

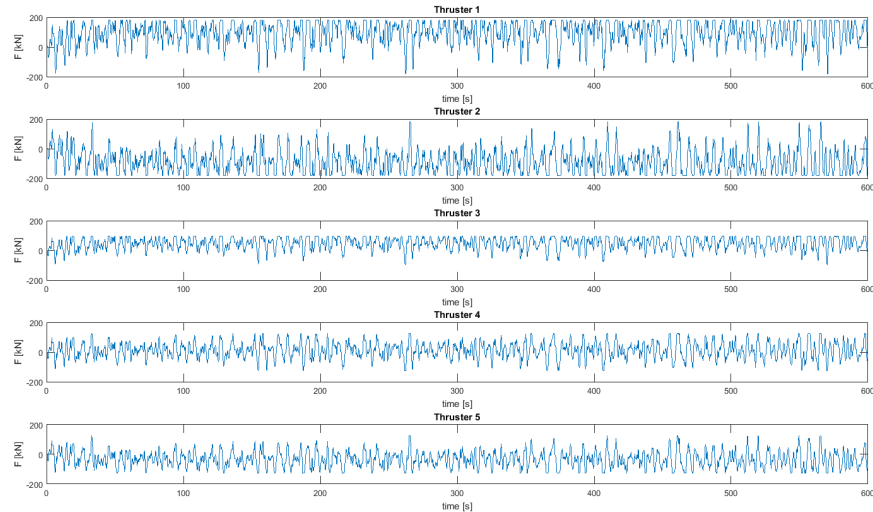


Figure E-28: Thrust forces for $c_{alloc} = 5e4$

MPC AMPL

Scenario 1: mean LF disturbance angle is 0°

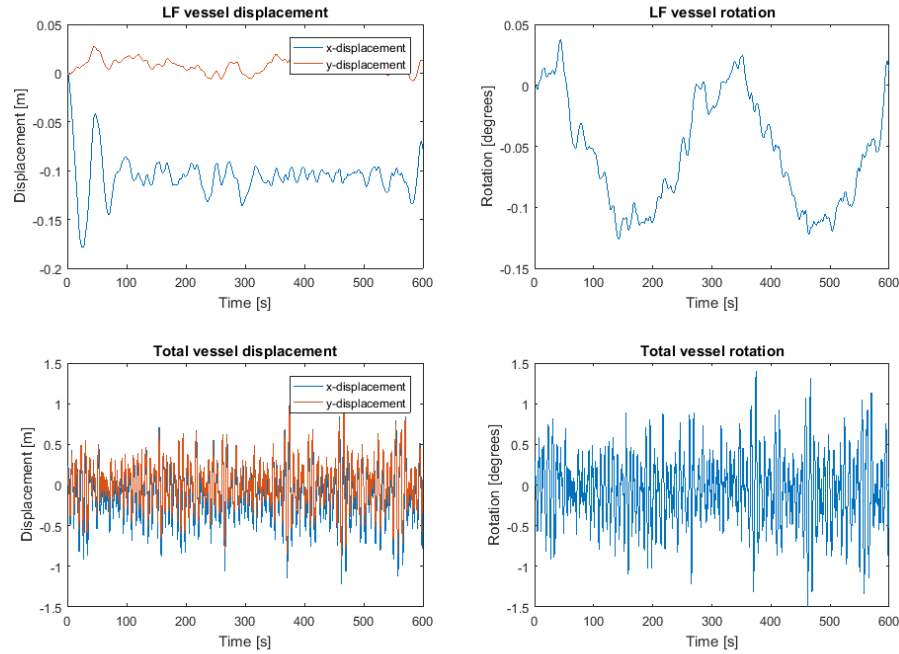


Figure E-29: η_{LF} and η_{tot} for $c_{alloc} = 5e2$

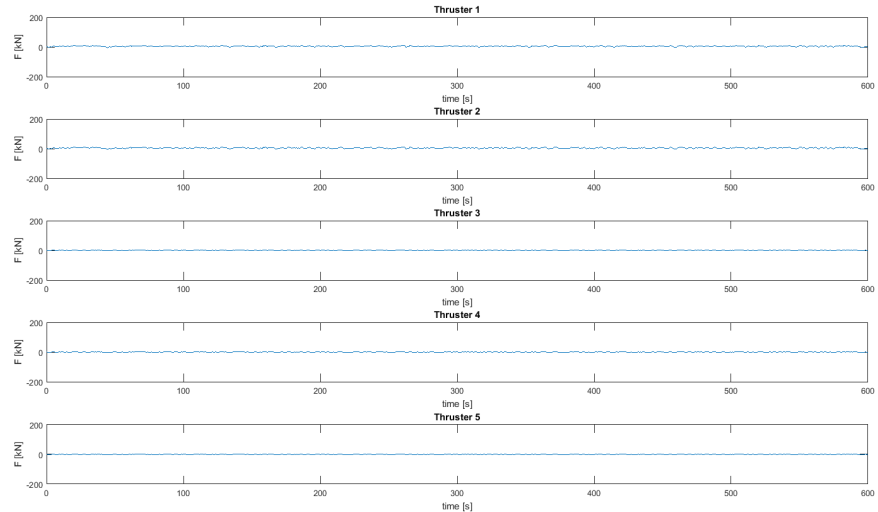


Figure E-30: Thrust forces for $c_{alloc} = 5e2$

Scenario 2: mean LF disturbance angle is 35°

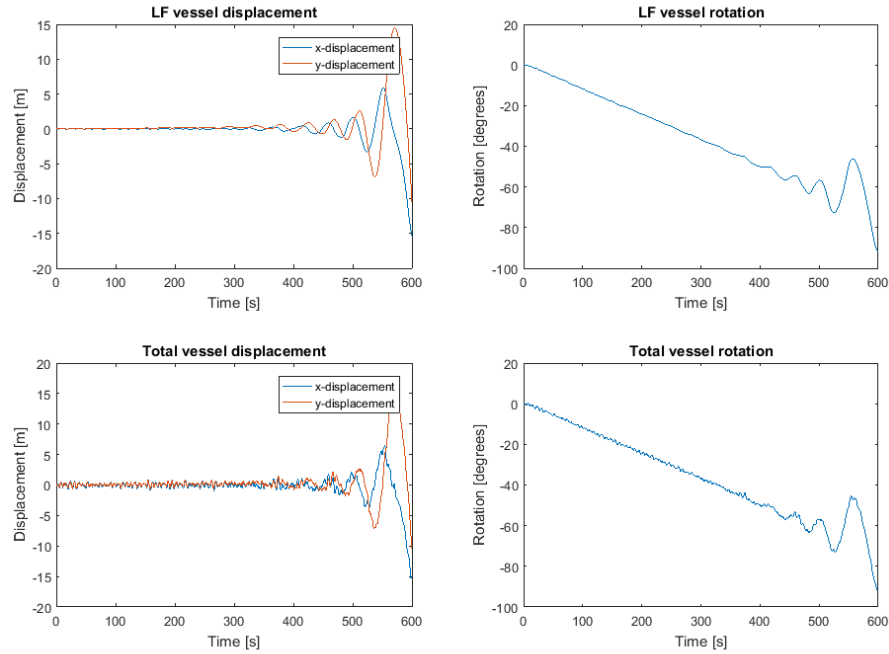


Figure E-31: η_{LF} and η_{tot} for $c_{alloc} = 5e4$

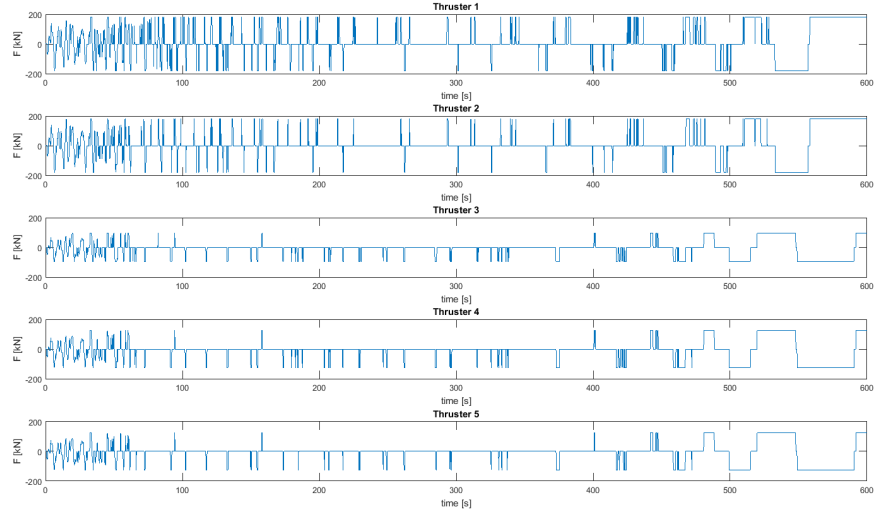


Figure E-32: Thrust forces for $c_{alloc} = 5e4$

Bibliography

- [1] AMPL Optimization inc. Ampl, December 2016.
- [2] M. Becerra-Vargas and E. Morgado Belo. Application of H-infinity theory to a 6 DOF flight simulator motion base. *Journal of the Brazilian Society of Mechanical Sciences and Engineering*, 34(2):193–204, 2012.
- [3] K G Cleasby and Andrew R Plummer. A novel high efficiency electro-hydrostatic flight simulator motion system. In *Fluid Power and Motion Control (FPMC 2008)*, pages 437–449. Centre for PTMC, UK, September 2008.
- [4] C. de Wit. Optimal thrust allocation methods for dynamic positioning of ships. Master’s thesis, Delft University of Technology, 2009.
- [5] T. I. Fossen. A nonlinear unified state-space model for ship maneuvering and control in a seaway. *International Journal of Bifurcation and Chaos*, 15(09):2717–2746, 2005.
- [6] T. I. Fossen. *Handbook of marine craft hydrodynamics and motion control*. John Wiley & Sons, 2011.
- [7] T. I. Fossen. Mathematical models of ships and underwater vehicles. *Encyclopedia of Systems and Control*, pages 701–706, 2015.
- [8] T. I. Fossen and T. A. Johansen. A survey of control allocation methods for ships and underwater vehicles. In *Control and Automation, 2006. MED’06. 14th Mediterranean Conference on*, pages 1–6. IEEE, 2006.
- [9] T.I. Fossen and T. Perez. Marine systems simulator (mss), 2004.
- [10] Y. Huang, D. M. Pool, O. Stroosma, Q. P. Chu, and M. Mulder. A review of control schemes for hydraulic stewart platform flight simulator motion systems. In *AIAA Modeling and Simulation Technologies Conference*, page 1436, 2016.
- [11] IHC Holland BV, December 2016.

- [12] Z. Liu. Sensor fusion and observer design for dynamic positioning. Master's thesis, Delft University of Technology, 2015.
- [13] Offshore Europe. Ampelmann company b.v., January 2017.
- [14] T. Perez and M. Blanke. *Mathematical ship modelling for control applications*. Ørsted-DTU, Automation, 2002.
- [15] T. Perez, Ø. N. Smogeli, T. I. Fossen, and A. J. Sørensen. An overview of the marine systems simulator (MSS): A simulink® toolbox for marine control systems. *Modeling, identification and Control*, 27(4):259–275, 2006.
- [16] SNAME. Nomenclature for treating the motion of a submerged body trough a fluid. *Technical and Research Bulletin*, (1-5), 1950.
- [17] A. J. Sørensen. A survey of dynamic positioning control systems. *Annual reviews in control*, 35(1):123–136, 2011.
- [18] A. J. Sørensen. Marine control systems—lecture notes. *Department of Marine Technology, Norwegian Univ. of Sci. and Tech*, 2013.
- [19] A. J. Sørensen. Dynamic positioning control systems for ships and underwater vehicles. *Encyclopedia of Systems and Control*, pages 329–337, 2015.
- [20] The MathWorks, Inc. Creating a stewart platform model using simmechanics, December 2016.
- [21] E. Thöndel. Electric motion platform for use in simulation technology—design and optimal control of a linear electromechanical actuator. In *Proceedings of the World Congress on Engineering and Computer Science*, volume 2. Citeseer, 2010.
- [22] T. van den Boom. Model predictive control. Lecture notes, 2013.
- [23] D.T.J. Van der Tempel, D.J.C. Salzmann, J. Koch, F. Gerner, and A.J. Göbel. Vessel, motion platform, method for compensating motions of a vessel and use of a stewart platform, April 11 2012. EP Patent 1,993,902.
- [24] J. van der Tempel, D. Cerdà Salzmann, and F. Gerner. Ampelmann demonstrator, 2008.
- [25] M. Verhaegen and V. Verdult. *Filtering and system identification: a least squares approach*. Cambridge university press, 2007.
- [26] C.A. Willemse, H.T. Grimmelius, and A.R. Tjallema. Dynamic positioning. Lecture notes, 2008.

Glossary

List of Acronyms

API	Application Programming Interface
b-frame	Body-fixed frame
CoG	Center of Gravity
DGPS	Differential Global Positioning System
DOF	Degrees of Freedom
DP	Dynamic Positioning
DR	Dead Reckoning
FPSO	Floating Production, Storage and Operation
h-frame	Hydrodynamic frame
HF	High-Frequency
HPR	Hydro-acoustic Position Reference
HPU	Hydraulic Power Unit
IMO	International Maritime Organization
IMU	Inertial Measurement Unit
LF	Low-Frequency
MPC	Model Predictive Control
MSS	Marine Systems Simulator
n-frame	North-east-down frame
PID	Proportional Integral Derivative

UKF Unscented Kalman Filter

VAF Variance Accounted For